

THE STREM CHEMIKER

VOL. XXV No. 2

September, 2011

Aminodiphosphines: Highly Versatile Ligands for Catalysis

by Dino Amoroso*, Kamaluddin Abdur-Rashid, Xuanhua Chen,
Rongwei Guo, Wenli Jia and Shuiming Lu

Nanosprings™: A Versatile Nanomaterial Platform

by Timothy C. Cantrell, Giancarlo Corti, David C. Hyatt,
David N. McIlroy, M. Grant Norton, Tejasvi Prakash
and Matthew Yahvah

Semiconductor Nanoparticles – A Review

by Daniel Neß and Jan Niehaus

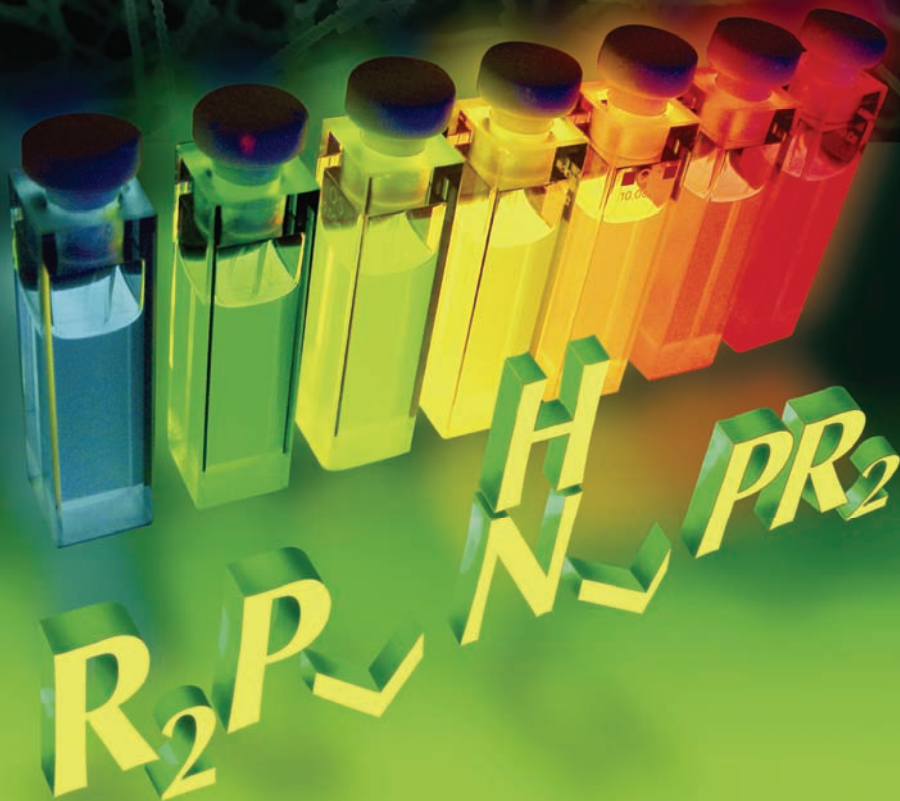


Table of Contents

Biographical Sketches

Kanata -	Dino Amoroso*, Kamaluddin Abdur-Rashid, Xuanhua Chen, Rongwei Guo, Wenli Jia and Shuiming Lu	1
GoNano -	Timothy C. Cantrell, Giancarlo Corti, David C. Hyatt, David N. McIlroy, M. Grant Norton, Tejasvi Prakash and Matthew Yahvah,	2-3
CANdot® -	Daniel Neß and Jan Niehaus	3
Aminodiphosphines: Highly Versatile Ligands for Catalysis		4-12
Aminodiphosphines Offered by Strem		12-26
Nanosprings™: A Versatile Nanomaterial Platform		27-38
Nanosprings™ Offered by Strem		38
Semiconductor Nanoparticles – A Review		39-47
CANdot® Quantum Dots Offered by Strem		47-49
New Products Introduced Since Chemiker XXV No. 1		50-66
New Kits Introduced Since Chemiker XXV No. 1		67-69
Available Booklets		69

BONUS OFFER: While supplies last, with any purchase of a Takasago product, receive 100mg of 44-0217 at no additional charge. Supplies are limited. This Bonus Offer is limited to one bonus per customer order. Please add 100mg of 44-0217 at the time your order is placed.

Congratulations to the following 2010 & 2011 recipients of awards sponsored by Strem:

**American Chemical Society Award
for Distinguished Service in the Advancement of Inorganic Chemistry**

2011 Charles P. Casey
2010 Richard D. Adams

Canadian Society for Chemistry Award for Pure or Applied Inorganic Chemistry

2011 Derek Gates
2010 Daniel B. Leznoff

©Copyright 2011 by

Headquarters:

Strem Chemicals, Inc.

7 Mulliken Way
Newburyport, MA 01950-4098
USA
Tel.: (978) 499-1600
Fax: (978) 465-3104
(Toll-free numbers below US & Canada only)
Tel.: (800) 647-8736
Fax: (800) 517-8736
Email: info@strem.com

European Offices:

15, rue de l'Atome
Zone Industrielle
67800 Bischheim
France
Tel.: (33) 03 88 62 52 60
Fax: (33) 03 88 62 26 81
Email: info.europe@strem.com

Postfach 1215
77672 Kehl
Germany
Telefon: 0 78 51 / 7 58 79
Email: info.europe@strem.com

Strem Chemicals UK, Ltd.

41 Hills Road
Cambridge, England CB2 1NT
Tel.: 0845 643 7263
Fax: 01223 368021
Email: enquiries@strem.co.uk



The Strem Chemiker
Vol. XXV No. 2
September, 2011

www.strem.com

"Cover design and art by Renegade Studios"

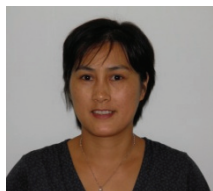
Biographical Sketches

Kanata



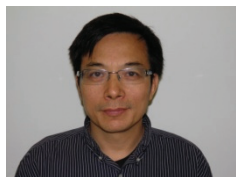
Dino Amoroso* received his Ph.D. from the University of Ottawa under the supervision of Prof. Deryn Fogg. His graduate studies focused on diversifying ligand scaffolds employed in ruthenium-catalyzed olefin metathesis reactions to affect stereochemical control. After graduation, he moved to industry where he has developed transition-metal catalysts for a range of transformations including olefin polymerization, C-X bond formation and hydrogenation. He is currently Manager, Business Development with Kanata Chemical Technologies, Inc. (KCT) in Toronto, Canada. KCT is a technology-based organization dedicated to the development of catalytic process technologies for chemical manufacturing.

Kamaluddin Abdur-Rashid received his Ph.D. in 1994 at the University of the West Indies, Mona Campus, Jamaica, under the supervision of Professor Tara Dasgupta. He joined Professor Bob Morris' group at the University of Toronto (1998-2002) as a Research Associate where he spearheaded the group's quest into pure and applied catalysis research. His discoveries led to the development of new classes of organometallic catalysts and their applications in organic synthesis, including industrial use. In 2004 he founded Kanata Chemical Technologies Inc. (KCT); an R&D company that is dedicated to the development and application of innovative catalyst technologies and processes.



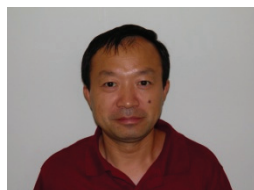
Xuanhua Chen received her M.Sc. in 1989 from Central China Normal University. She subsequently worked in the Department of Chemistry, Central China Normal University researching catalytic asymmetric reactions and also taught physical chemistry. She joined Kanata Chemical Technologies in 2006 as a Research Scientist.

Rongwei Guo received his Ph.D. in 2002 from the Hong Kong Polytechnic University, Hong Kong, China, under the supervision of Professor Albert S. C. Chan. His research focused on novel chiral ligand synthesis and applications in asymmetric catalysis. Then he joined Professor Morris' group at the University of Toronto in 2003, where he worked on the enantioselective hydrogenation of C=O and C=N double bonds and the formation of C-C bonds. In 2005, he joined Kanata Chemical Technologies in Toronto, Canada where he is currently Manager, Research and Development.



Wenli Jia received his Ph.D. in 2001 from Nankai University, China, under the supervision of Professor Jitao Wang. He then joined Professor Suning Wang at Queen's University (2001-2005) where his research focused on the synthesis of novel luminescent organic and organometallic compounds for use in OLED applications. He joined Kanata Chemical Technologies, Inc. (KCT) in 2005 as a Research Scientist.

Shuiming Lu received his Ph.D. in 1996 from the Nankai University in Tianjin, China, under the supervision of Professor Ruyu Chen. He became an Associate Professor in the Department of Chemistry at the Huazhong Normal University in Wuhan, China. After postdoctoral research appointments at the Hebrew University of Jerusalem with Professor Eli Breuer and at the University of Ottawa with Professor Howard Alper, he joined Kanata Chemical Technologies, where he is currently a Research Scientist.





Timothy C. Cantrell received his MS in Chemistry from the University of Idaho in 2007 under Dr. Pamela Shapiro. He joined GoNano Technologies, Inc. in the spring of 2008 and is serving as the project lead in Nanospring scale-up and material development. Mr. Cantrell has 5 years experience coating 1-D nanomaterials. In addition, he is listed on 3 patents and involved with many paper and technical presentations through GoNano.

Giancarlo Corti obtained his Ph.D. in Mechanical Engineering from the University of Idaho where he also completed his postdoctoral appointment prior to joining GoNano Technologies as Manager of Research and Development. During his postdoctoral appointment Giancarlo was responsible of the micro-fabrication, design and development for micro devices containing nano components such as Nanosprings and nanowires. He has made several contributions in the areas of acoustics in fluids, MEMS, NEMS, and biosensors. Currently Giancarlo is the Vice President of Research and Development and his present work include the design and development of equipment and procedures for mass production of nanomaterials, mainly silica Nanosprings. In addition, he oversees the different research programs at GoNano Technologies.



David C. Hyatt received his Ph.D. in Biochemistry from the University of Arizona where he studied enzyme mechanistic details using X-ray crystallography. He went on to do postdoctoral work at the Cleveland Clinic Foundation and later at Washington State University. During this time he has gained experience in plant natural product biochemistry and computational modeling of proteins. He has also worked on enzyme redesign through mutagenesis and maintains an active interest in this area. In 2011, David joined GoNano Technologies to lead the effort in immobilized enzyme technology.

David N. McIlroy received his Ph.D. in Physics in 1993 from the University of Rhode Island and postdoc in at the University of Nebraska-Lincoln. He joined the Department of Physics at the University of Idaho in 1996, where he is currently the department Chair and the Dyess Faculty Fellow. Professor McIlroy started his career over 20 years ago in the field of surface science and has over ten years of experience in the field of 1-D nanomaterials, such as nanowires, and most notably, silica Nanosprings that he developed in his laboratory. His interests in 1-D materials includes chemical interactions at their surfaces, as well as composite 1-D nanostructures consisting of metal nanoparticle decorated nanowires and nanosprings. In 2007, David co-formed GoNano Technologies, Inc.



M. Grant Norton is Professor of Materials Science and Engineering in the School of Mechanical and Materials Engineering at Washington State University and former Associate Dean of Research and Graduate Programs in the College of Engineering and Architecture. Professor Norton obtained his Ph.D. in Materials from Imperial College, London and spent a two-year postdoctoral at Cornell University before joining the Washington State University faculty in 1991. In 2003 and 2004 he was an AFOSR Faculty Research Associate at Wright-Patterson Air Force Base and spent the 1999/2000 academic year as a Visiting Professor at Oxford University. From 2000 to 2005 Professor Norton was Chair of Materials Science at Washington State University. He is author or co-author of about 200 papers in the archival literature, several book chapters, and two textbooks, one on X-ray diffraction and most recently *Ceramic Materials: Science and Engineering*, published by Springer. Professor Norton serves as Deputy Editor-in-Chief of *Journal of Materials Science* and is on the Editorial Board of *Journal of Nanotechnology*. The National Science Foundation, the Department of Homeland Security,

GoNano (cont.)

M. Grant Norton (cont)

Boeing Commercial Airplane Company, and REC Silicon are currently sponsoring Professor Norton's research. Prior to entering academia, Norton worked for two major European multinationals. He has consulted for a number of companies and organizations and is an advisor to CH2M Hill in the area of nanomaterials processing. In 2009, Governor Christine Gregoire appointed Professor Norton to the Board of Directors of the Washington Technology Center. In 2007, Norton co-formed GoNano Technologies, Inc., a university spin off company focused on alternative energy applications for nanomaterials.

Tejasvi Prakash obtained his BE in Electronics and communication from Bangalore University, India and a ME in Electrical Engineering from University of Idaho, Moscow, Idaho. He is pursuing a Ph.D. in Physics under Dr. McIlroy. He has experience in nanomaterial synthesis and characterization and has focused on Nanosprings enabled applications like carbon capture and recycling, continuous flow reactors and ultra capacitors.



Matthew Yahvah received his M.S. in Chemical Engineering from the University of Idaho in 2010. He worked several months in a biodiesel plant before joining GoNano's research team in fall 2010. He has worked on research involving industrial carbon capture, and biofuels from algae. Matt's primary focus at GoNano has been optimizing catalyst deposition on the Nanosprings as well as the validation of Nanosprings in catalytic converter applications. He has been enjoying his work very much.

CANdot®



Daniel Neß started his study of chemistry in April 2004 at the University of Hamburg. During 2007 he completed a three month internship at the University of Minnesota with Prof. Lawrence Que, Jr. where he also wrote his diploma thesis in the field of "Non-heme iron complexes for cis-dihydroxylation" from June through December 2008.

Since January 2009 he is working on his Ph.D. thesis "Synthesis of nanoparticles in a continuous flow system" in the Center of Applied Nanotechnology (CAN) GmbH.

Jan Niehaus studied chemistry at the University of Hamburg. He first came in contact with nanochemistry during his diploma thesis about the "synthesis and characterization of PbTe nanoparticles" in the working group of Prof. Weller in 2004. Between 2005 and 2008 he worked on his Ph.D. thesis developing a "continuous flow reactor for the production of monodispersed nanoparticles". Since 2008 he is leading the synthesis unit responsible for fluorescent and magnetic particles at the Center of Applied Nanotechnology (CAN) GmbH.



Aminodiphosphines: Highly Versatile Ligands for Catalysis

Dino Amoroso*, Kamaluddin Abdur-Rashid, Xuanhua Chen, Rongwei Guo,
Wenli Jia and Shuiming Lu
Kanata Chemical Technologies, Inc., MaRS Centre, South Tower
101 College St., Office 230, Toronto, ON M5G 1L7 Canada

Introduction

A simple and effective strategy for expanding ligand libraries which is often employed is the elaboration of known ligand designs based on denticity. That is, increasing the number of coordinating atoms within a given ligand framework while the general compositional and structural features are retained ultimately affords expanded applications or capabilities in catalysis. In the case of aminophosphine ligands (Figure 1), one such elaboration of the denticity is recognised in the development of aminodiphosphine ligands. Here, a second chelating arm is added to the amine affording a series of tridentate 'PNP' ligands. Given the versatility of the bidentate congeners,¹ it is no surprise that such tridentate PNP ligands have been deployed with high levels of success in a number of catalytic applications ranging from hydrogenation to amine alkylation. Some recent examples of their application to catalysis are described herein.

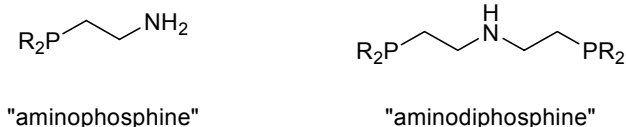
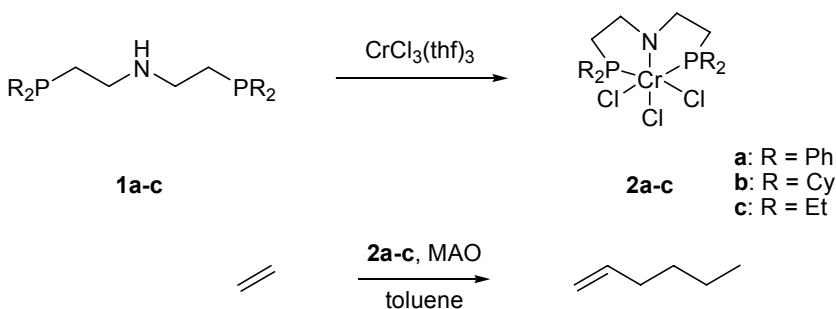


Figure 1 General structure of aminophosphine versus aminodiphosphine ligands.

Trimerisation of Ethylene

The use of aminodiphosphine ligands in the oligomerisation of ethylene has resulted in the development of a highly active and selective system for ethylene trimerisation.² A series of chromium complexes (Scheme 1) were prepared in high yields and subsequently tested in the oligomerisation of ethylene. It was determined that, in combination with methylaluminoxane (MAO), the Cr complexes display exceptional activity and selectivity with appropriate selection of the substituents on the phosphorus atoms. The highest activity was observed with the ethyl-substituted catalyst, **2c**, where a turnover frequency (TOF) of just less than 70,000 h⁻¹ was measured. In this case, selectivity for hexenes was 94 wt% with a 1-hexene selectivity of 99.1 wt%. Selectivity for trimerisation to linear 1-hexene is of great interest given the use of this product as a co-monomer in the production of polyethylene. For phenyl-substituted **2a**, a decrease in activity was observed (although selectivity was similar to **2c**). In the case of the bulkier cyclohexyl-substituted catalyst, **2b**, a propensity for polymerisation was observed (85.7 wt% polyethylene) rather than oligomerisation or trimerisation. The decreased tendency toward elimination is likely a result of the increased steric protection afforded by the bulkier ligand.

Scheme 1 Preparation of chromium-PNP pre-catalysts for ethylene oligomerisation.



Hydrogen Storage

The identification of viable alternative energy sources represents an area of burgeoning interest. Accordingly, the use and storage of hydrogen for this purpose has likewise become an intensely studied area. As it pertains to the use of ammonia borane (AB) as a storage medium for hydrogen, aminodiphosphine ligands and catalysts derived therefrom have been found to be of particular utility. Several reports have identified catalysts of a related nature (i.e. employing aminodiphosphine ligands) that can be deployed with a notable degree of success.³⁻⁸

In the case of ammonia borane dehydrogenation, Blaquiere et al.⁵ reported on the use of an Ir-based catalyst (**3**, Figure 2) which displayed modest efficacy at low catalyst loadings. Interestingly, the authors found that more active catalysts were identified amongst the series of ruthenium aminophosphine complexes, **4a-c** and **5a-b**. The latter complexes were found to yield as much as 2 (molar) equivalents of hydrogen per mole of methylammonia borane (MeAB) with loadings as low as 0.03 mol%. Reactions carried out at high MeAB concentrations led to systems with gravimetric hydrogen content of up to 3.6 wt% H₂.

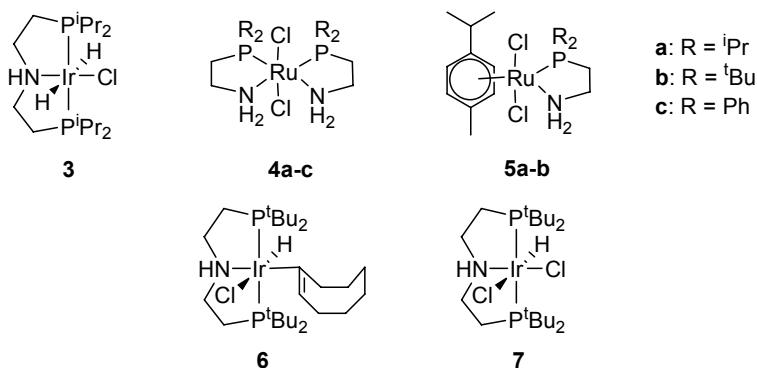
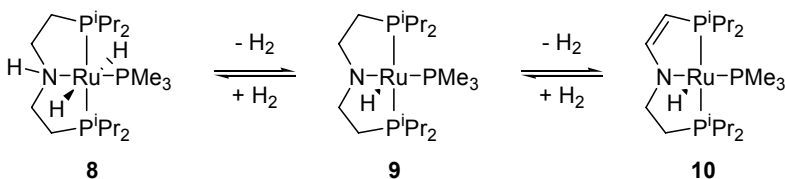


Figure 2 Iridium aminodiphosphine and ruthenium aminophosphine complexes for the dehydrogenation and/or hydrolysis of ammonia borane(s)

In the case of iridium catalysts **6** and **7**, these were found to be exceptionally active in the hydrolysis of ammonia borane (rather than dehydrogenation).⁷ Indeed, catalyst **7** was found to yield as much as 2.93 equivalents of hydrogen per mole of AB. Notable features of this particular catalyst/system are that the high performance was obtained in a water/alcohol solvent mixture and that the catalyst itself showed no degradation or loss of activity after storage at 100°C for 30 days. Catalyst loadings of 0.01 mol% were employed and repeated dosing (10 times) with AB of a single aliquot of catalyst showed consistent performance with no observable decrease in the volume of hydrogen liberated and a consistent rate throughout. Perhaps most remarkable was the use of the catalyst in a solid mixture with AB (i.e. no solvent) which when exposed to water vapour displayed similar levels of performance for hydrogen generation. In fact, this solid mixture translates to a system with gravimetric hydrogen content of 9.1 wt% far exceeding DOE targets.

Scheme 2 Interconversion of ruthenium PNP complexes through hydrogenation/dehydrogenation equilibria.



$$\text{H}_3\text{BNH}_3 \xrightarrow{[\text{Ru}]} \text{H}_2 + [\text{H}_2\text{BNH}_2]_n + \begin{array}{c} \text{H} \\ | \\ \text{HN} \text{---} \text{B} \text{---} \text{NH} \\ | \quad \quad | \\ \text{HB} \quad \quad \text{BH} \\ | \\ \text{N} \\ | \\ \text{H} \end{array} \quad (1)$$
$$2 \text{ Me}_2\text{HNBH}_3 \xrightarrow{\text{8 or 9}} 2 \text{ H}_2 + \begin{array}{c} \text{Me}_2\text{N}-\text{BH}_2 \\ | \quad | \\ \text{H}_2\text{B}-\text{NMe}_2 \end{array} \quad (2)$$

Hydrogenation has been perhaps the most heavily exploited application in catalysis for the aminodiphosphine ligands discussed here. This is almost certainly due to the fact that the most broadly exploited area for the closely related aminophosphines (Figure 1) has been this same area.¹ In general, their behaviour is thought to be similar in nature to the aminophosphine analogues where an outer-sphere mechanism is operative (Scheme 3).¹⁰⁻¹⁶

Transfer Hydrogenation

In transfer hydrogenation,^{13,17} the series of iridium hydride complexes shown in Scheme 4 were found to be implicated in the catalytic process. The dihydride complex, **11**, was found to be inactive in transfer hydrogenations until activated with base. Conversion to the trihydride **13**, led to exceptional activity in the reduction of a series of polar substrates. In the case of acetophenone, catalyst loadings as low as 100,000:1 (substrate:catalyst) could be employed to give 92 % conversion to the corresponding alcohol, 1-phenylethanol. Table 1 shows the complete set of results for the transfer hydrogenation of the various substrates examined. Ketones, aldehydes and imines are promptly reduced to the corresponding alcohols and amines. Notably, the unsaturated ketone of Entry 5 is reduced at both the ketone and olefin functionality yielding only the saturated alcohol.

Scheme 4 Iridium hydride complexes implicated in hydrogenation of ketones and aldehydes and imines.

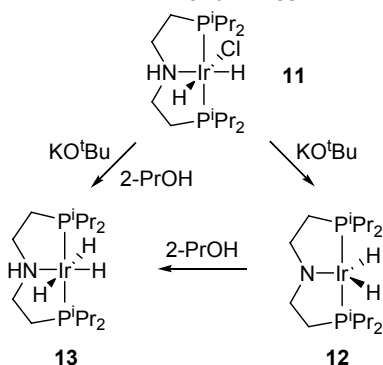
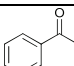
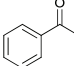
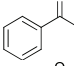
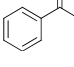
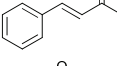
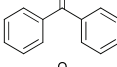
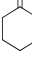
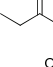
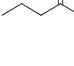
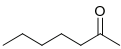
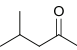
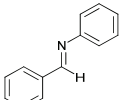


Table 1. Transfer hydrogenation of polar substrates using **11-13** in 2-ProH.

Entry	Catalyst	Substrate	Temp (°C)	S:C	Time (h)	Conv. (%)	Yield (%)
1	13		25	5,000	2	>99	98
2	13		60	100,000	12	92	90
3	12		25	5,000	2	>99	98
4 ^a	11		25	5,000	2	>99	98
5 ^b	13		25	5,000	2	>99	95
6	13		25	10,000	2.5	>99	97
7	13		25	5,000	1	>99	98
8	13		40	2,500	2	98	90
9	13		40	2,500	2	95	81

Entry	Catalyst	Substrate	Temp (°C)	S:C	Time (h)	Conv. (%)	Yield (%)
10	13		40	2,500	2	92	82
11	13		40	2,500	2	94	90
12	13		80	1,000	1	93	90

^a With added base. ^b Saturated alcohol is the only product.

The same family of iridium complexes, **11-13** (Scheme 3), have been considered for direct (H₂) hydrogenations.^{12,18} In this case, **11** and **13** were tested for hydrogenation activity in non-hydrogen donor solvents to ensure the transfer hydrogenation mechanism was not active. It was indeed verified that in methanol (a non-hydrogen-donor solvent) and in the absence of base **13** catalyzes the reduction of acetophenone to phenylethanol within 5 hours at loadings of 5000:1 (substrate:catalyst). As expected, when **11** was tested under the same conditions no reaction was observed. Upon addition of base, the result was identical to that observed with **13** (i.e. the supposed active catalyst) thus establishing **11** as a convenient, air-stable entry point to the active catalyst. The convenience and versatility of this hydrogenation system was further highlighted in its ability to carry out the hydrogenation in a broad range of solvents including chlorinated solvents such as dichloromethane and chloroform (Entry 9 – 10, Table 2) where traditional Noyori-type catalysts become deactivated via formation of the corresponding hydrido-chloro complex. The only solvent in which the iridium system was found to be inactive is acetonitrile (Entry 11).

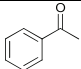
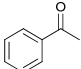
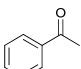
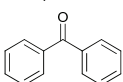
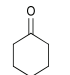
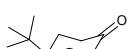
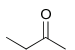
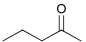
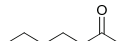
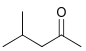
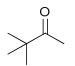
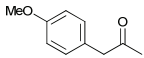
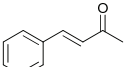
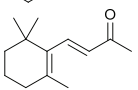
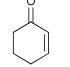
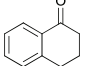
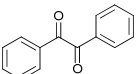
Table 2. Hydrogenation of acetophenone using **11**/KO^tBu (1:10) as catalyst in various solvents (10 atm. H₂) at room temperature.

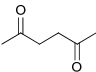
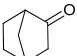
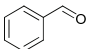
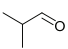
Entry	Solvent	S:C	Time (h)	Conv. (%)
1	methanol	450	0.5	100
2	ethanol	450	1	100
3	2-propanol	450	0.5	100
4	ether	450	1	100
5	THF	450	0.5	100
6	ethyl acetate	450	0.5	100
7	hexane	450	0.5	100
8	toluene	450	1	100
9	dichloromethane	450	1	100
10	chloroform	450	1	100
11	acetonitrile	450	2	0

Table 3 shows the results of the direct hydrogenation of a broad range of ketones and aldehydes in methanol using **11** as the entry point to the catalytic cycle. The results clearly demonstrate the broad utility of this system as a number of dialkyl ketones were readily reduced (Entries 5 – 12). The sterically hindered and electronically deactivated pinacolone (Entry 11) was readily reduced. For the purposes of comparison, the unsaturated ketone, benzalacetone (Entry 13) was reduced to the unsaturated alcohol under the direct hydrogenation conditions whereas under transfer hydrogenation conditions only the saturated alcohol was obtained (Table 1, Entry 5). In the case of pro-chiral ketones, the achiral catalyst lead to the formation of mainly the *meso* diol of benzil (Entry 17) while reduction of 2,5-hexanedione resulted in only rac-2,5-hexanediol (Entry 18) and a 6:1 mixture of *endo:exo*

norborneol resulted from the hydrogenation of norcamphor (Entry 19). It is worth noting that chiral derivatives are now commercially available.¹⁹

Table 3. Direct hydrogenation of ketones and aldehydes using **11**/KO^tBu (1:10) as catalyst in methanol.

Entry	Substrate	S:C	Time (h)	Conv. (%)
1		900	1	100
2		6000	5	100
3		30000	12	100
4		500	1	100
5		1100	1.5	100
6 ^a		700	1	100
7		1050	2	100
8		1200	2	100
9		900	2	100
10		1500	2	100
11		1050	72	100
12		100	1	100
13 ^b		360	2	100
14 ^b		300	1	100
15 ^c		1100	2	100
16		250	2	100
17 ^d		200	0.5	100

Entry	Substrate	S:C	Time (h)	Conv. (%)
18 ^e		600	2	100
19 ^f		900	1	100
20		1000	2.5	100
21		750	1.5	100

^aRatio of *cis*:*trans* alcohol = 1:2; ^bonly carbonyl group is reduced; ^cratio of saturated:allyl alcohol = 1:1; ^dratio of *meso*:*rac* alcohol = 3:1; ^e*rac*-alcohol is the only product; ^fratio of *endo*:*exo* = 6:1.

Some details have recently emerged on the use of ruthenium-PNP complexes as effective catalysts for the hydrogenation of esters and lactones.²⁰ At this point, a limited amount of information is available however this will almost certainly generate significant interest as more information becomes available.²¹

Dehydrogenation and Dehydrogenative Couplings

A series of osmium and ruthenium PNP complexes (Figure 3) have been prepared and tested in a number of dehydrogenation and dehydrogenative coupling protocols including acceptorless dehydrogenative coupling (ADC) of alcohols and alkylation of primary amines.^{22,23} The ADC protocol represents a powerful route to a range of esters (**3**). In this case, catalysts **15**, **16** and **18** were found to become efficient catalysts above temperatures of 120°C yielding esters of isoamyl alcohol, hexanol and benzyl alcohol in approximately 90% conversion within anywhere from 2-8 hours (depending on temperature). In fact, these catalysts were found to be stable and active at temperatures of up to 200°C with loadings of 0.1 mol%.

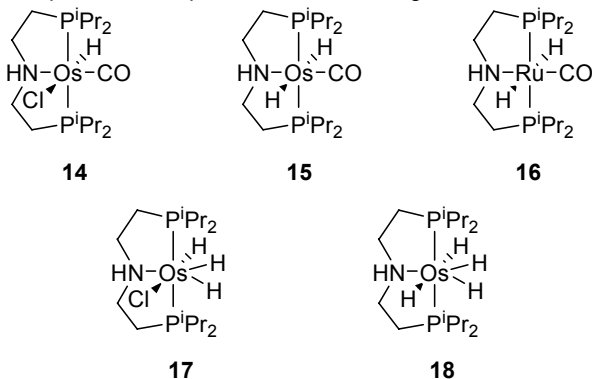
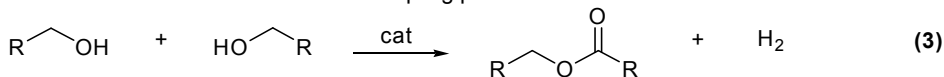
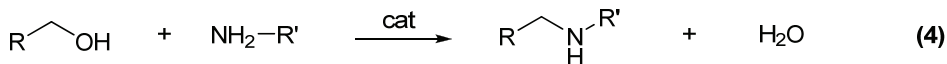


Figure 3 Osmium and ruthenium complexes for dehydrogenation and dehydrogenative coupling protocols.

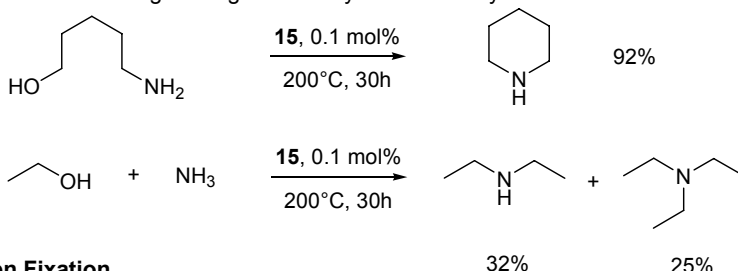


For use in amine alkylation (**4**), catalysts **15**, **16** and **18** were similarly found to offer their best results at 200°C such that no imine by-products were detected. Amines employed included hexyl, cyclohexyl, benzyl and aniline while isoamyl, benzyl, methyl and ethyl alcohol were used to prepare a number of unsymmetrical secondary amines. Catalysts **14** and **17** were also used in this protocol however these required the addition of a base to become active. Two particularly attractive examples using **15** are given in Scheme 5. The first example is a ring-

closing reaction using only molten 5-aminopentanol to derive piperidine. The second is the direct alkylation of ammonia using only a 2.0M solution of ammonia in ethanol (i.e. as purchased) to give a mixture of diethylamine and triethylamine. In general, it is believed that the amine alkylation proceeds via dehydrogenation of the alcohol to the aldehyde which subsequently reacts with the amine to form an intermediate imine. The imine is thus hydrogenated (using the hydrogen which was removed from the alcohol) to form the amine.



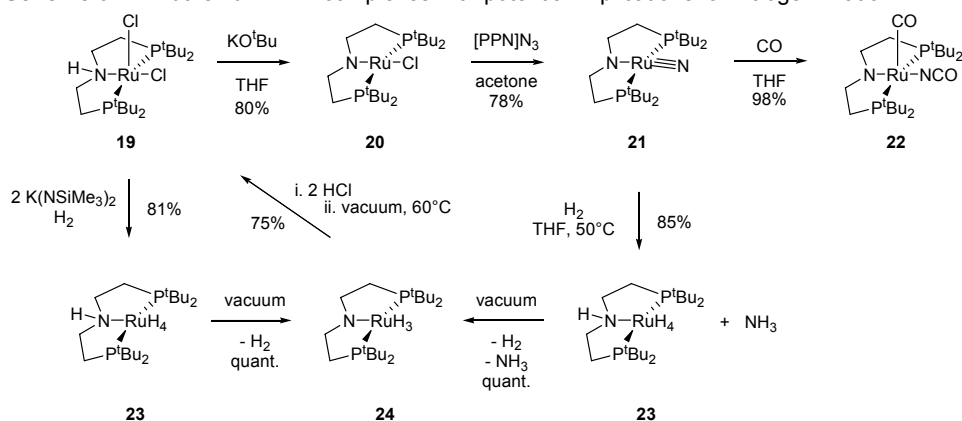
Scheme 5 Ring-closing amine alkylation and alkylation of ammonia.



Nitrogen Fixation

Perhaps the most exciting prospect for the application of PNP-type ligands in catalysis is in the area of nitrogen fixation. Very recently several ruthenium PNP complexes, which are correlated through a series of reactions (Scheme 6), where shown to form the basis of a process for the synthesis of ammonia from nitrogen.^{24,25} The rare, four-coordinate ruthenium complex **20**, which was derived from the readily accessible dichloride **19**, is the key species within the series of complexes. Once converted to the azide and then exposed to hydrogen, an equivalent of ammonia is released. The resulting Ru(IV) tetrahydride was then restored to the dichloride **19** in two steps through exposure to vacuum (to liberate one equivalent of hydrogen), treatment with acid (HCl) and a second vacuum treatment (to liberate a second equivalent of hydrogen). In the same report, the nitride ruthenium complex **21** was also shown to react with CO to form a terminal isocyanate complex.

Scheme 6 Ruthenium PNP complexes with potential implications for nitrogen fixation.



Conclusion

The range of transformations that have been reported thus far serve to underscore the potential of PNP-type ligands in catalysis. Without doubt, the greater availability of such ligands and catalysts will continue to foster the development of new and exciting applications and establish this class of ligands as a particularly effective scaffold in the preparation of practical catalysts.

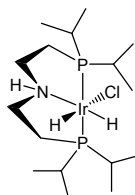
References:

- (1) Amoroso, D.; Graham, T. W.; Guo, R.; Tsang, C.-W.; Abdur-Rashid, K. *Aldrichimica Acta* **2008**, *41*, 15-26.
- (2) McGuinness, D. S.; Wasserscheid, P.; Keim, W.; Hu, C.; Englert, U.; Dixon, J. T.; Grove, C. *Chem. Commun.* **2003**, 334-335.
- (3) Abdur-Rashid, K.; Graham, T. W.; Tsang, C.-W.; Chen, X.; Guo, R.; Jia, W. **2011**, US 2011/0104046.
- (4) Abdur-Rashid, K.; Graham, T. W.; Tsang, C.-W.; Chen, X.; Guo, R.; Jia, W.; Amoroso, D.; Sui-Seng, C. **2011**, US 2011/0070152.
- (5) Blaquiere, N.; Diallo-Garcia, S.; Gorelsky, S. I.; Black, D. A.; Fagnou, K. *J. Am. Chem. Soc.* **2008**, *130*, 14034-14035.
- (6) Friedrich, A.; Drees, M.; Schneider, S. *Chem. Eur. J.* **2009**, *15*, 10339-10342.
- (7) Graham, T. W.; Tsang, C.-W.; Chen, X.; Guo, R.; Jia, W.; Lu, S.-M.; Sui-Seng, C.; Ewart, C. B.; Lough, A. J.; Amoroso, D.; Abdur-Rashid, K. *Angew. Chem. Int. Ed.* **2010**, *49*, 8708-8711.
- (8) Kaß, M.; Friedrich, A.; Drees, M.; Schneider, S. *Angew. Chem. Int. Ed.* **2009**, *48*, 905-907.
- (9) Staubitz, A.; Sloan, M. E.; Robertson, A. P. M.; Friedrich, A.; Schneider, S.; Gates, P. J.; Günne, J. S. a. d.; Manners, I. *J. Am. Chem. Soc.* **2010**, *132*, 13332-13345.
- (10) Abdur-Rashid, K.; Clapham, S. E.; Hadzovic, A.; Lough, A. J.; Morris, R. H. *J. Am. Chem. Soc.* **2002**, *124*, 15104-15118.
- (11) Abdur-Rashid, K.; Faatz, M.; Lough, A. J.; Morris, R. H. *J. Am. Chem. Soc.* **2001**, *123*, 7473-7474.
- (12) Chen, X.; Jia, W.; Guo, R.; Graham, T. W.; Gullons, M. A.; Abdur-Rashid, K. *Dalton Transactions* **2009**, 1407-1410.
- (13) Clarke, Z. E.; Maragh, P. T.; Dasgupta, T. P.; Gusev, D. G.; Lough, A. J.; Abdur-Rashid, K. *Organometallics* **2006**, *25*, 4113-4117.
- (14) Comas-Vives, A.; Ujaque, G.; Lledos, A. *Organometallics* **2007**, *26*, 4135.
- (15) Shvo, Y.; Czarkie, D.; Rahamim, Y.; Chodosh, D. F. *J. Am. Chem. Soc.* **1986**, *108*, 7400-7402.
- (16) Xu, Y.; Docherty, G. F.; Woodward, G.; Wills, M. *Tetrahedron: Asymmetry* **2006**, *17*, 2925.
- (17) Abdur-Rashid, K. **2007**, US 7,291,753.
- (18) Abdur-Rashid, K.; Guo, R.; Chen, X.; Jia, W. **2010**, US 7,777,083.
- (19) Chiral derivatives are now available from Strem Chemicals Inc. For details see: <http://www.strem.com/catalog/v/15-7301/> and <http://www.strem.com/catalog/v/15-7302/>.
- (20) Kuriyama, W.; Matsumoto, T.; Ino, Y.; Ogata, O. **2011**, WO 2011/048727.
- (21) At the time of preparation of this review, only the patent application as submitted in Japan was available.
- (22) Bertoli, M.; Choualeb, A.; Gusev, D. G.; Lough, A. J.; Major, Q.; Moore, B. *Dalton Transactions* **2011**, in press.
- (23) Bertoli, M.; Choualeb, A.; Lough, A. J.; Moore, B.; Spasyuk, D.; Gusev, D. G. *Organometallics* **2011**, *30*, 3479-3482.
- (24) Askevold, B.; Nieto, J. T.; Tussupbayev, S.; Diefenbach, M.; Herdtweck, E.; Holthausen, M. C.; Schneider, S. *Nature Chemistry* **2011**, *3*, 532-536.
- (25) Askevold, B.; Khushniyarov, M. M.; Herdtweck, E.; Meyer, K.; Schneider, S. *Angew. Chem. Int. Ed.* **2010**, *49*, 7566-7569.

Products Referenced in the Article

IRIDIUM (Compounds)

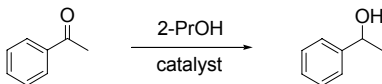
77-0500 Chlorodihydrido[bis(2-di-i-propylphosphino-ethyl)amine]iridium(III), min. 98% [791629-96-4]
 $\text{IrClH}_2(\text{C}_{16}\text{H}_{37}\text{NP}_2)_2$; FW: 535.10;
 white powd.
 Note: Sold under license from Kanata for research purposes only. Patent WO04096735; US 10/985,058.
 Technical Note: The product is predominately cis-dihydrido.



250mg
1g

Technical Note:

1. Catalyst used for transfer hydrogenation.



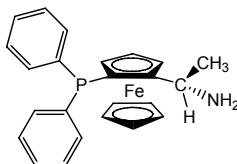
Reference:

1. *Organometallics*, **2006**, *25*, 4113.

Products Referenced in the Article

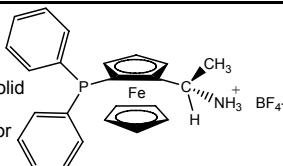
IRON (Compounds)

26-1425 **(R)-1-((S)-2-Diphenylphosphino)ferrocenylethylamine** **[607389-84-4]** 100mg
NEW→ **ferrocenylethylamine** 500mg
 $C_{24}H_{24}FeNP$; FW: 413.27;
 yellow solid



26-1426 **(S)-1-((R)-2-Diphenylphosphino)ferrocenylethylamine** 100mg
NEW→ **ferrocenylethylamine** 500mg
 $C_{24}H_{24}FeNP$; FW: 413.27; yellow solid

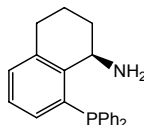
26-1704 **(R)-1-((S)-2-Diphenylphosphino)ferrocenylethylaminium tetrafluoroborate, min. 97%** 100mg
NEW→ **ferrocenylethylaminium tetrafluoroborate, min. 97%** 500mg
 $C_{24}H_{25}BF_4FeNP$; FW: 501.08; orange solid
air sensitive
 Note: Sold under license from Kanata for research purposes only.
 PCT/CA2009/001412.



26-1705 **(S)-1-((R)-2-Diphenylphosphino)ferrocenylethylaminium tetrafluoroborate, min. 97%** 100mg
NEW→ **ferrocenylethylaminium tetrafluoroborate, min. 97%** 500mg
 $C_{24}H_{25}BF_4FeNP$; FW: 501.08; orange solid
air sensitive
 Note: Sold under license from Kanata for research purposes only.
 PCT/CA2009/001412.

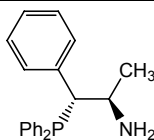
PHOSPHORUS (Compounds)

15-7143 **(R)-1-Amino-8-(diphenylphosphino)-1,2,3,4-tetrahydronaphthalene, min. 97%** 250mg
NEW→ **[960128-64-7]** 1g
 $C_{22}H_{22}NP$; FW: 331.39; white solid
air sensitive



15-7144 **(S)-1-Amino-8-(diphenylphosphino)-1,2,3,4-tetrahydronaphthalene, min. 97%** 250mg
NEW→ **[960128-64-7]** 1g
 $C_{22}H_{22}NP$; FW: 331.39; white solid
air sensitive

15-7107 **(1R,2R)-2-Amino-1-phenylpropyldiphenylphosphine, min. 97%** 100mg
NEW→ **[799297-44-2]** 500mg
 $C_{21}H_{22}NP$; FW: 319.38; white solid
air sensitive



Technical Note:

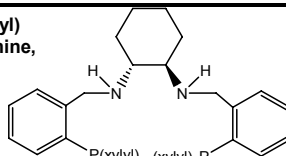
1. See 44-6022 (page 25).

15-7108 **(1S,2S)-2-Amino-1-phenylpropyldiphenylphosphine, min. 97%** 100mg
NEW→ **[341968-71-6]** 500mg
 $C_{21}H_{22}NP$; FW: 319.38; white solid
air sensitive

Technical Note:

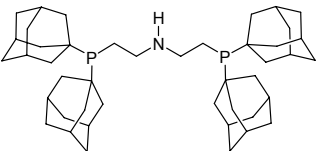
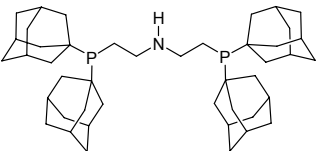
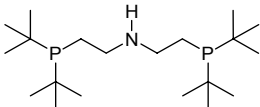
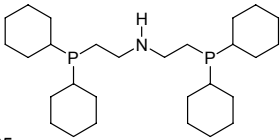
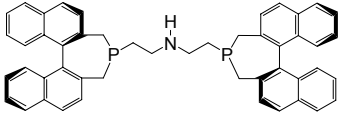
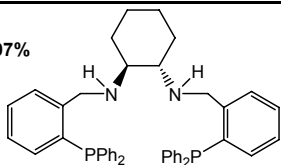
1. See 44-6023 (page 26).

15-7320 **(1R,2R)-N,N-Bis(2-[bis(3,5-dimethylphenyl)phosphino]benzyl)cyclohexane-1,2-diamine, min. 97%** 100mg
NEW→ **[1150113-66-8]** 500mg
 $C_{52}H_{60}N_2P_2$; FW: 774.99;
 yellow solid
air sensitive



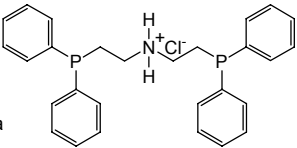
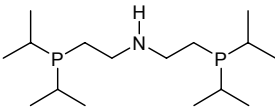
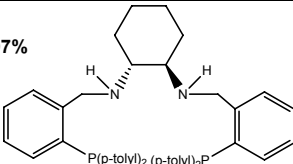
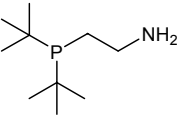
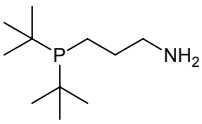
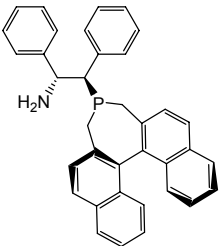
Products Referenced in the Article

PHOSPHORUS (Compounds)

15-7321 NEW→	(1S,2S)-N,N-Bis[2-[bis(3,5-dimethylphenyl)phosphino]benzyl]cyclohexane-1,2-diamine, min. 97% [1086138-36-4] $C_{52}H_{60}N_2P_2$; FW: 774.99; yellow solid <i>air sensitive</i>		100mg 500mg
15-7312 NEW→	Bis[2-(di-1-adamantyl-phosphino)ethyl]amine, min. 97% [1086138-36-4] $C_{44}H_{68}NP_2$; FW: 673.97; white solid <i>air sensitive</i> Note: Sold under license from Kanata for research purposes only. WO 2004096735.		250mg 1g
15-7308 NEW→	Bis[2-(di-<i>t</i>-butylphosphino)ethyl]amine, min. 97% [944710-34-3] $C_{20}H_{46}NP_2$; FW: 361.53; pale yellow to colorless liq. <i>air sensitive</i> Note: Sold under license from Kanata for research purposes only. WO 2004096735.		500mg 2g
15-7310 NEW→	Bis[2-(dicyclohexyl-phosphino)ethyl]amine, min. 97% [550373-32-5] $C_{28}H_{53}NP_2$; FW: 465.67; white solid <i>air sensitive</i> Note: Sold under license from Kanata for research purposes only. WO 2004096735.		250mg 1g
15-7301 NEW→	Bis[2-[(1<i>b</i>R)-3,5-dihydro-4H-dinaphtho[2,1-c:1',2'-e]phosphepin-4-yl]ethyl]amine, min. 97% [851870-89-8] $C_{48}H_{41}NP_2$; FW: 693.79; white solid <i>air sensitive</i> Note: Sold under license from Kanata for research purposes only. WO2004096735.		100mg 500mg
15-7302 NEW→	Bis[2-[(1<i>b</i>S)-3,5-dihydro-4H-dinaphtho[2,1-c:1',2'-e]phosphepin-4-yl]ethyl]amine, min. 97% $C_{48}H_{41}NP_2$; FW: 693.79; white solid <i>air sensitive</i> Note: Sold under license from Kanata for research purposes only. WO2004096735.		100mg 500mg
15-7325 NEW→	(1<i>R</i>,2<i>R</i>)-N,N-Bis[2-(diphenyl-phosphino)benzyl]cyclo-hexane-1,2-diamine, min. 97% [174758-63-5] $C_{44}H_{44}N_2P_2$; FW: 662.78; yellow solid <i>air sensitive</i>		250mg 1g
15-7326 NEW→	(1<i>S</i>,2<i>S</i>)-N,N-Bis[2-(diphenylphosphino)benzyl]cyclohexane-1,2-diamine, min. 97% [174677-83-9] $C_{44}H_{44}N_2P_2$; FW: 662.78; yellow solid <i>air sensitive</i>		250mg 1g

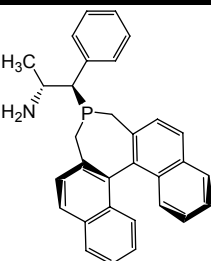
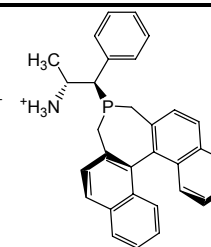
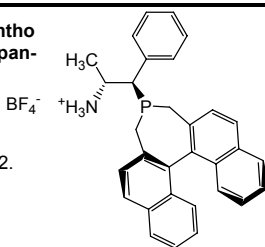
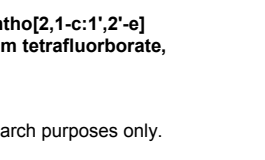
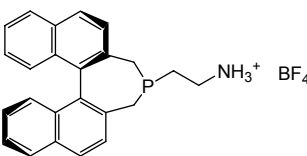
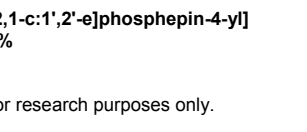
Products Referenced in the Article

PHOSPHORUS (Compounds)

15-7306 NEW→	<p>Bis[(2-diphenylphosphino)ethyl] ammonium chloride, min. 97% [66534-97-2] $C_{28}H_{30}ClNP_2$; FW: 477.95; white solid <i>air sensitive</i> Note: Sold under license from Kanata for research purposes only. WO2004096735.</p>		500mg 2g
15-7304 NEW→	<p>Bis[(2-di-i-propylphosphino)ethyl] amine, min. 97% [131890-26-1] $C_{16}H_{37}NP_2$; FW: 305.42; pale yellow to colorless liq. <i>air sensitive</i> Note: Sold under license from Kanata for research purposes only. WO2004096735.</p>		500mg 2g
15-7328 NEW→	<p>(1R,2R)-N,N-Bis[2-(di-p-tolylphosphino)benzyl]cyclohexane-1,2-diamine, min. 97% [1150113-65-7] $C_{48}H_{52}N_2P_2$; FW: 718.89; yellow solid <i>air sensitive</i></p>		250mg 1g
15-7329 NEW→	<p>(1S,2S)-N,N-Bis[2-(di-p-tolylphosphino)benzyl]cyclohexane-1,2-diamine, min. 97% $C_{48}H_{52}N_2P_2$; FW: 718.89; yellow solid <i>air sensitive</i></p>		250mg 1g
15-7128 NEW→ HAZ	<p>2-(Di-t-butylphosphino)ethylamine, min. 97% (10 wt% in THF) [1053658-84-6] $C_{10}H_{24}P$; FW: 189.28; pale yellow to colorless liq. <i>air sensitive</i></p>		5g 25g
15-7130 NEW→ HAZ	<p>3-(Di-t-butylphosphino)propylamine, min. 97% (10 wt% in THF) [1196147-72-4] $C_{11}H_{26}NP$; FW: 203.30; pale yellow to colorless liq. <i>air sensitive</i></p>		5g 25g
15-7137 NEW→	<p>(1R,2R)-2-[(4S,11bR)-3,5-dihydro-4H-dinaphtho[2,1-c:1',2'-e]phosphepin-4-yl]-1,2-diphenylethanamine, min. 97% $C_{36}H_{30}NP$; FW: 507.60; white solid <i>air sensitive</i> Note: Sold under license from Kanata for research purposes only. WO 2008148202.</p>		100mg 500mg
15-7136 NEW→	<p>(1S,2S)-2-[(4R,11bS)-3,5-dihydro-4H-dinaphtho[2,1-c:1',2'-e]phosphepin-4-yl]-1,2-diphenylethanamine, min. 97% [1092064-02-2] $C_{36}H_{30}NP$; FW: 507.60; white solid <i>air sensitive</i> Note: Sold under license from Kanata for research purposes only. WO 2008148202.</p>		100mg 500mg

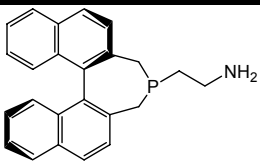
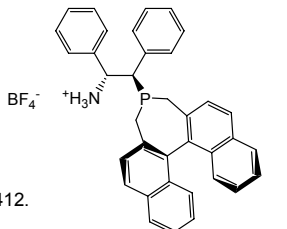
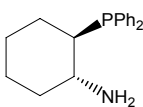
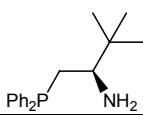
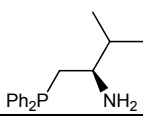
Products Referenced in the Article

PHOSPHORUS (Compounds)

15-7141 NEW→	(1R,2R)-2-[(4S,11bR)-3,5-dihydro-4H-dinaphtho[2,1-c:1',2'-e]phosphepin-4-yl]-1-phenylpropan-2-amine, min. 97% $C_{31}H_{28}NP$; FW: 445.53; white solid <i>air sensitive</i> Note: Sold under license from Kanata for research purposes only. WO 2008148202.		100mg 500mg
15-7140 NEW→	(1S,2S)-2-[(4R,11bS)-3,5-dihydro-4H-dinaphtho[2,1-c:1',2'-e]phosphepin-4-yl]-1-phenylpropan-2-amine, min. 97% $[1092064-04-4]$ $C_{31}H_{28}NP$; FW: 445.53; white solid <i>air sensitive</i> Note: Sold under license from Kanata for research purposes only. WO 2008148202.		100mg 500mg
15-7187 NEW→	(1R,2R)-2-[(4S,11bR)-3,5-dihydro-4H-dinaphtho[2,1-c:1',2'-e]phosphepin-4-yl]-1-phenylpropan-2-aminium tetrafluoroborate, min. 97% $C_{31}H_{29}BF_4NP$; FW: 533.35; white solid <i>air sensitive</i> Note: Sold under license from Kanata for research purposes only. PCT/CA2009/001412.		100mg 500mg
15-7186 NEW→	(1S,2S)-2-[(4R,11bS)-3,5-dihydro-4H-dinaphtho[2,1-c:1',2'-e]phosphepin-4-yl]-1-phenylpropan-2-aminium tetrafluoroborate, min. 97% $C_{31}H_{29}BF_4NP$; FW: 533.35; white solid <i>air sensitive</i> Note: Sold under license from Kanata for research purposes only. PCT/CA2009/001412.		100mg 500mg
15-7180 NEW→	2-[(11bR)-3,5-dihydro-4H-dinaphtho[2,1-c:1',2'-e]phosphepin-4-yl]ethaninium tetra-fluoroborate, min. 97% $C_{24}H_{23}BF_4NP$; FW: 443.22; white solid <i>air sensitive</i> Note: Sold under license from Kanata for research purposes only. PCT/CA2009/001412.		100mg 500mg
15-7181 NEW→	2-[(11bS)-3,5-dihydro-4H-dinaphtho[2,1-c:1',2'-e]phosphepin-4-yl]ethaninium tetrafluoroborate, min. 97% $C_{24}H_{23}BF_4NP$; FW: 443.22; white solid <i>air sensitive</i> Note: Sold under license from Kanata for research purposes only. PCT/CA2009/001412.		100mg 500mg

Products Referenced in the Article

PHOSPHORUS (Compounds)

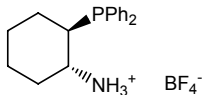
15-7132 NEW→	2-[(11bR)-3,5-dihydro-4H-di-naphtho [2,1-c:1',2'-e]phosphpepin-4-yl]ethyl] amine, min. 97% [1092064-00-0] $C_{24}H_{22}NP$; FW: 355.41; pale yellow solid <i>air sensitive</i> Note: Sold under license from Kanata for research purposes only. WO2008148202.		100mg 500mg
15-7134 NEW→	2-[(11bS)-3,5-dihydro-4H-dinaphtho[2,1-c:1',2'-e]phosphpepin-4-yl] ethyl]amine, min. 97% [1053659-64-5] $C_{24}H_{22}NP$; FW: 355.41; pale yellow solid <i>air sensitive</i> Note: Sold under license from Kanata for research purposes only. WO2008148202.		100mg 500mg
15-7184 NEW→	(1R,2R)-2-((4S,11bR)-3H-dinaphtho [2,1-c:1',2'-e]phosphpepin-4(5H)-yl)-1,2-diphenylethanaminium tetrafluoroborate, min. 97% $C_{36}H_{31}BF_4NP$; FW: 595.42; white solid <i>air sensitive</i> Note: Sold under license from Kanata for research purposes only. PCT/CA2009/001412.		100mg 500mg
15-7183 NEW→	(1S,2S)-2-((4R,11bS)-3H-dinaphtho[2,1-c:1',2'-e]phosphpepin-4(5H)-yl)-1,2-diphenylethanaminium tetrafluoroborate, min. 97% $C_{36}H_{31}BF_4NP$; FW: 595.42; white solid <i>air sensitive</i> Note: Sold under license from Kanata for research purposes only. PCT/CA2009/001412.		100mg 500mg
15-7153 NEW→	(1R,2R)-2-(Diphenylphosphino)-1-amino-cyclohexane, min. 97% [452304-59-5] $C_{18}H_{22}NP$; FW: 283.35; white solid <i>air sensitive</i>		100mg 500mg
15-7154 NEW→	(1S,2S)-2-(Diphenylphosphino)-1-aminocyclohexane, min. 97% [452304-63-1] $C_{18}H_{22}NP$; FW: 283.35; white solid <i>air sensitive</i>		100mg 500mg
15-7150 NEW→	(R)-1-(Diphenylphosphino)-2-amino-3,3-dimethylbutane, min. 97% $C_{18}H_{24}NP$; FW: 285.36; colorless liq. <i>air sensitive</i>		100mg 500mg
15-7151 NEW→	(S)-1-(Diphenylphosphino)-2-amino-3,3-dimethylbutane, min. 97% [286454-86-2] $C_{18}H_{24}NP$; FW: 285.36; colorless oil <i>air sensitive</i>		100mg 500mg
15-7146 NEW→	(R)-1-(Diphenylphosphino)-2-amino-3-methylbutane, min. 97% $C_{17}H_{22}NP$; FW: 271.34; colorless oil <i>air sensitive</i>		100mg 500mg

Products Referenced in the Article

PHOSPHORUS (Compounds)

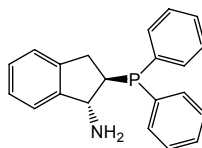
15-7147 (S)-1-(Diphenylphosphino)-2-amino-3-methylbutane, min. 97% 100mg
NEW→ [146476-37-1] 500mg
 $C_{17}H_{22}NP$; FW: 271.34; colorless oil
air sensitive

15-7195 (1R,2R)-2-(Diphenylphosphino)cyclohexanaminium tetrafluoroborate, min. 97% 100mg
NEW→ $C_{18}H_{23}BF_4NP$; FW: 371.16; white to pale yellow solid 500mg
air sensitive
 Note: Sold under license from Kanata for research purposes only. PCT/CA2009/001412.



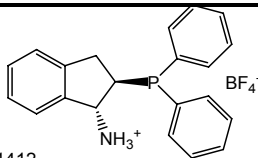
15-7196 (1S,2S)-2-(Diphenylphosphino)cyclohexanaminium tetrafluoroborate, min. 97% 100mg
NEW→ $C_{18}H_{23}BF_4NP$; FW: 371.16; white to pale yellow solid 500mg
air sensitive
 Note: Sold under license from Kanata for research purposes only. PCT/CA2009/001412.

15-7110 (1R,2R)-2-(Diphenylphosphino)-2,3-dihydro-1H-inden-1-amine, min. 97% 1g
NEW→ (10wt% in THF) [1091606-70-0] 5g
 $C_{21}H_{20}NP$; FW: 317.36; colorless to pale yellow liq.
air sensitive
 Note: Sold under license from Kanata for research purposes only. O2008148202.



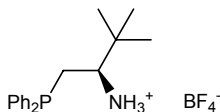
15-7111 (1S,2S)-2-(Diphenylphosphino)-2,3-dihydro-1H-inden-1-amine, min. 97% (10wt% in THF) [1091606-69-7] 1g
NEW→ $C_{21}H_{20}NP$; FW: 317.36; colorless to pale yellow liq. 5g
air sensitive
 Note: Sold under license from Kanata for research purposes only. WO2008148202.

15-7162 (1R,2R)-2-(Diphenylphosphino)-2,3-dihydro-1H-inden-1-aminium tetrafluoroborate, min. 97% 100mg
NEW→ $C_{21}H_{21}BF_4NP$; FW: 405.17; white solid 500mg
air sensitive
 Note: Sold under license from Kanata for research purposes only. PCT/CA2009/001412.



15-7163 (1S,2S)-2-(Diphenylphosphino)-2,3-dihydro-1H-inden-1-aminium tetrafluoroborate, min. 97% 100mg
NEW→ $C_{21}H_{21}BF_4NP$; FW: 405.17; white solid 500mg
air sensitive
 Note: Sold under license from Kanata for research purposes only. PCT/CA2009/001412.

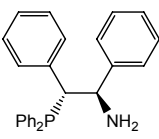
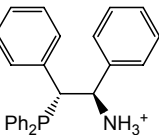
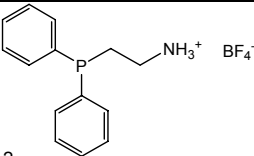
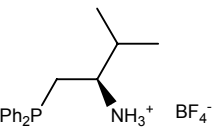
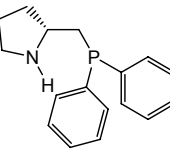
15-7193 (R)-1-(Diphenylphosphino)-3,3-dimethylbutan-2-aminium tetrafluoroborate, min. 97% 100mg
NEW→ $C_{18}H_{26}BF_4NP$; FW: 373.18; white solid 500mg
air sensitive
 Note: Sold under license from Kanata for research purposes only. PCT/CA2009/001412.



15-7194 (S)-1-(Diphenylphosphino)-3,3-dimethylbutan-2-aminium tetrafluoroborate, min. 97% 100mg
NEW→ $C_{18}H_{26}BF_4NP$; FW: 373.18; white solid 500mg
air sensitive
 Note: Sold under license from Kanata for research purposes only. PCT/CA2009/001412.

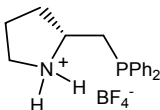
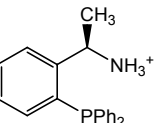
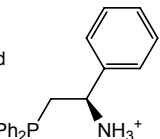
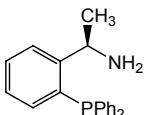

Products Referenced in the Article

PHOSPHORUS (Compounds)

15-7102 NEW→	(1R,2R)-2-(Diphenylphosphino)-1,2-diphenylethylamine, min. 97% <i>[1091606-68-6]</i> $C_{26}H_{24}NP$; FW: 318.45; white solid <i>air sensitive</i> Note: Sold under license from Kanata for research purposes only. WO2008148202.		100mg 500mg
15-7103 NEW→	(1S,2S)-2-(Diphenylphosphino)-1,2-diphenylethylamine, min. 97% <i>[1091606-67-5]</i> $C_{26}H_{24}NP$; FW: 318.45; white solid <i>air sensitive</i> Note: Sold under license from Kanata for research purposes only. WO2008148202.		100mg 500mg
15-7156 NEW→	(1R,2R)-2-(Diphenylphosphino)-1,2-diphenylethylaminium tetrafluoroborate, min. 97% $C_{26}H_{25}BF_4NP$; FW: 469.26; white solid <i>air sensitive</i> Note: Sold under license from Kanata for research purposes only. PCT/CA2009/001412.		100mg 500mg
15-7157 NEW→	(1S,2S)-2-(Diphenylphosphino)-1,2-diphenylethylaminium tetrafluoroborate, min. 97% $C_{26}H_{25}BF_4NP$; FW: 469.26; white solid <i>air sensitive</i> Note: Sold under license from Kanata for research purposes only. PCT/CA2009/001412.		100mg 500mg
15-7174 NEW→	2-(Diphenylphosphino)ethanaminium tetrafluoroborate, min. 97% $C_{14}H_{17}BF_4NP$; FW: 317.06; white to beige solid <i>air sensitive</i> Note: Sold under license from Kanata for research purposes only. PCT/CA2009/001412.		500mg 2g
15-7191 NEW→	(R)-1-(Diphenylphosphino)-3-methylbutan-2-aminium tetrafluoroborate, min. 97% $C_{17}H_{23}BF_4NP$; FW: 359.15; white to pale yellow solid <i>air sensitive</i> Note: Sold under license from Kanata for research purposes only. PCT/CA2009/001412.		100mg 500mg
15-7192 NEW→	(S)-1-(Diphenylphosphino)-3-methylbutan-2-aminium tetrafluoroborate, min. 97% $C_{17}H_{23}BF_4NP$; FW: 359.15; white to pale yellow solid <i>air sensitive</i> Note: Sold under license from Kanata for research purposes only. PCT/CA2009/001412.		100mg 500mg
15-7115 NEW→	(R)-2-[(Diphenylphosphino)methyl]pyrrolidine, min. 97% [428514-91-4] $C_{17}H_{20}NP$; FW: 269.32; colorless oil <i>air sensitive</i>		250mg 1g

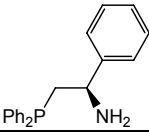
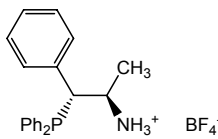
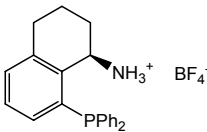
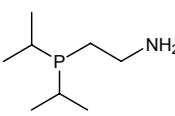
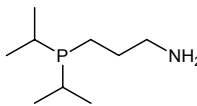
Products Referenced in the Article

PHOSPHORUS (Compounds)

15-7116 NEW→	(S)-2-[(Diphenylphosphino)methyl]pyrrolidine, min. 97% [60261-46-3] $C_{17}H_{20}NP$; FW: 269.32; colorless oil <i>air sensitive</i>		250mg 1g
15-7165 NEW→	(R)-2-[(Diphenylphosphino)methyl]pyrrolidinium tetrafluoroborate, min. 97% $C_{17}H_{21}BF_4NP$; FW: 357.13; white solid <i>air sensitive</i> Note: Sold under license from Kanata for research purposes only. PCT/CA2009/001412.		100mg 500mg
15-7166 NEW→	(S)-2-[(Diphenylphosphino)methyl]pyrrolidinium tetrafluoroborate, min. 97% $C_{17}H_{21}BF_4NP$; FW: 357.13; white solid <i>air sensitive</i> Note: Sold under license from Kanata for research purposes only. PCT/CA2009/001412.		100mg 500mg
15-7168 NEW→	(R)-1-[2-(Diphenylphosphino)phenyl]ethanaminium tetrafluoroborate, min. 97% $C_{20}H_{21}BF_4NP$; FW: 393.16; white solid <i>air sensitive</i> Note: Sold under license from Kanata for research purposes only. PCT/CA2009/001412.		100mg 500mg
15-7169 NEW→	(S)-1-[2-(Diphenylphosphino)phenyl]ethanaminium tetrafluoroborate, min. 97% $C_{20}H_{21}BF_4NP$; FW: 393.16; white solid <i>air sensitive</i> Note: Sold under license from Kanata for research purposes only. PCT/CA2009/001412.		100mg 500mg
15-7171 NEW→	(R)-2-(Diphenylphosphino)-1-phenylethanaminium tetrafluoroborate, min. 97% $C_{20}H_{21}BF_4NP$; FW: 393.16; white to pale yellow solid <i>air sensitive</i> Note: Sold under license from Kanata for research purposes only. PCT/CA2009/001412.		100mg 500mg
15-7172 NEW→	(S)-2-(Diphenylphosphino)-1-phenylethanaminium tetrafluoroborate, min. 97% $C_{20}H_{21}BF_4NP$; FW: 393.16; white to pale yellow solid <i>air sensitive</i> Note: Sold under license from Kanata for research purposes only. PCT/CA2009/001412.		100mg 500mg
15-7118 NEW→	(R)-1-[2-(Diphenylphosphino)phenyl]ethylamine, min. 97% [192057-60-6] $C_{20}H_{20}NP$; FW: 305.35; white solid <i>air sensitive</i>		250mg 1g
15-7119 NEW→	(S)-1-[2-(Diphenylphosphino)phenyl]ethylamine, min. 97% [913196-43-7] $C_{20}H_{20}NP$; FW: 305.35; white solid <i>air sensitive</i>		250mg 1g

Products Referenced in the Article

PHOSPHORUS (Compounds)

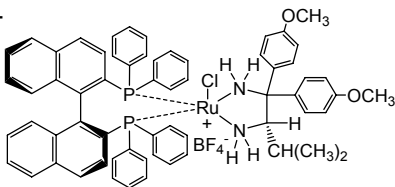
15-7121 NEW→	(R)-2-(Diphenylphosphino)-1-phenylethylamine, min. 97% [141096-35-7] $C_{20}H_{20}NP$; FW: 381.45; white solid <i>air sensitive</i>		250mg 1g
15-7122 NEW→	(S)-2-(Diphenylphosphino)-1-phenylethylamine, min. 97% [1103533-85-2] $C_{20}H_{20}NP$; FW: 381.45; white solid <i>air sensitive</i>		250mg 1g
15-7159 NEW→	(1R,2R)-1-(Diphenylphosphino)-1-phenylpropan-2-aminium tetrafluoroborate, min. 97% $C_{21}H_{23}BF_4NP$; FW: 407.19; white solid <i>air sensitive</i> Note: Sold under license from Kanata for research purposes only. PCT/CA2009/001412.		100mg 500mg
15-7160 NEW→	(1S,2S)-1-(Diphenylphosphino)-1-phenylpropan-2-aminium tetrafluoroborate, min. 97% $C_{21}H_{23}BF_4NP$; FW: 407.19; white solid <i>air sensitive</i> Note: Sold under license from Kanata for research purposes only. PCT/CA2009/001412.		100mg 500mg
15-7189 NEW→	(R)-8-(Diphenylphosphino)-1,2,3,4-tetrahydronaphthalen-1-aminium tetrafluoroborate, min. 97% $C_{22}H_{23}BF_4NP$; FW: 419.20; white solid <i>air sensitive</i> Note: Sold under license from Kanata for research purposes only. PCT/CA2009/001412.		100mg 500mg
15-7190 NEW→	(S)-8-(Diphenylphosphino)-1,2,3,4-tetrahydronaphthalen-1-aminium tetrafluoroborate, min. 97% $C_{22}H_{23}BF_4NP$; FW: 419.20; white solid <i>air sensitive</i> Note: Sold under license from Kanata for research purposes only. PCT/CA2009/001412.		100mg 500mg
15-1812 NEW→ HAZ	2-(Di-i-propylphosphino)ethylamine, min. 97% (10 wt% in THF) [1053657-14-9] $(C_3H_7)_2PCH_2CH_2NH_2$; FW: 161.23; pale yellow to colorless liq. <i>air sensitive</i>		5g 25g
15-1831 NEW→ HAZ	3-(Di-i-propylphosphino)propylamine, min. 97% (10 wt% in THF) [1196147-69-9] $(C_3H_7)_2PCH_2CH_2CH_2NH_2$; FW: 175.25; colorless to pale yellow liq. <i>air sensitive</i>		5g 25g

Products Referenced in the Article

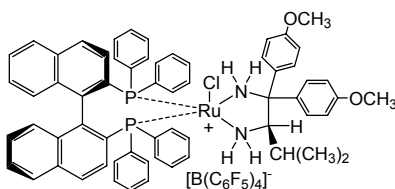
RUTHENIUM (Compounds)

44-0136 **NEW→** **Chloro[(R)-(-)-2,2'-bis(diphenylphosphino)-1,1'-binaphthyl] [(R)-1,1'-bis(4-methoxyphenyl)-3-methylbutane-1,2-diamine]ruthenium(II) tetrafluoroborate, min. 97%** 100mg
500mg
 $C_{63}H_{58}BClF_4N_2O_2P_2Ru$; FW: 1160.42; orange pwdr.
Note: Sold under license from Kanata for research purposes only.
PCT/CA2008/001905.

44-6063 **NEW→** **Chloro[(S)-(-)-2,2'-bis(diphenylphosphino)-1,1'-binaphthyl] [(S)-1,1-bis(4-methoxyphenyl)-3-methylbutane-1,2-diamine] ruthenium(II) tetrafluoroborate, min. 97% [1150112-86-9]** 100mg
500mg
 $C_{63}H_{58}BClF_4N_2O_2P_2Ru$; FW: 1160.40; orange-red solid
Note: Sold under license from Kanata for research purposes only. WO 2009055912.



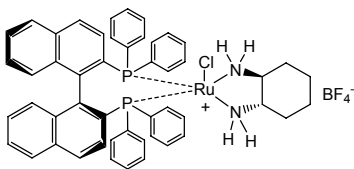
44-6065 **NEW→** **Chloro[(R)-(-)-2,2'-bis(diphenylphosphino)-1,1'-binaphthyl] [(R)-1,1-bis(4-methoxyphenyl)-3-methylbutane-1,2-diamine] ruthenium(II) tetrakis(pentafluorophenyl)borate, min. 97%** 100mg
500mg
 $C_{87}H_{58}BClF_{20}N_2O_2P_2Ru$; FW: 1752.70; orange-red solid
Note: Sold under license from Kanata for research purposes only. WO 2009055912.



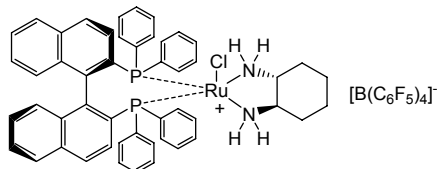
44-6066 **NEW→** **Chloro[(S)-(-)-2,2'-bis(diphenylphosphino)-1,1'-binaphthyl] [(S)-1,1-bis(4-methoxyphenyl)-3-methylbutane-1,2-diamine]ruthenium(II) tetrakis(pentafluorophenyl)borate, min. 97% [1150112-87-0]** 100mg
500mg
 $C_{87}H_{58}BClF_{20}N_2O_2P_2Ru$; FW: 1752.70; orange-red solid
Note: Sold under license from Kanata for research purposes only.
WO 2009055912.

44-0134 **NEW→** **Chloro[(R)-2,2'-bis(diphenylphosphino)-1,1'-binaphthyl] [(1R,2R)-cyclohexane-1,2-diamine]ruthenium(II) tetrafluoroborate, min. 97%** 100mg
500mg
 $C_{50}H_{46}BClF_4N_2P_2Ru$; FW: 960.19; orange solid
Note: Sold under license from Kanata for research purposes only.
PCT/CA2008/001905.

44-6053 **NEW→** **Chloro[(S)-2,2'-bis(diphenylphosphino)-1,1'-binaphthyl] [(1S,2S)-cyclohexane-1,2-diamine]ruthenium(II) tetrafluoroborate, min. 97%** 100mg
500mg
 $C_{50}H_{46}BClF_4N_2P_2Ru$; FW: 960.19; yellow solid
air sensitive
Note: Sold under license from Kanata for research purposes only. WO 2009055912.



44-6054 **NEW→** **Chloro[(R)-2,2'-bis(diphenylphosphino)-1,1'-binaphthyl] [(1R,2R)-cyclohexane-1,2-diamine]ruthenium(II) tetrakis(pentafluorophenyl)borate, min. 97% [1150112-55-2]** 100mg
500mg
 $C_{74}H_{46}BClF_{20}N_2P_2Ru$; FW: 1552.42; yellow solid
Note: Sold under license from Kanata for research purposes only.
WO 2009055912.

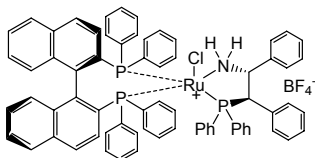


Products Referenced in the Article

RUTHENIUM (Compounds)

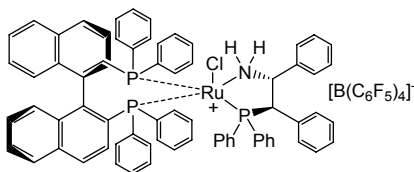
44-6055 **NEW→** **Chloro[(S)-2,2'-bis(diphenylphosphino)-1,1'-binaphthyl]** 100mg
500mg
[(1S,2S)-cyclohexane-1,2-diamine]ruthenium(II)
tetrakis(pentafluorophenyl)borate, min. 97%
 $C_{74}H_{46}BClF_{20}N_2P_2Ru$; FW: 1552.42; yellow solid
 Note: Sold under license from Kanata for research purposes only.
 WO 2009055912.

44-6057 **NEW→** **Chloro[(R)-2,2'-bis(diphenylphosphino)-1,1'-binaphthyl]** 100mg
500mg
[(1R,2R)-2-(diphenylphosphino)-1,2-diphenylethanamine]
ruthenium(II) tetrafluoroborate, min. 97% [1150112-54-1]
 $C_{70}H_{56}BClF_4NP_3Ru$; FW: 1227.45; orange to brown solid
 Note: Sold under license from Kanata for research purposes only. WO 2009055912.

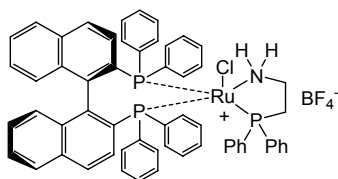


44-6058 **NEW→** **Chloro[(S)-2,2'-bis(diphenylphosphino)-1,1'-binaphthyl]** 100mg
500mg
[(1S,2S)-2-(diphenylphosphino)-1,2-diphenylethanamine]
ruthenium(II) tetrafluoroborate, min. 97% [1150316-02-1]
 $C_{70}H_{56}BClF_4NP_3Ru$; FW: 1227.45; orange to brown solid
 Note: Sold under license from Kanata for research purposes only.
 WO 2009055912.

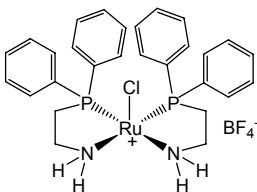
44-6070 **NEW→** **Chloro[(R)-2,2'-bis(diphenylphosphino)-1,1'-binaphthyl]** 100mg
500mg
[(1R,2R)-2-(diphenylphosphino)-1,2-diphenylethanamine]
ruthenium(II), tetrakis(pentafluorophenyl)borate, min. 97% [1150112-53-0]
 $C_{94}H_{56}BClF_{20}NP_3Ru$; FW: 1819.68; orange to brown solid
 Note: Sold under license from Kanata for research purposes only.
 WO 2009055912.



44-6056 **NEW→** **Chloro[(R)-2,2'-bis(diphenylphosphino)-1,1'-binaphthyl]** 100mg
500mg
[2-(diphenylphosphino)ethanamine]
ruthenium(II) tetrafluoroborate, min. 97% [1150112-44-9]
 $C_{58}H_{48}BClF_4NP_3Ru$; FW: 1075.26; yellow solid
 Note: Sold under license from Kanata for research purposes only. WO 2009055912.



44-6060 **NEW→** **Chlorobis[2-(diphenylphosphino)ethanamine]** 100mg
500mg
ruthenium(II) tetrafluoroborate, min. 97% [1150112-46-1]
 $C_{28}H_{32}BClF_4N_2P_2Ru$; FW: 681.84; yellow solid
 Note: Sold under license from Kanata for research purposes only.
 WO 2009055912.



Products Referenced in the Article

RUTHENIUM (Compounds)

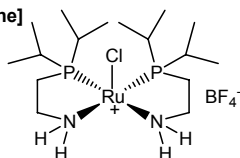
44-6068

NEW→

Chlorobis[2-(di-*i*-propylphosphino)ethanamine] ruthenium(II) tetrafluoroborate, min. 97%

$C_{16}H_{40}ClBF_4N_2P_2Ru$; FW: 546.14; red-brown solid

Note: Sold under license from Kanata for research purposes only. WO 2009055912.

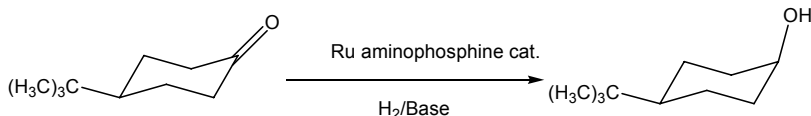


100mg

500mg

Technical Note:

1. Excellent catalyst for the hydrogenation of ketones and imines.



Reference:

1. *J. Chem. Soc., Dalton Trans.*, **2009**, 8301.

98% d.e.

44-0232

NEW→

Dichloro[(*R*)-2,2'-bis[bis(4-methylphenyl)]-1,1'-binaphthyl] [(1*R*,2*R*)-2-amino-1-phenylpropyldiphenylphosphine]ruthenium(II), min. 97%

$C_{60}H_{62}Cl_2NP_3Ru$; FW: 1170.13; orange solid

air sensitive

Note: Sold under license from Kanata for research purposes only.

US Patents 7,579,295 and 7,317,131.

Technical Note:

1. Precursor to cationic hydrogenation catalyst for synthesis of chiral alcohols from ketones.

Reference:

1. WO2009055912 A1.

100mg

500mg

44-6050

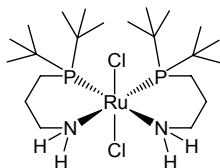
NEW→

Dichlorobis[3-(di-*t*-butylphosphino)propylamine]ruthenium(II), min. 97%

[1196147-60-0]

$C_{22}H_{52}Cl_2N_2P_2Ru$; FW: 578.58; brown solid

Note: Sold under license from Kanata for research purposes only. US 7317131 and US 7579295.



250mg

1g

Technical Note:

1. See 44-6068 (page 24).

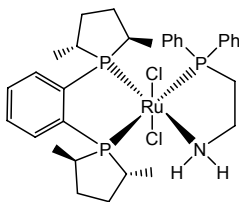
44-6015

NEW→

Dichloro{1,2-bis[(2*R*,5*R*)-2,5-dimethylphospholanobenzene]} [2-diphenylphosphino)ethylamine] ruthenium(II), min. 97%

$C_{32}H_{44}Cl_2NP_3Ru$; FW: 707.60; yellow solid

Note: Sold under license from Kanata for research purposes only.



100mg

500mg

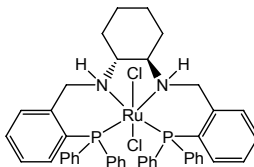
Products Referenced in the Article

RUTHENIUM (Compounds)

44-6018

NEW→

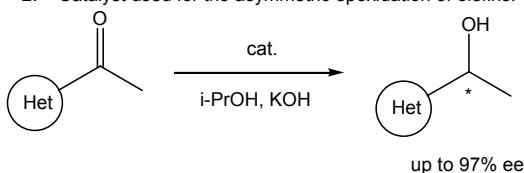
Dichloro{[(1R,2R)-N,N-bis[2-(diphenylphosphino)benzyl]cyclohexane-1,2-diamine}ruthenium(II), min. 97% [429678-11-5]
C₄₄H₄₄Cl₂N₂P₂Ru; FW: 834.76; orange solid



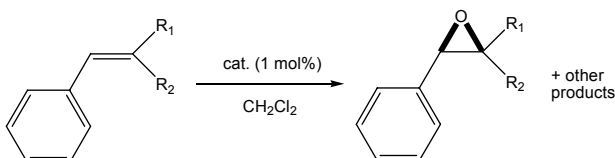
100mg
500mg

Technical Notes:

1. Catalyst used for the highly-enantioselective synthesis of heteroaromatic alcohols.
2. Catalyst used for the asymmetric epoxidation of olefins.



Tech. Note (1)
Ref. (1)



Tech. Note (2)
Ref. (2)

References:

1. *Synthesis*, **2009**, 2413.
2. *Organometallics*, **2000**, 19(20), 4117.

44-6019

NEW→

Dichloro{[(1S,2S)-N,N-bis[2-(diphenylphosphino)benzyl]cyclohexane-1,2-diamine}ruthenium(II), min. 97% [302924-37-4]
C₄₄H₄₄Cl₂N₂P₂Ru; FW: 834.76; orange solid

100mg
500mg

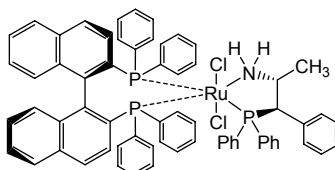
Technical Note:

1. See 44-6068 (page 24).

44-6022

NEW→

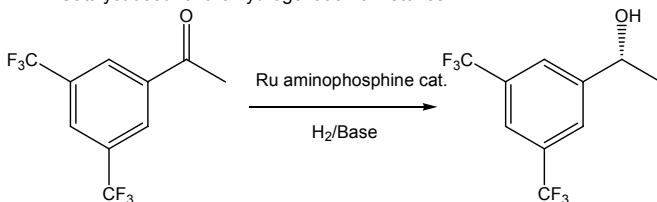
Dichloro{(R)-bis(diphenylphosphino)-1,1'-binaphthyl}[(1R,2R)-2-amino-1-phenylpropyldiphenylphosphine]ruthenium(II), min. 97%
C₆₆H₅₇Cl₂NP₃Ru; FW: 1129.06; yellow solid
Note: Sold under license from Kanata for research purposes only. US 7317131 and US 7579295.



100mg
500mg

Technical Note:

1. Catalyst used for the hydrogenation of ketones.



Tech. Note (1)
Ref. (1)

References:

1. *J. Am. Chem. Soc.*, **2005**, 127, 516.

95% e.e.

Products Referenced in the Article

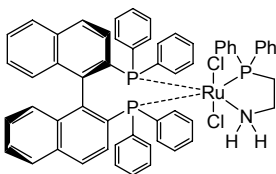
RUTHENIUM (Compounds)

- 44-6023** **Dichloro[(R)-bis(diphenylphosphino)-1,1-binaphthyl][1S,2S)-2-amino-1-phenylpropyldiphenylphosphine]ruthenium(II), min. 97%** 100mg
NEW→ 500mg
 $C_{66}H_{57}Cl_2NP_3Ru$; FW: 1129.06; yellow solid
 Note: Sold under license from Kanata for research purposes only.
 US 7317131 and US 7579295.

Technical Note:

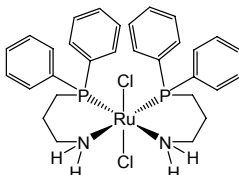
- See 44-6022 (page 25).

- 44-6025** **Dichloro[(R)-bis(diphenylphosphino)-1,1-binaphthyl][2-(diphenylphosphino)ethylamine]ruthenium(II), min. 97% [1097731-98-0]** 100mg
NEW→ 500mg
 $C_{58}H_{48}Cl_2NP_3Ru$; FW: 1023.91; yellow solid
 Note: Sold under license from Kanata for research purposes only. US 7317131 and US 7579295.

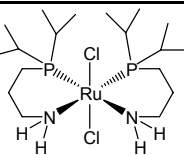


- 44-6026** **Dichloro[(S)-bis(diphenylphosphino)-1,1-binaphthyl][2-(diphenylphosphino)ethylamine]ruthenium(II), min. 97%** 100mg
NEW→ 500mg
 $C_{58}H_{48}Cl_2NP_3Ru$; FW: 1023.91; yellow solid
 Note: Sold under license from Kanata for research purposes only.
 US 7317131 and US 7579295.

- 44-6040** **Dichlorobis[3-(diphenylphosphino)propylamine]ruthenium(II), min. 97% [1196467-26-1]** 250mg
NEW→ 1g
 $C_{30}H_{36}Cl_2N_2P_2Ru$; FW: 658.54; yellow-brown solid
 Note: Sold under license from Kanata for research purposes only. US 7317131 and US 7579295.



- 44-6043** **Dichlorobis[3-(di-i-propylphosphino)propylamine]ruthenium(II), min. 97% [1196147-57-5]** 250mg
NEW→ 1g
 $C_{18}H_{44}Cl_2N_2P_2Ru$; FW: 522.48; yellow-orange solid
 Note: Sold under license from Kanata for research purposes only. US 7317131 and US 7579295.



Technical Note:

- See 44-6068 (page 24).

Nanosprings™: A Versatile Nanomaterial Platform

Timothy C. Cantrell, Giancarlo Corti, David C. Hyatt, David N. McIlroy,
M. Grant Norton, Tejasvi Prakash and Matthew Yahvah

GoNano Technologies, Moscow, ID 83843, USA

1. Introduction

Nanosprings™ are a unique high surface area one-dimensional nanomaterial. Although Nanosprings can be formed from a number of different materials, the most versatile and commercially important forms are those made of amorphous silica [1], [2]. Silica Nanosprings offer several advantages over other one-dimensional nanostructures, such as carbon nanotubes and silicon nanowires:

- The silica surface is compatible with the wide variety of glass modification reactions, which have been developed and optimized over decades [3], [4]. However, in the majority of cases the Nanospring surface is actually more straightforward to coat or modify than bulk silica glass.
- The hydrophilicity of the silica Nanospring surface facilitates the formation of metal nanoparticles and nanocrystalline metal oxides using multiple techniques, including wet impregnation, spray pyrolysis, atomic layer deposition (ALD), and chemical vapor deposition (CVD).
- The material has a surface area $> 350\text{m}^2/\text{g}$, which is 100% accessible with zero closed porosity, as determined by the absence of hysteresis in Brunauer, Emmett, Teller (BET) measurements.
- Nanosprings are thermally stable $>1000^\circ\text{C}$ in air and chemically durable.
- Nanosprings are produced with a scalable, catalyst-mediated growth mechanism that leaves the Nanosprings strongly attached to the substrate.
- The processing method is photolithography compatible, allowing, for example, the formation of compact arrays of sensors on a single device.
- The mild growth conditions of 350°C and atmospheric pressure allows the material to be coated on a wide variety of substrates including, aluminum, polyimide, glass, silicon, stainless steel, carbon.
- The processing method allows Nanosprings to be formed in and on three-dimensional structures such as micromachined silicon, cordierite monoliths, fiberglass cloth, carbon fibers, micron-sized silica beads, and particles of activated carbon.

Functionalized silica Nanosprings [1], [2], [5-12], are an ideal nanomaterial platform for a broad range of applications, including:

- Continuous flow chemistry
- Chemical and biological sensors
- Catalyst supports, including photocatalysis
- Molecular hydrogen storage

2. Synthesis and Growth Mechanism

Silica Nanosprings are synthesized in a standard atmospheric CVD process at temperatures as low as 350°C . The Nanosprings grow via a modified vapor-liquid-solid (VLS) mechanism, which is facilitated by the presence of gold nanoparticle catalysts at the tips [13]. The Nanosprings form as randomly oriented mats on a substrate as shown in figure 1. The process is compatible with a wide range of substrates; the only requirement is that the substrate must withstand the 350°C growth temperature. Typical mat thicknesses can be controlled within the range 3 to $300\text{ }\mu\text{m}$. A $100\text{ }\mu\text{m}$ mat requires a growth time of approximately 15 minutes. An individual Nanospring is shown in the transmission electron microscope (TEM) image in figure 2. The Nanosprings are amorphous, as evidenced by the absence of sharp diffraction patterns, note the gold nanoparticle catalyst at the tip of the Nanospring.

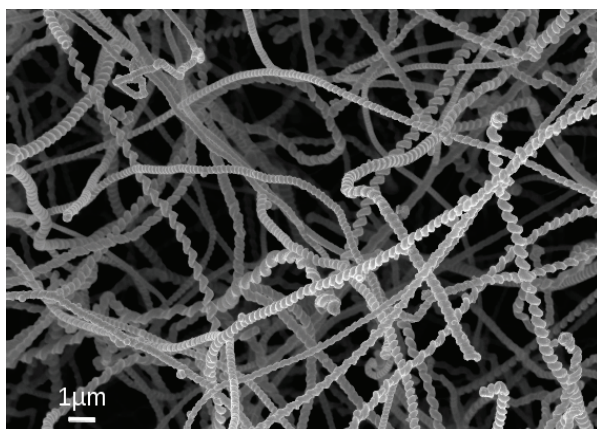


Figure 1

SEM image of a silica Nanospring mat

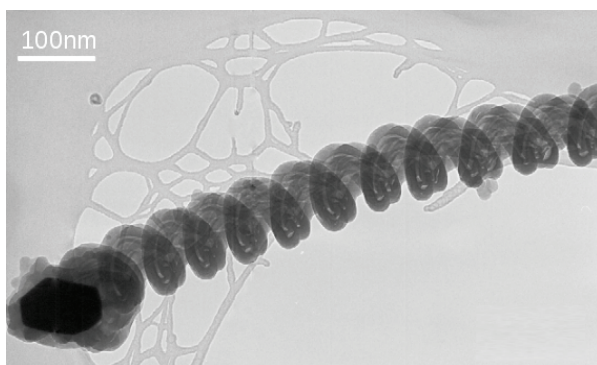


Figure 2

A TEM image of a single silica Nanospring

Standard photolithography techniques can be employed to form silica Nanospring mats in specific, well-defined locations, as shown in figure 3. Patterning is an important approach for fabricating continuous flow reactors and sensor applications.

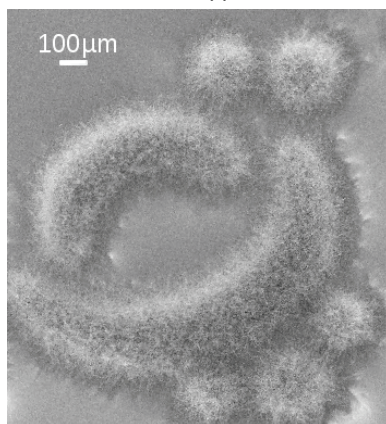


Figure 3

A patterned mat of silica Nanosprings

3. Coating and Functionalization

Vapor-phase coating techniques, such as atomic layer deposition (ALD) and CVD, as well as liquid-phase processes (impregnation and spray pyrolysis) can be used to coat Nanosprings. Figure 4 shows silica Nanosprings coated by ALD with zinc oxide. Suitable ALD precursors are diethyl zinc and titanium tetrachloride, respectively [14], [15]. The nanocrystalline TiO_2 forms in the anatase phase and 500 ALD cycles produce a crystallite size of 40 nm.

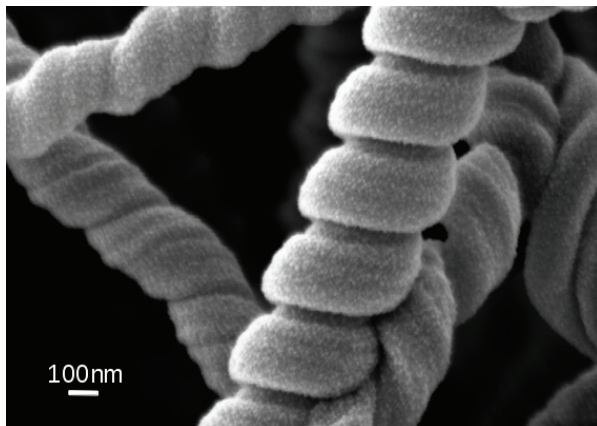


Figure 4 SEM picture of a zinc oxide coated Nanospring

The Nanosprings allow for a conformal and controlled coating of numerous metal oxides by ALD and more recently, semiconducting gallium nitride has been successfully deposited by ALD (private communication, D. McIlroy, U. of Idaho). Gallium nitride is of particular interest for sensor applications [16] and forming it directly onto the Nanosprings provides an excellent support structure with a high amount of accessible surface area. In addition to metal oxides and nitrides, metal nanoparticles can also be deposited on the Nanospring surface. Wet impregnation and spray pyrolysis are common deposition techniques for metal nanoparticles. Figure 5 shows a TEM image of silica Nanosprings coated with palladium nanoparticles. The palladium was deposited using a solution of palladium acetylacetonate (5.94 mg/ml in benzene, 10.4 μL) to coat $1 \times 1 \text{ cm}^2$ samples of Nanosprings. Upon evaporative drying, it was placed in an oven at 500°C for 15 minutes and reduced with 40sccm H_2 and 15sccm N_2 . This procedure will deposit approximately 0.4wt% palladium.

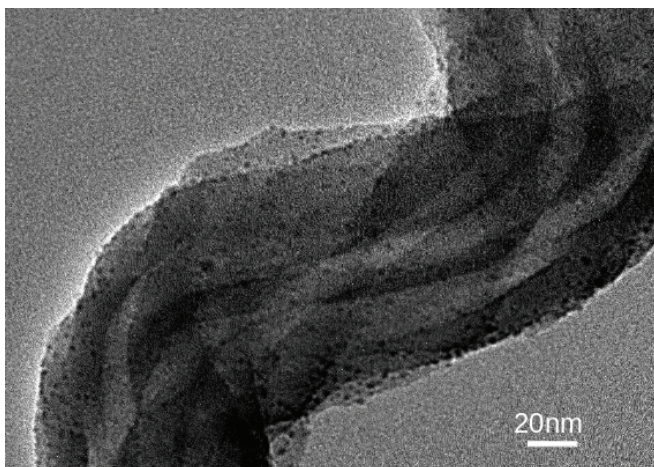


Figure 5 TEM image of a palladium coated Nanospring

4. Applications

4.1 Biological Reactors

The use of enzymes as industrial catalysts is a growing technology that holds great promise for the production of specialized compounds. Many industrial and pharmaceutical compounds, and other high value molecules, have complex chemical structures that make them difficult to produce by conventional chemical synthesis, e.g., the antimalarial compound artemisinin, represented in figure 6, a sesquiterpene lactone from annual wormwood [17]. The chemical complexity of artemisinin makes its complete chemical synthesis from organic reagents impractical. If the appropriate enzymes were available, it would be possible to synthesize complex compounds like these at the laboratory bench from abundant, low cost precursors. The sequences of enzymatic reactions involved in the natural biosynthesis of many high value natural products have been established [18], and could be used for commercial production. However, this technology is limited by the high cost of enzymes. To be cost effective, an enzyme used as an industrial catalyst must produce more products, last longer, and function under higher product concentrations than it would under its natural conditions [19]. An effective way to improve the performance of an enzyme under industrial conditions is to immobilize it on a fixed support in a continuous flow reactor (CFR).

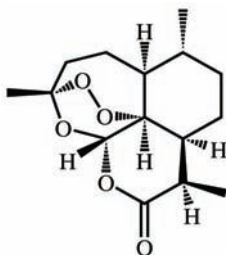


Figure 6 Artemisinin

Immobilization allows continuous recycling of the catalyst, mitigates product inhibition, and often increases the working life of the enzyme [20]. To be effective, however, an enzyme-based CFR must employ a high concentration of enzyme in a small area without causing a prohibitive restriction in flow. Nanosprings appear to be an excellent support material for these applications because they:

- Provide a high surface area for enzyme attachment
- Offer minimal flow resistance
- Have a surface chemistry that is suitable for the reversible thiol-based attachment of virtually any soluble enzyme

A model CFR using Nanosprings and β -galactosidase from *Aspergillus oryzae* has recently been described [21]. That work utilized the model substrate *o*-nitrophenol- β -D-galactosylpyranoside (*o*-NPG) to monitor the reaction. In the physiological reaction catalyzed by β -galactosidase, lactose is hydrolyzed into glucose and galactose. In the model reaction, *o*-NPG is hydrolyzed into galactose and *o*-nitrophenol, which can be spectrophotometrically monitored. We have been using this same enzyme/substrate system, with some modifications, as a means of method development. In our work, Nanosprings were functionalized with thiol groups by reacting them with 3-mercaptopropyltrimethoxysilane (MPTMS), shown in figure 7. This was accomplished by incubating a Nanosprings covered silicon wafer (25×75 mm²) in a 5% MPTMS solution in acetone. The enzyme was functionalized by reacting with *N*-succinimidyl 3-(2-pyridyldithiol) propionate (SPDP), resulting in the attachment of pyridyldithiol groups to lysine side chains on the enzyme surface (See Figure 8). This was accomplished by first making a 20 mg/mL solution of β -galactosidase in PBS with 1mM EDTA added. To the enzyme solution was added 50 mL/mL of a 20 mM solution of SPDP in DMSO. The mixture was incubated for 30 minutes at room temperature and then passed through a 6K MWCO polyacrylamide desalting column to remove unreacted components. The column fractions were assayed for maximum activity, and the active fractions were pooled and used for Nanospring attachment. To covalently link the enzyme to the Nanosprings, the SPDP-modified enzyme solution was then placed on top of the thiol-functionalized wafer and incubated for one hour at

room temperature. The enzyme-coated wafer was then washed with reaction buffer (20 mM sodium phosphate, 10 mM sodium citrate, pH 4.5) and placed into the reactor chamber. A syringe pump was used to pump several reactor volumes of reaction buffer through the reactor at 0.1 mL/min.

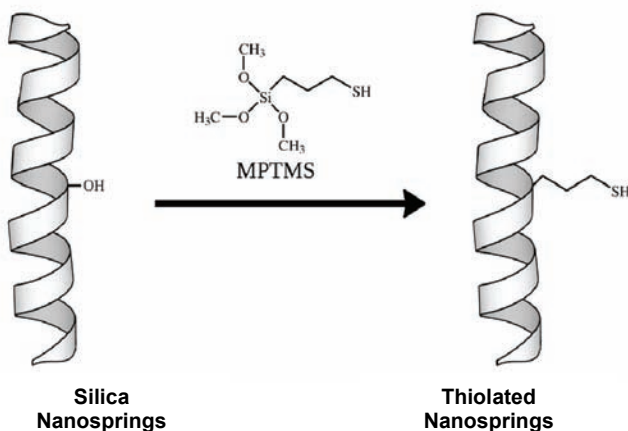


Figure 7 Thiolation of Nanosprings

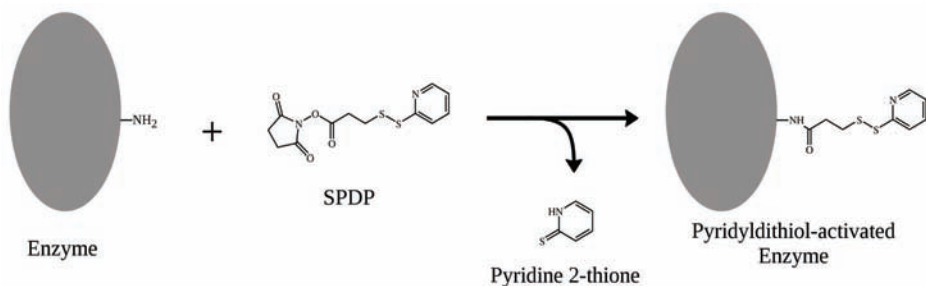


Figure 8 Modification of enzyme for Nanospring attachment

Activity of the reactor was measured by pumping varying concentrations of substrate (*o*-NPG in reaction buffer) through the reactor at 0.1 or 0.2 mL/min. After several reactor volumes of substrate had been pumped through, 0.2 mL fractions were collected into vials containing 0.6 mL of quench buffer (100 mM sodium borate, pH 9.8). The high pH of the quench buffer stops the reaction and converts the reaction product, *o*-nitrophenol, to its colored form [22]. The quantity of product was determined by measuring the absorbance at 415 nm. Product concentrations were calculated using the empirically determined extinction coefficient for *o*-nitrophenol of $4800 \text{ M}^{-1}\text{cm}^{-1}$. In general, lower flow rates resulted in higher conversion efficiencies. When substrate concentration was varied, there was an inverse relationship between conversion efficiency and quantity of product produced per minute, as shown in figure 9. At low substrate concentrations conversion efficiency is > 90%, but the amount of product produced per minute is relatively low. Product volume per minute increases at higher substrate concentrations, but at the expense of conversion efficiency. These data suggest that both high product volume and complete conversion could be achieved by linking reactors together in series.

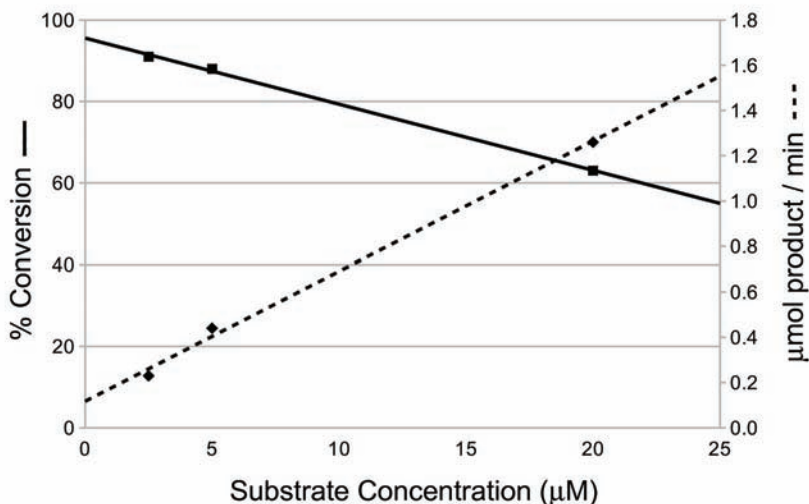


Figure 9: Conversion efficiency and product volume vs. substrate concentration for β -galactosidase reactor at 0.1 mL/min

4.2 Chemical Reactors

The concept of immobilized enzyme reactors can be carried forward into general heterogeneous catalysis applications by the use of catalysts coated on the Nanosprings. Higher reaction rates in existing heterogeneously catalyzed reactions like alkylation, amination, C-C coupling, hydrogenation, oxidation, can be expected due to the high accessible surface area of the Nanosprings. The catalysts deposited on the Nanosprings are thermally stable, as discussed in section 4.3, leading to an expectation that catalyst lifetimes could be extended. In addition, it has been demonstrated that the Nanospring surface aids in some catalytic reactions.

Currently, we are studying hydrogenation of 4-nitrophenol into 4-aminophenol as a representative reaction. Catalytic hydrogenation processes in the liquid phase present challenges and difficulties due to the three-phase system formed by the solution, the solid-state catalyst and the gaseous hydrogen. Design of reliable experiments and analysis of the experimental data are the main points to be considered in these reactions. A CFR consisting of a mat of palladium-decorated Nanosprings simplifies the study of the kinetics of liquid-phase hydrogenation processes. In addition, a CFR eliminates the post-processing work required to separate the catalyst particles from the reaction products. In the present work, we report the results obtained in a CFR using palladium, silver and palladium nanoparticles on zinc oxide coated silica Nanosprings for the reduction of 4-nitrophenol with sodium borohydride or hydrogen gas.

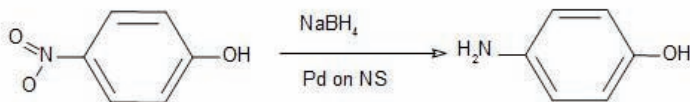


Figure 10 Reduction of 4-nitrophenol with sodium borohydride

To assess the performance of the catalytic material 0.5 mL of 1.12 mM 4-nitrophenol was placed in a cuvette with a $10 \times 5 \text{ mm}^2$ stainless steel coated with silica Nanosprings. Immediately, 0.5 mL of 10 mM NaBH_4 was added to the cuvette. Changes in absorbance were measured at $\lambda=400\text{nm}$ over a period of 45 minutes. Palladium was the most active catalyst, as

shown in figure 11, with a reaction efficiency of 13.71 % per min, compared to 3.3 % per min for the Ag nanoparticles and 0.03 % per min for the Pd on ZnO-coated Nanosprings as indicated in figure 11. It has to be noted that the ZnO-coated Nanosprings were completely inert demonstrating that the Nanospring surface can be an active catalyst support. Compared to an equivalent amount of 5% palladium on activated carbon, the Nanospring-supported catalyst provides more than 3 times the reaction rate. In addition, the reaction efficiency of palladium nanoparticles was measured at various concentrations of 4-nitrophenol, shown in figure 12. The results obtained in these tests, show a remarkable catalytic activity for this particular process.

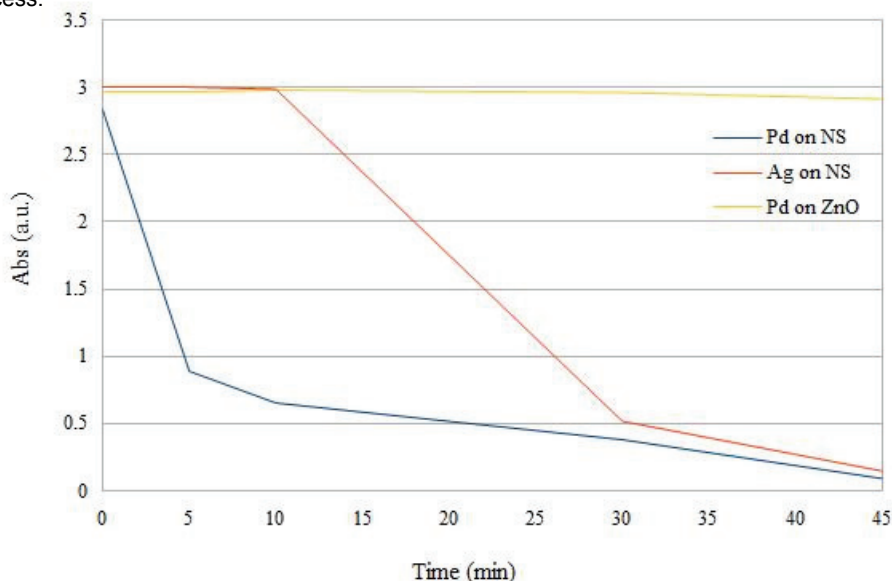


Figure 11 Disappearance of 4-nitrophenol due to different catalysts

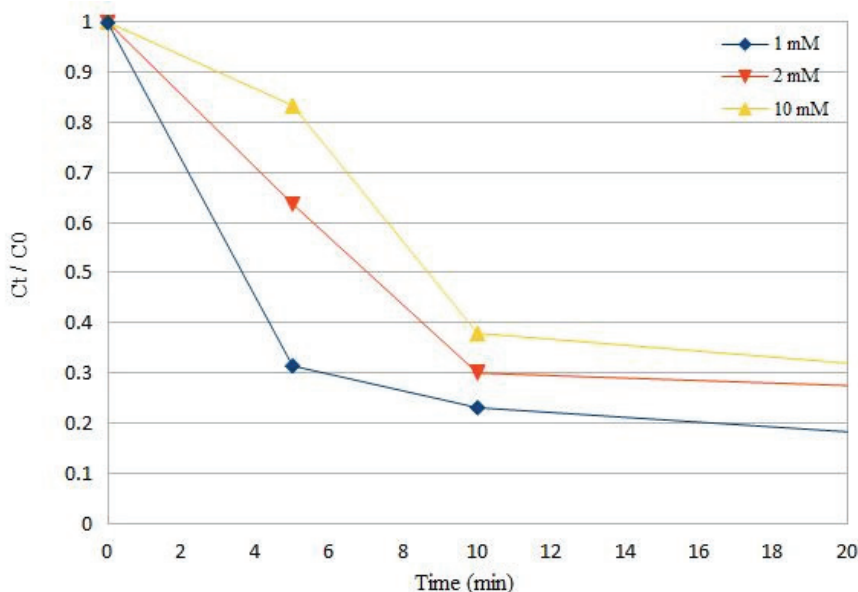


Figure 12 Variation of reaction rates at various nitrophenol concentrations

The performance of the catalyst inside the CFR was evaluated by feeding a solution of 4-nitrophenol (0.1 mM) into the reactor at different flow rates using a syringe pump. The reducing solution of sodium borohydride (0.3125 g/L) was supplied at a flow rate of 25 mL/h. The conversion was calculated by measuring the absorbance of the liquid product at $\lambda=400$ nm. The space velocity was calculated by dividing the total flow rate of reactants by the volume of the reactor (0.1 mL). The result shown in figure 13 indicates that the Nanosprings-based CFR displays a high performance at moderate space velocities.

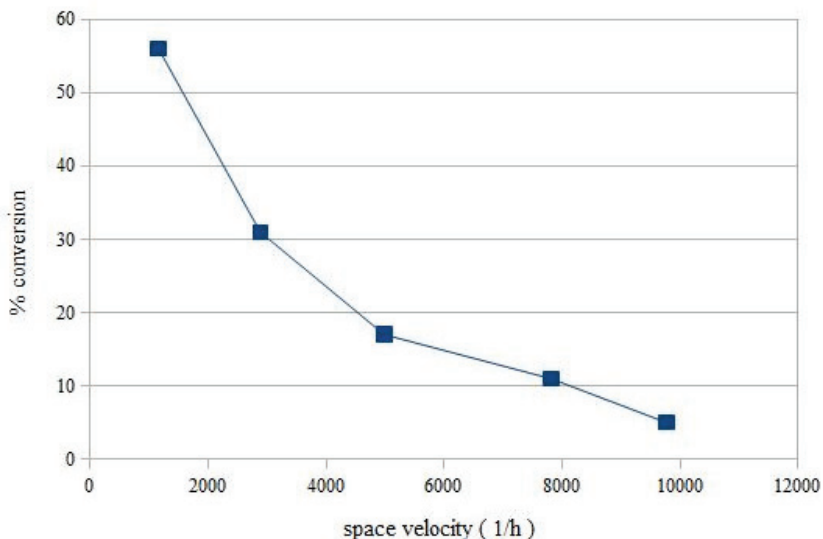


Figure 13 Conversion efficiency as a function of space velocities

Figure 14 indicates pressure drop measurements across the CFR at different flow rates. It can be seen that the pressure drops with the steel foil substrate with and without Nanosprings are almost identical implying very little resistance to the flow by the Nanospring mat.

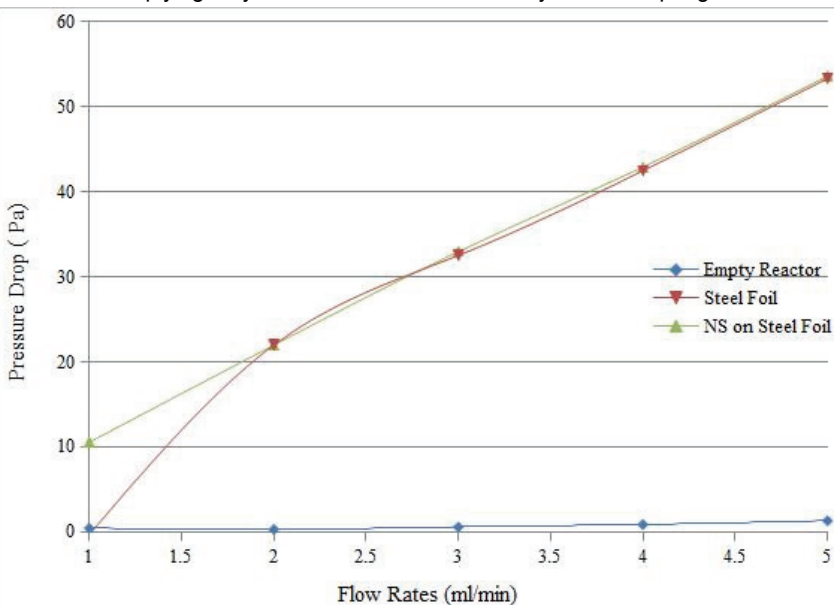


Figure 14 Pressure drop versus flow rates to measure resistance to flow

The following conclusions can be drawn from these preliminary results:

- The immobilization of palladium nanoparticles on silica Nanosprings produces a highly active catalyst
- Catalyst performance was enhanced due to forced contact between catalyst film and reactants
- For higher conversion efficiencies the CFR can be operated in recirculating mode
- The versatility of possible Nanospring coatings enable CFR for a multitude of catalysis reactions

4.3 Catalytic Converters

Nanosprings have been deposited on the two major substrate materials used for catalytic converters: cordierite monoliths and stainless steel foils. Figure 15 shows a Nanospring mat formed on the walls of a ceramic (cordierite) monolith.

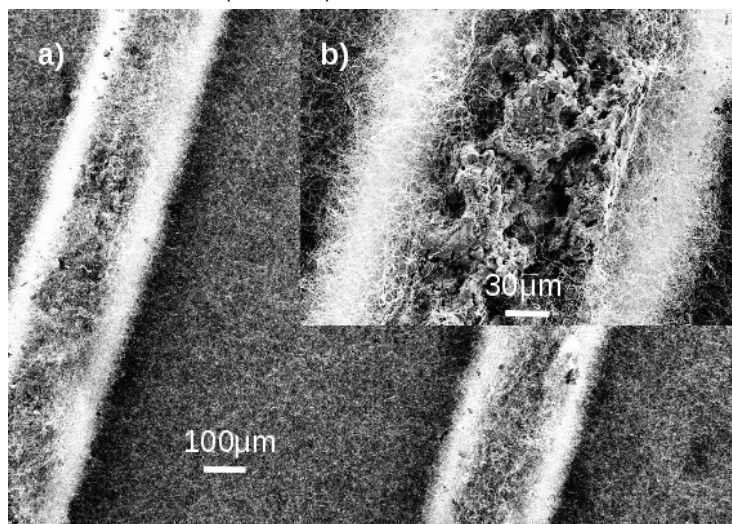


Figure 15 SEM image of a cordierite monolith coated with silica Nanosprings

The Nanospring coating shows some advantages over the standard catalyst impregnated γ -alumina “wash-coat” that is deposited on these substrates. The density of the Nanospring coating on the catalytic converters is much less. On a core where the alumina wash-coat would add approximately 152 g/L, the Nanospring coating would only add 14 g/L. The back pressure of the core due to the Nanospring coating is slightly lower than a standard alumina coated core. Due to the high accessible surface area of the Nanosprings, a greater amount of the active catalyst is exposed to the reactants. This avoids problems found in porous structures where reactions can be diffusion limited, or the catalyst can be encapsulated in the pores at high temperatures. In addition, tests were done showing that both platinum and palladium nanoparticles were able to resist sintering under hydrothermal aging (800°C with 10% relative humidity) for 16 h and still remain catalytically active. This shows an anomaly to the observed problems of catalyst being poisoned by silica, and shows promise of reducing cost and boosting performance of future catalytic converters.

Palladium and platinum nanoparticles (3.3 ± 1.6 nm and 4.4 ± 1.6 nm, respectively) were deposited on the Nanosprings using simple metal precursor solutions. The particles were counted and sized using transmission electron microscopy (TEM) to get a representative size distribution. The samples were then hydrothermally aged at 800°C with 10% relative humidity for 16 h. Under these conditions the palladium particles grow to 4.7 ± 2 nm and the platinum particles grow to 6.4 ± 3.8 nm. As reported by Suzuki *et al.* [23] and Liu *et al.* [24], under these hydrothermal aging conditions the palladium particle size would typically be around 10 to 20 nm and the platinum particle size could be as large as 80 nm, depending on the substrate.

Tests were done to confirm that platinum and palladium were still catalytically active after hydrothermal aging. Nanosprings were grown on corrugated stainless steel foil and on flat stainless steel foil, which were rolled together to form a small monolith. The Nanospring-coated monolith was placed in a tube furnace where a calibrated gas (1200ppm CO, 400ppm ethene, 12.5% O₂, 6.0% CO₂, and a balance of N₂) was metered through the monolith at space velocities of 50,000 h⁻¹ and 75,000 h⁻¹. An exhaust gas analyzer measured the effluent CO concentration. The percent conversion of CO was plotted against oven temperature to create "light-off" curves for the two different space velocities. This was done before and after hydrothermal aging to show the comparison. The "light-off" temperature is defined as the temperature where 50% conversion is reached.

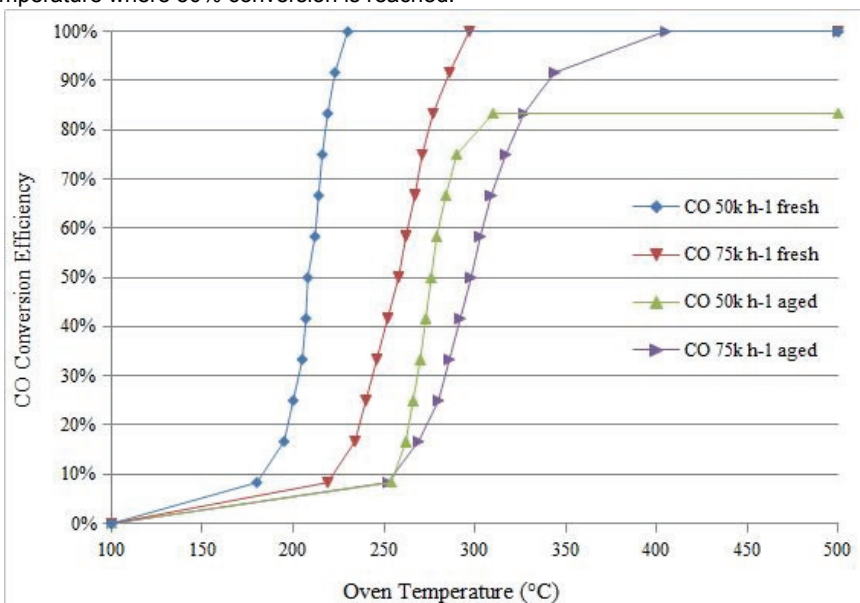


Figure 16 Light off curves of Carbon Monoxide

In addition to showing added catalyst stability and cost reduction the flexible nature of the Nanospring mat shows promise with metal catalytic converters where thermal expansion issues can create problems between the metal and ceramic wash-coat interface.

4.4 Sensors

Timalsina et al. [25], [26] have recently published two studies on the development of biological sensors based on silica Nanosprings. These studies used a capacitive-type sensor consisting of two glass substrates coated with indium tin oxide (ITO), where the vertically-aligned Nanosprings (VANS) were used as the sensing media. Following a top-down approach, VANS were grown in the patterned areas of the substrates [7]. A second patterned blank substrate, sans VANS, with a center hole of 3 mm in diameter was placed on top of the sensing electrode with a 200 μ m thick polydimethylsiloxane (PDMS) gasket. These sensors were characterized by alternating current impedance spectroscopy [3][2], and later were used for the detection of glucose oxidase [26]. Silica Nanosprings were initially treated with 1 mg/mL biotinylated immunoglobulin (B-IgG). The direct adsorption of B-IgG on the Nanosprings simplify the whole sensing procedure, since the avidin-conjugated glucose oxidase (Av-GOx) can directly be immobilized on the B-IgG. Timalsina et al. showed a 77% increase in signal for the VANS-based biosensor, which is significantly more sensitive to the biological solutions relative to the planar ITO sensors. An example of the sensor response is presented in figure 17. Note, the impedance data is a log-log scale, where the sensor exhibits excellent response to changes in functionalization. This work lays down the foundation for the development of fully-functional VANS-based sensors.

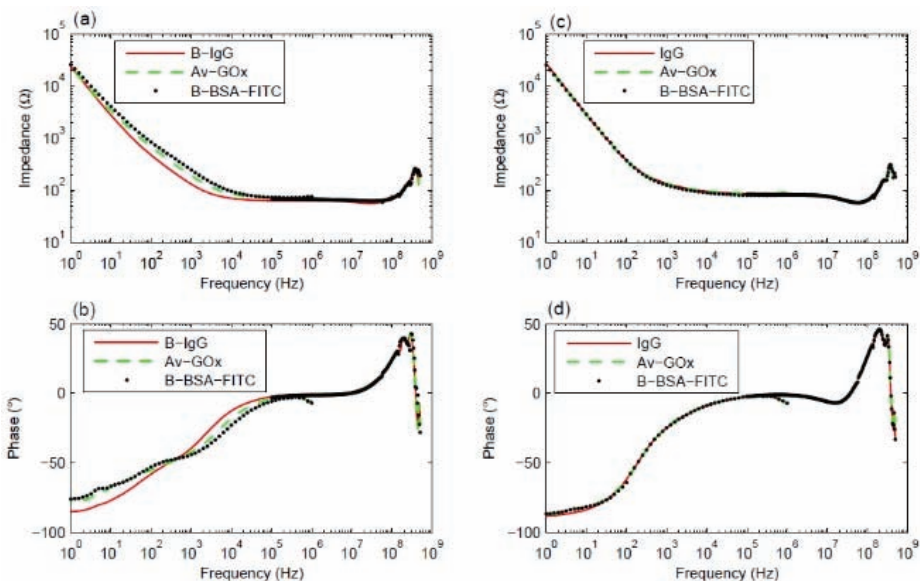


Figure 17 Impedance spectra measured at 10 mV applied V_{rms} after the subsequent addition of B-IgG (or IgG), Av-GOx and B-BSA-FITC: (a) impedance magnitude plot and (b) impedance phase plot as a function of frequency of the VANS sensor; (c) impedance magnitude plot and (d) impedance phase plot as a function of frequency of the control (VANS sensor without biotin)[26] .

References:

- [1] D. N. McIlroy, A. Alkhateeb, D. Zhang, D. E. Aston, A. C. Marcy, and M. G. Norton, "Nanospring formation- unexpected catalyst mediated growth," *Journal of Physics: Condensed Matter*, vol. 16, no. 12, p. R415-R440, Mar. 2004.
- [2] L. Wang, D. Major, P. Paga, D. Zhang, M. G. Norton, and D. N. McIlroy, "High yield synthesis and lithography of silica-based Nanospring mats," *Nanotechnology*, vol. 17, no. 11, p. S298-S303, 2006.
- [3] A. Legrand, *The surface properties of silicas*. Chichester; New York: John Wiley, 1998.
- [4] E. Plueddemann, *Silane coupling agents*, 2nd ed. New York: Plenum Press, 1991.
- [5] H. F. Zhang, C. M. Wang, E. C. Buck and L. S. Wang, "Synthesis, characterization, and manipulation of helical SiO₂ Nanosprings," *Nano Letters*, vol. 3, no. 5, pp. 577-580, May. 2003.
- [6] D. N. McIlroy, D. Zhang, Y. Kranov, and M. G. Norton, "Nanosprings," *Applied Physics Letters*, vol. 79, no. 10, p. 1540, 2001.
- [7] G. Corti et al., "Nanospring-based biosensors for electrical DNA microarrays," in *Mater. Res. Soc. Symp. Proc.*, 2007, vol. 1010, pp. V05-03.
- [8] G. Corti, T. Cantrell, M. F. Beaux II, D. N. McIlroy, and M. G. Norton, "Next generation Nanospring-enhanced catalytic converters," presented at the Nanotech Conference & Expo 2010, Anaheim, CA, 2010.
- [9] M. G. Norton, D. N. McIlroy, G. Corti, and M. A. Miller, "Silica Nanosprings – a novel nanostructured material for hydrogen storage," in *Clean Technology 2009*, Houston, 2009, pp. 202-205.
- [10] D. C. Hyatt, T. Cantrell, M. Yahvah, M. G. Norton, D. N. McIlroy, and G. Corti, "Use of silica Nanosprings in an enzyme-based continuous flow reactor," presented at the Microtech conference & Expo 2011, Boston, 2011.
- [11] D. N. McIlroy, G. Corti, T. Cantrell, M. F. Beaux II, T. Prakash, and M. G. Norton, "Engineering high surface area catalysts for Clean Tech Applications," in *Clean Technology 2009*, Houston, 2009, pp. 195-198.
- [12] T. Prakash, O. Marin-Flores, T. Cantrell, M. G. Norton, D. N. McIlroy, and G. Corti, "Carbon capture and recycling by photocatalysts supported on silica Nanosprings," presented at the Nanotech conference and Expo 2011, Boston, 2011.
- [13] D. N. McIlroy, D. Zhang, Y. Kranov, and M. G. Norton, "Nanosprings," *Applied Physics Letters*, vol. 79, no. 10, p. 1540, 2001.
- [14] Z. Hu and C. H. Turner, "Atomic layer deposition of TiO₂ from TiI₄ and H₂O onto SiO₂ surfaces: ab initio calculations of the initial reaction mechanisms," *Journal of the American Chemical Society*, vol. 129, no. 13, pp. 3863-3878, Apr. 2007.
- [15] J. W. Elam and S. M. George, "Growth of ZnO/Al₂O₃ alloy films using atomic layer deposition techniques," *Chemistry of Materials*, vol. 15, no. 4, pp. 1020-1028, Feb. 2003.
- [16] V. Dobrokhotov et al., "Principles and mechanisms of gas sensing by GaN nanowires functionalized with gold nanoparticles," *Journal of Applied Physics*, vol. 99, no. 10, p. 104302, 2006.

References (cont.):

- [17] P. Newton, BM, DPhil, MRCP and N. White, DSc, MD, FRCP, "MALARIA: new developments in treatment and prevention," *Annual Review of Medicine*, vol. 50, no. 1, pp. 179-192, Feb. 1999.
- [18] P. Bernhardt and S. E. O'Connor, "Opportunities for enzyme engineering in natural product biosynthesis," *Current Opinion in Chemical Biology*, vol. 13, no. 1, pp. 35-42, Feb. 2009.
- [19] D. J. Pollard and J. M. Woodley, "Biocatalysis for pharmaceutical intermediates: the future is now," *Trends in Biotechnology*, vol. 25, no. 2, pp. 66-73, Feb. 2007.
- [20] C. Mateo, J. M. Palomo, G. Fernandez-Lorente, J. M. Guisan, and R. Fernandez-Lafuente, "Improvement of enzyme activity, stability and selectivity via immobilization techniques," *Enzyme and Microbial Technology*, vol. 40, no. 6, pp. 1451-1463, May. 2007.
- [21] K. F. Schilke, K. L. Wilson, T. Cantrell, G. Corti, D. N. McIlroy, and C. Kelly, "A novel enzymatic microreactor with *Aspergillus oryzae* β -galactosidase immobilized on silicon dioxide Nanosprings," *Biotechnology Progress*, vol. 26, no. 6, pp. 1597-1605, 2010.
- [22] T. Haider and Q. Husain, "Immobilization of β galactosidase from *Aspergillus oryzae* via immunoaffinity support," *Biochemical Engineering Journal*, vol. 43, no. 3, pp. 307-314, Mar. 2009.
- [23] A. Suzuki et al., *Multi-scale theoretical study of sintering dynamics of Pt for automotive catalyst*. Warrendale, PA: SAE International, 2009.
- [24] R.-J. Liu, P. A. Crozier, C. M. Smith, D. A. Hucul, J. Blackson, and G. Salaita, "In situ electron microscopy studies of the sintering of palladium nanoparticles on alumina during catalyst regeneration processes," *Microscopy and Microanalysis*, vol. 10, no. 1, Jan. 2004.
- [25] Y. P. Timalisina et al., "Characterization of a vertically aligned silica Nanospring-based sensor by alternating current impedance spectroscopy," *Journal of Micromechanics and Microengineering*, vol. 20, no. 9, p. 095005, Sep. 2010.
- [26] Y. P. Timalisina et al., "Alternating current impedance spectroscopic analysis of biofunctionalized vertically-aligned silica Nanospring surface for biosensor applications," *Journal of Applied Physics*, vol. 110, no. 1, p. 014901, 2011.

Products Referenced in the Article

NEW Silica Nanosprings™

14-6010 NEW→	Silica Nanosprings™ grown on aluminum foil substrate (3.5 x 8cm) reddish white plate; S.A. 350m ² /g	1pc 5pc
14-6012 NEW→	Silica Nanosprings™ grown on fiber glass substrate (3.5 x 8cm) reddish white plate; S.A. 350m ² /g	1pc 5pc
14-6014 NEW→	Silica Nanosprings™ grown on glass slide substrate (2.5 x 7.5cm) reddish white plate; S.A. 350m ² /g	1pc 5pc
14-6030 NEW→	Silica Nanosprings™ coated with titanium dioxide and grown on aluminum foil substrate (3.5 x 8cm) white plate	1pc 5pc
14-6032 NEW→	Silica Nanosprings™ coated with titanium dioxide and grown on fiber glass substrate (3.5 x 8cm) white plate	1pc 5pc
14-6034 NEW→	Silica Nanosprings™ coated with titanium dioxide and grown on glass slide substrate (2.5 x 7.5cm) white plate	1pc 5pc
14-6050 NEW→	Silica Nanosprings™ coated with zinc oxide and grown on aluminum foil substrate (3.5 x 8cm) white to beige plate	1pc 5pc
14-6052 NEW→	Silica Nanosprings™ coated with zinc oxide and grown on fiber glass substrate (3.5 x 8cm) white to beige plate	1pc 5pc
14-6054 NEW→	Silica Nanosprings™ coated with zinc oxide and grown on glass slide substrate (2.5 x 7.5cm) white to beige plate	1pc 5pc

Note: Sold under license from GoNano for research purposes only. US 11-993,452 & PCT WO2007/002369A3.

Semiconductor Nanoparticles – A Review

Daniel Neß and Jan Niehaus
CANdot®

Introduction:

The synthesis, characterization and applications of nanocrystals were the subject of extensive research in the past decade. Nanocrystals are crystalline objects that are less than 100 nm in at least two dimensions.^[1] As a result, nanoparticles are made up of a small number of atoms and found in the transition region between atoms or molecules and infinitely large solids. This is why the electronic, optical, structural and thermodynamic properties can be a function of the crystallite dimensions and thus change with the radius.^[2-7]

Since semiconductors are of widespread use in electronic and optical applications the possibility of being able to adjust the bandgap in semiconductor nanoparticles to the required specifications by varying the size alone and not the chemical composition makes them extremely interesting.

Size quantization effect:

It was observed for the first time in 1981 that in nanocrystalline CuCl_2 the band gap apparently increases with decreasing particle size.^[8] Because the size of the band gap E_g determines the frequency at which the onset of absorption takes place, this effect can be observed with the naked eye in nanoparticles that have a band gap E_g of 1.8 – 3.1 eV and already start to absorb in the visible range. For example, it is possible to adjust the band gap of CdSe, which in the solid state is 1.7 eV, to up to 2.5 eV by reducing particle size.

Shown in Figure 1 are colloidal solutions of CdSe nanoparticles. The material in every cuvette has the same chemical composition. The samples differ only in their particle size from 3 nm (blue) to 7 nm (red).



Fig. 1 Colloidal solutions of CdSe nanoparticles of different size

This phenomenon is called the size quantization effect. It is due to formation of two charge carriers confined to a finite area by excitation of an electron from the valence band to the conduction band during light absorption. This electron/hole pair, also termed an exciton, has a structure very similar to that of the hydrogen atom but usually a low binding energy due to the small effective masses and therefore a large radius. Accordingly, the binding energy of the hydrogen atom in the ground state is 13.51 eV and its radius 0.53 Å,^[9] while for CdSe the binding energy of the exciton is only 0.02 eV and the resulting radius 49 Å.

The radius of the electron/hole pair is a decisive factor in the properties of nanoparticles. If absorption takes place in a nanocrystal that has dimensions similar to or even smaller than the Bohr radius of the exciton, then the exciton can no longer be in the ground state but must have a higher kinetic energy. Hence, the energy level of the exciton is influenced by the particle walls. This quantum mechanical effect described as a particle-in-a-box is stronger the smaller the dimensions of the particle, i.e. the box, becomes. The band gap E_g increases with decreasing particle size, and the onset of light absorption shifts to shorter wavelengths.^[4]

The particle-in-a-box model allows calculation of the size quantization effect.^[10,11] By assuming a box potential with infinitely high potential barriers and taking into consideration the Coulomb interaction between the electron and hole, the following expression, the so-called Brus equation, is obtained for the change in the band gap as a function of the particle radius:^[12]

$$\Delta E = \frac{\pi^2 \cdot \hbar^2}{2 \cdot R^2} \left(\frac{1}{m_e} + \frac{1}{m_h} \right) - \frac{1.8 \cdot e^2}{4 \cdot \pi \cdot \epsilon \cdot R}$$

Eq. 1

where ΔE change in band gap E_g relative to macroscopic solid
 R radius of nanoparticle
 $m_{e/h}$ effective mass electron / hole
 ϵ dielectric constant

The first term includes the relationship known from the particle-in-a-box that the energy is a function of $1/R^2$. The second term includes the Coulomb interaction. This equation can also be used very effectively to calculate the radius of semiconductor nanoparticles from the absorption spectrum alone.

However, because the values used to calculate the effective masses are derived from microcrystalline solids and the assumption of a box potential is a stark simplification as well, the calculated values agree approximately with the measured values only for larger particles. For smaller radiuses, very large deviations are obtained, making it necessary to perform significantly more precise and hence also more complicated calculations.

The change in electronic structure on transition from the atom to the macrocrystalline solid can be explained using the LCAO approach.^[13-15] To understand the special properties of nanoparticles, however, it is better to start from the bulk solid and observe the changes in the electronic structure from there. This is shown in Figure 2.

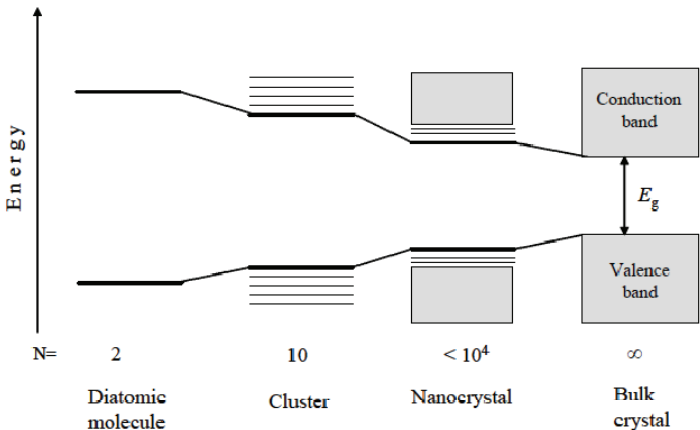


Fig. 2 Diagram of the change in energy levels with increasing agglomeration number N ^[16]

It can be seen in Figure 2 that the band character in bulk solids, i.e. where there is a large number of atoms, is strong and the band gap small. If the number N of atoms decreases in the solid, the energy level density within the bands, on the one hand, decreases. On the other, the distance between the HOMO (top band edge of the valence band) and the LUMO (bottom band edge of the conduction band) increases. In a molecule the transition to discrete energy levels is complete and there are no longer any bands.

Nanoparticles with a smaller radius resulting in a smaller number N of atoms therefore have a larger "band gap" than particles with a larger radius. However, the term band gap is not fully applicable to nanoparticles because the density and accordingly the band character of the electronic states also decrease with decreasing radius and instead discrete energy levels tend to form. As a result, transitions of increased oscillator strength take place, which can also be observed in the absorption spectrum of monodisperse samples.^[17]

Shown in Figure 3 is a typical absorption spectrum for nanoparticles, in this case CdSe nanoparticles in n-hexane.

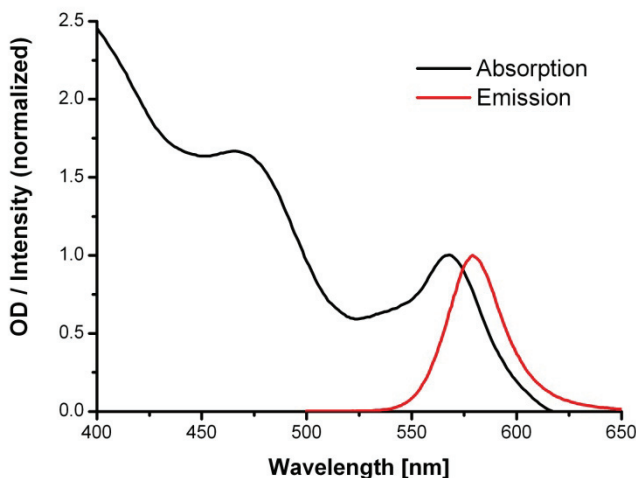


Fig. 3 Absorption and emission of CdSe nanoparticles

Clearly distinguishable are two maxima that show a strong blue shift relative to the absorption edge at 715 nm in macrocrystalline CdSe.

The first maximum at 570 nm is produced by excitation of an electron from the top band edge of the valence band into the bottom band edge of the conduction band. The energy of this transition therefore corresponds to the width of the band gap and can be used in the Brus equation to calculate the particle size. The second transition at 470 nm represents excitation of the electron from the HOMO of the valence band into a higher level of the conduction band. The difference between the two transitions shows how strongly the size quantization effect has reduced the density of the energy levels in the bands. Further absorption maxima would represent transition into the next higher level of the conduction band. Consequently, both impacts of the size quantization effect, the increase in band gaps as well as decrease in level density in the bands, can be seen in the absorption spectra of nanoparticles.

If the size distribution of the sample is somewhat larger, however, these characteristics disappear from the absorption spectrum because nanoparticles of different size also have a different band gap E_g . As a result, the absorption is distributed over a larger range of wavelengths and the peak usually can no longer be seen.

The size quantization effect can also be observed in the emission spectrum of nanocrystals. Here the energy of the radiation emitted by the nanocrystals after excitation is measured. This is therefore energy released when the electron returns to the valence band from the conduction band, i.e. on recombination of the electron and hole. Because the distance

separating the conduction and valence band edge in nanocrystals is influenced not only by the particle structure, the surface characteristics, lattice voltages and environment (solvent) but also by the size of the particles, the peak is usually very broad.

It is noticeable in Figure 3 that the emission spectrum, unlike the absorption spectrum, shows only one transition at 580 nm. This radiation-emitting transition always occurs from the bottom band edge of the conduction band to the top band edge of the valence band. All other transitions within the conduction band release only little energy and can therefore proceed radiationless. This energy is transferred to the lattice as vibrational energy.^[18]

Furthermore, in this sample the emission maximum is shifted by 11 nm from the first absorption maximum. This phenomenon is called the Stokes shift and reduces the reabsorption of emitted light by semiconductor particles. This leads to an increase of the measured intensity. The Stokes shift is strongly affected by the particle shape. For dots 10 to 20 nm are common values.

Core particles:

The simplest semiconductor nanoparticles are composed of a homogeneous, crystalline core with a surface coating of stabilizing molecules to saturate free valences. These molecules, commonly called ligands, also prevent agglomeration of the particles and thus allow formation of a homogeneous dispersion of long-term stability. Typical examples of this substance class are CdSe, CdTe and PbS nanoparticles, with the CdSe-based particles covering the VIS (480 – 650 nm), the CdTe-based the NIR (600 800 nm) and the PbS-based the IR range (1000 – 1600 nm). All of these materials show the direct correlation of core size with band gap already described. Figure 4 presents the absorption and emission spectra of CdSe particles of different size.

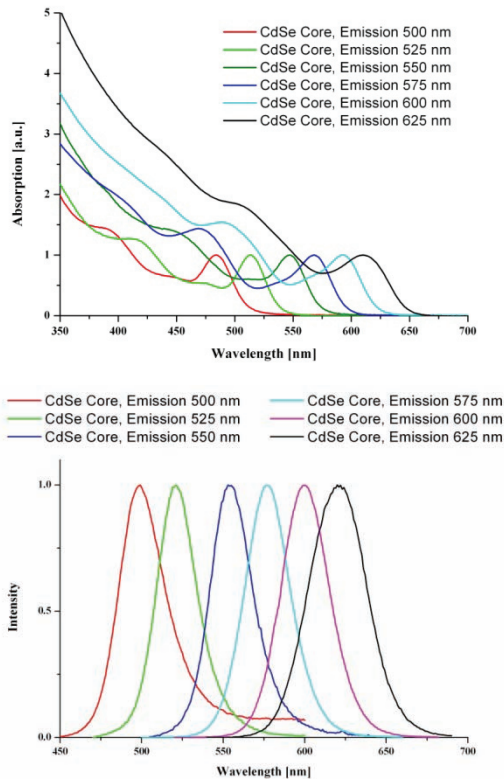


Fig. 4 Absorption and emission spectra of CdSe nanoparticles 3 to 7 nm in size

Because the structure of these particles results in direct contact of the free charge carriers with the particle surface after excitation, they usually are not very stable and have a quantum yield of less than 20%. These particles are, however, very suitable for applications where nanoparticles are to serve as the absorber material and not the fluorescent color. This is the case especially in the field of solar cell research.

Core/shell particles:

Core/shell particles have a conventional nanoparticle as the core on which a shell made up of another substance is grown. In the case of semiconductor nanoparticles, growth of an external coating passivates the valences on the core surface, thereby increasing the stability and quantum yield.^[19,20]

The alignment of the valence and conduction bands of the core and shell material is very important for achieving the desired positive effect on the quantum yield. In a type I core/shell particle the valence band of the shell material is lower energetically than the valence band of the core and the conduction band of the shell material higher than the conduction band of the core material. Consequently, after generation of an exciton by absorption both charge carriers are confined in the core. Valences on the outside of the shell therefore do not affect the quantum yield and there is no change in the band gap. The quantum yield of these particles is significantly higher than that of core particles.

In type II core/shell particles the conduction band of the core material is lower than the conduction band of the core material. Whereas the hole remains confined to the core, the probability of finding the electrons in the shell material is high. Because of the spacial separation of both charge carriers hardly any recombination takes place and the quantum yield is very low. Moreover, the real band gap decreases and absorption and emission show a strong red shift.^[19] Both possibilities can be seen in Figure 5.

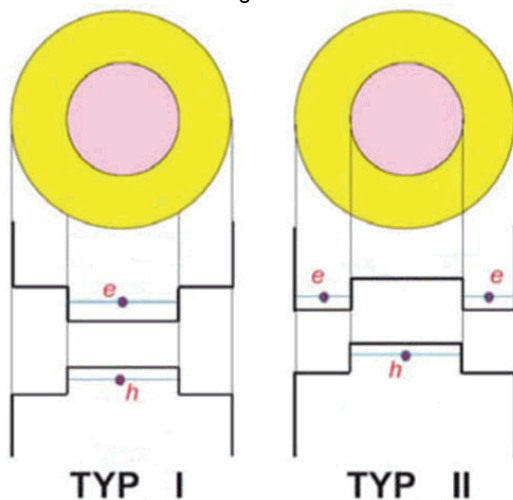


Fig. 5 Type I and Type II core/shell particles

Core/shell/shell particles:

For the shell to grow, the lattice constants of the core and shell materials should not be too different. For example, it would be preferable to grow a ZnS shell on a CdSe core because the band gap of zinc sulfide is much larger and confinement of the charge carriers in the core would be much greater. Both semiconductors have a zinc blende (sphalerite) crystal structure but the lattice constants differ by 12% (6.05Å for CdSe, 5.42 Å for ZnS). Therefore a CdS layer is grown between the core and outer shell that has a lattice constant lying between that of CdSe and ZnS.^[21] This band gap alignments and lattice mismatches are shown in Figure 6:

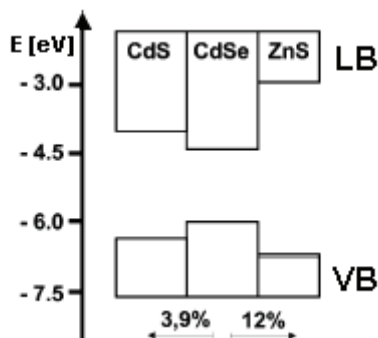


Fig. 6 Alignment of bands in CdSe, CdS and ZnS^[21]

In such cases a core/shell/shell system is fabricated to maintain a small difference between lattice constants of adjacent materials. The result is primarily a higher stability than in conventional core/shell systems. These particles are therefore especially suited for demanding applications such as an LED fluorescent material or transfer into aqueous media.

Organometallic synthesis:

Nanoparticles can be produced by many different methods that generally can be classified into two groups: "top down" and "bottom up".

The "top down" methods are processes in which macroscopic material is broken down. This is accomplished primarily by crushing or laser fragmentation. The advantages of these production methods are relatively low costs and normally large production volumes. The disadvantages are a mostly large particle size distribution, production of particles with no stabilizing surface ligands and restriction to simple core structures. These disadvantages make these production methods for the most part unsuitable for semiconductor nanoparticles.

The "bottom up" methods are generally processes in which nanoparticles are built up from their atomic building blocks. These syntheses are often carried out in solution and enable a high degree of size control and stabilization of the particles. However, the normally smaller production volumes and significantly higher costs are disadvantages.^[22]

The so-called *hot injection* method is a very common example of this type of synthesis. In this method a starting component is combined with surface ligands in a flask, heated to the nucleation temperature and then rapidly combined with the second component. This instantly results in nucleation and subsequent growth. By varying the reaction conditions it is possible to influence the size of the nanocrystals formed. Increasing the reaction time normally results in larger particles because more material can attach to the seeds. Another phenomenon known as Ostwald ripening additionally leads to an increase in the mean particle diameter.^[25] Here larger particles grow while smaller particles, which are energetically less favored due to a large surface, dissolve. This is only possible, however, if the attachment step of the educts to a nanoparticle is reversible.^[20,22,23] Presented in Figure 7 are TEM micrographs of three PbS samples after different reaction times.^[24]

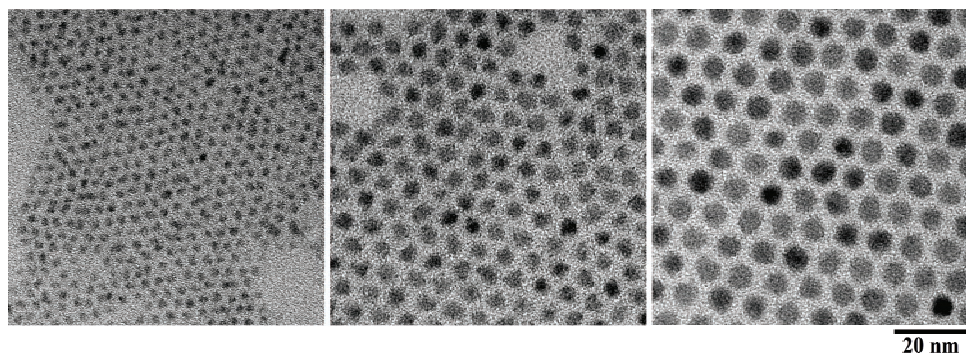


Fig. 7 PbS nanoparticles with an emission of 1000 nm (left), 1400 nm (center) und 1600 nm (right)^[24]

The disadvantage of the “*hot injection*” method is a limited production volume because the amount injected cannot be increased indefinitely. Batch-to-batch reproducibility of the optical properties is also problematic because both nucleation and growth of the particles must take place consecutively in the same flask.

These problems can be avoided by synthesizing the particles in a continuous flow reactor. The system developed by CAN GmbH in collaboration with the University of Hamburg is based on the layout shown in Figure 8.

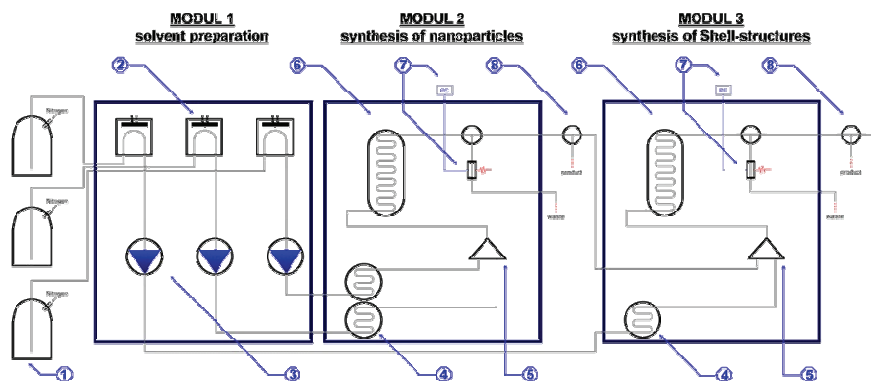


Fig. 8 Layout of a continuous flow unit for synthesis of semiconductor nanoparticles

This system is set up to emulate the “*hot injection*” process. The precursor solutions are stored under an inert atmosphere (1) and can be degassed before the reaction (2). Pulsation-free pumps (3) are used to pump the fluids to the reaction module 2. The solutions are heated separately to the nucleation temperature (4) before they are mixed in the micro fluidic mixing chamber (5). There nucleation of the particles takes place. Because the inner volume of the mixing chamber is only a few μL , the nuclei are immediately pumped to the growth oven (6). This oven is usually heated to a temperature slightly below that of the mixing chamber to prevent further nucleation. After the growth process, the solution is cooled to room temperature and absorption and emission spectra can be recorded with the in-situ spectroscopy unit (7). This separation of nucleation and the growth process leads to a high reproducibility of the particle properties. Figure 9 shows absorption and emission spectra of three different batches of quantum dots. Using “design of experiments” calculations it can be shown that the significance is lower than 0.1%. If further inorganic shells are needed, the solution containing the core particles leaving module 2 can be pumped to module 3, where further precursors can be added. For example, this can be used to produce CdSe/ZnS core/shell particles with enhanced optical properties.

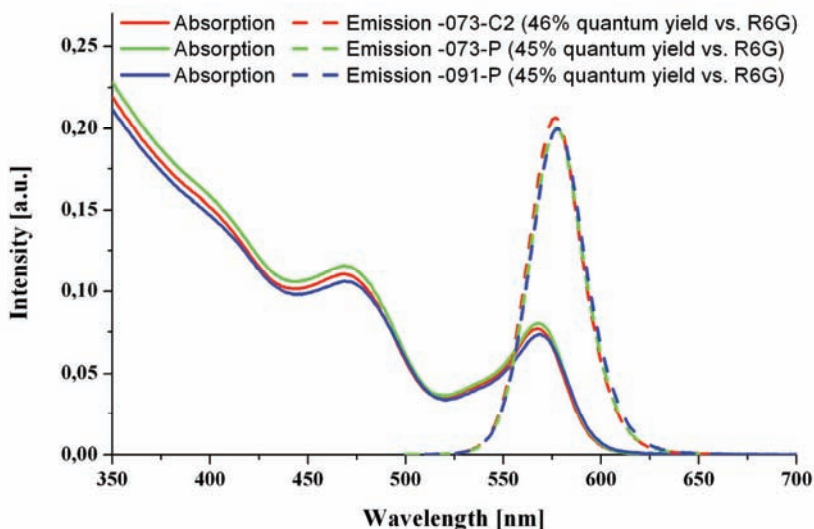


Fig. 9 Absorption and emission spectra of three continuously produced CdSe samples

Applications:

Because of their unique properties semiconductor nanoparticles have a broad range of applications. Adjustment of the band gap through variation of the particle size allows their use everywhere that absorption materials or fluorescent colors for specific wavelengths are required. Due to the inorganic nature of the particle semiconductor nanocrystals show a superior stability compared to common organic dyes. This comes to great effect especially in applications where the fluorescent component is exposed to heat, intensive light or aggressive chemicals like acids during the process. Because of the exchangeability of the surface ligands the same kind of nanoparticle can be used in different solvents or can be homogeneously incorporated in different materials without a change of the optical properties.^[4]

Another advantage of the semiconductor quantum dots is the broad absorption of light which is shown in figure 3 and 9. In contrast to organic dyes, which usually exhibit a quite narrow absorption range, the particles can be excited with nearly every wavelength shorter than the emission maximum. For example all CdSe samples shown in figure 4 can be excited with radiation below 480 nm simultaneously. This can be very useful for all applications where different colors have to be detected in one sample, because this can be done with one excitation wavelength and one emission scan.

Core particles are especially well suited for use in solar cells. The nanoparticle is excited by the incident light and the resulting charge carriers are sucked through the cell. Further isolating shells would reduce the efficiency of the cells in this process taking place on the nanoparticle surface. The CdSe particles used should, however, be as large as possible in order to absorb as much of the solar radiation range as possible. Even more effective are PbS particles, which in addition to visible light convert also IR radiation up to 1000 nm into charge carriers.

Core/shell particles are characterized by a higher stability and quantum yield than core particles. This makes them a less expensive alternative to core/shell/shell particles, for example, as fluorescent material in LEDs or as fluorescent markers in nonpolar organic media.







Core/shell/shell particles have the highest fluorescence intensity and stability against environmental influences and should therefore be used for all demanding applications. They are especially well suited for transfer into aqueous media and hence for use in the biomedical field. After functionalization they can be used there, for example, in cancer research.

References:

- [1] W. Rasband: National Institutes of Health, USA, Java, 1.3.1, **2003**.
- [2] A. Henglein, *Chem. Rev.* **89** (1989), 1861.
- [3] M. G. Bawendi, M. Steigerwald, L. E. Brus, *Annu. Rev. Phys. Chem.* **41** (1990), 477.
- [4] H. Weller, *Angew. Chem. Int. Ed. Eng.* **32** (1993), 41.
- [5] A. P. Alivisatos, *J. Phys. Chem.* **100** (1996), 13226.
- [6] A. Eychmüller, *J. Phys. Chem. B* **104** (2000), 6514.
- [7] T. Trindade, P. O'Brien, N. L. Pickett, *Chem. Mater.* **13** (2001), 3843.
- [8] A. I. Ekimov, A. A. Onushchenko, *JETP Lett.* **34** (1981), 345.
- [9] Gaponenko, S.V., *Optical Properties of Semiconductor Nanocrystals*, Cambridge University Press, 1998.
- [10] A. L. Efros, *Sov. Phys. Semicond.* **16**, (1982), 772.
- [11] Y. Nosaka, *J. Phys. Chem.* **95** (1991), 5054.
- [12] L. E. Brus, *J. Chem. Phys.* **80** (1984), 4403.
- [13] P. E. Lippens, M. Lannoo, *Phys. Rev. B* **39** (1989), 10935.
- [14] N. A. Hill, K. B. Whaley, *J. Chem. Phys.* **99** (1993), 3703.
- [15] N. A. Hill, K. B. Whaley, *J. Chem. Phys.* **100** (1994), 2831.
- [16] H. Döllefeld, *Diss. Universität Hamburg* **2001**.
- [17] D. M. Mittleman, V. L. Colvin, *et al. Phys. Rev. B: Condens Matter* **49** (1994), 14435.
- [18] C. Kittel, Einführung in die Festkörperphysik, 12. A., Oldenbourg Verlag, München Wien, **1999**.
- [19] V. Klimov, s. Ivanov, *Nature* **447** (2007), 441.
- [20] D. Talapin, H. Weller, *Nano Let., Vol. 3* **12** (2003), 1677.
- [21] R. Xie, A. Mefs, *J. Am. Chem. Soc.* **127** (2005), 7480.
- [22] V. F. Puentes, K. M. Krishnan, A. P. Alivisatos, *Science* **291** (2001), 2115.
- [23] S. Sun, C. B. Murray, *J. Appl. Phys.* **85** (1999), 4325.
- [24] M. Nagel, *Diss. Universität Hamburg* **2007**.
- [25] J. H. Nakat, G. D. Willet, *Inorg. Chem.* **30** (1991), 2957.

Products Referenced in the Article

NEW CANdot® Quantum Dots

48-1005  HAZ	Cadmium selenide CANdot® quantum dot (core), 50umol/L in hexane, 500nm peak emission CdSe	5ml 25ml
48-1011  HAZ	Cadmium selenide CANdot® quantum dot (core), 50umol/L in hexane, 525nm peak emission CdSe	5ml 25ml
48-1017  HAZ	Cadmium selenide CANdot® quantum dot (core), 50umol/L in hexane, 550nm peak emission CdSe	5ml 25ml
48-1023  HAZ	Cadmium selenide CANdot® quantum dot (core), 50umol/L in hexane, 575nm peak emission CdSe	5ml 25ml
48-1030  HAZ	Cadmium selenide CANdot® quantum dot (core), 50umol/L in hexane, 600nm peak emission CdSe	5ml 25ml
48-1035  HAZ	Cadmium selenide CANdot® quantum dot (core), 50umol/L in hexane, 625nm peak emission Note: Sold in collaboration with CAN for research purposes.	5ml 25ml
48-1040  HAZ	Cadmium selenide/cadmium sulfide CANdot® quantum dot (core/shell), 50umol/L in hexane, 550nm peak emission CdSe/CdS	1ml 5ml
48-1046  HAZ	Cadmium selenide/cadmium sulfide CANdot® quantum dot (core/shell), 50umol/L in hexane, 575nm peak emission CdSe/CdS	1ml 5ml
48-1052  HAZ	Cadmium selenide/cadmium sulfide CANdot® quantum dot (core/shell), 50umol/L in hexane, 600nm peak emission CdSe/CdS	1ml 5ml
48-1057  HAZ	Cadmium selenide/cadmium sulfide CANdot® quantum dot (core/shell), 50umol/L in hexane, 625nm peak emission CdSe/CdS	1ml 5ml

Products Referenced in the Article

NEW CANdot® Quantum Dots			
48-1063 NEW→ HAZ	Cadmium selenide/cadmium sulfide/zinc sulfide CANdot® quantum dot (core/shell/shell), 50umol/L in hexane, 550nm peak emission CdSe/CdS/ZnS	1ml 5ml	
48-1070 NEW→ HAZ	Cadmium selenide/cadmium sulfide/zinc sulfide CANdot® quantum dot (core/shell/shell), 50umol/L in hexane, 575nm peak emission CdSe/CdS/ZnS	1ml 5ml	
48-1075 NEW→ HAZ	Cadmium selenide/cadmium sulfide/zinc sulfide CANdot® quantum dot (core/shell/shell), 50umol/L in hexane, 600nm peak emission CdSe/CdS/ZnS	1ml 5ml	
48-1080 NEW→ HAZ	Cadmium selenide/cadmium sulfide/zinc sulfide CANdot® quantum dot (core/shell/shell), 50umol/L in hexane, 625nm peak emission CdSe/CdS/ZnS	1ml 5ml	
48-1086 NEW→ HAZ	Cadmium selenide/cadmium sulfide/zinc sulfide CANdot® quantum dot (core/shell/shell), 50umol/L in hexane, 650nm peak emission CdSe/CdS/ZnS	1ml 5ml	
<i>air sensitive, (store cold)</i>			
Note: Sold in collaboration with CAN for research purposes.			

CADIUM Selenide CANdot® QUANTUM DOT (core) KIT, 50umol/L in hexane, 500-625nm peak emissions			
Peak Emission	Particle Size (diameter)	Strem Catalog No. (in hexane)†	Quantum Yield
CdSe core			
500nm	2.7nm	48-1005	>10%
525nm	2.8nm	48-1011	>10%
550nm	3.5nm	48-1017	>10%
575nm	3.9nm	48-1023	>10%
600nm	4.7nm	48-1030	>10%
625nm	5.3nm	48-1035	>10%
Kit: 500-625nm		96-0800	>10%
Kit contains 5ml of each of the above 6 products. Ligand capping agent oleylamine. Stable in dispersions 6 months.			
*Particle size reported excludes ligand capping agent.			
All sizes determined by TEM except for 650nm CdSe/CdS/ZnS which is calculated.			
† Available at nanoparticle concentration of 50umol per liter.			

96-0800 NEW→ HAZ	Cadmium selenide CANdot® quantum dot (core) Kit, 50umol/L in hexane, 500-625nm peak emissions Components available for individual sale. Contains the following:	
48-1005	Cadmium selenide CANdot® quantum dot (core), 50umol/L in hexane, 500nm peak emission	See page 47
48-1011	Cadmium selenide CANdot® quantum dot (core), 50umol/L in hexane, 525nm peak emission	See page 47
48-1017	Cadmium selenide CANdot® quantum dot (core), 50umol/L in hexane, 550nm peak emission	See page 47
48-1023	Cadmium selenide CANdot® quantum dot (core), 50umol/L in hexane, 575nm peak emission	See page 47
48-1030	Cadmium selenide CANdot® quantum dot (core), 50umol/L in hexane, 600nm peak emission	See page 47
48-1035	Cadmium selenide CANdot® quantum dot (core), 50umol/L in hexane, 625nm peak emission	See page 47
<i>air sensitive, (store cold in dark under inert atmosphere)</i>		
Sold in collaboration with CAN for research purposes.		

CADMIUM SELENIDE/CADMIUM SULFIDE CANdot® QUANTUM DOT (core/shell) KIT, 50umol/L in hexane, 550-625nm peak emissions

Peak Emission	Particle Size (diameter)	Strem Catalog No. (in hexane)†	Quantum Yield
CdSe/CdS core/shell			
550nm	3.7nm	48-1040	>30%
575nm	4.1nm	48-1046	>30%
600nm	4.9nm	48-1052	>30%
625nm	5.6nm	48-1057	>30%
Kit: 550-625nm		96-0810	>30%

Kit contains 1ml of each of the above 4 products. Ligand capping agent oleylamine. Stable in dispersions >6 months.

*Particle size reported excludes ligand capping agent.

All sizes determined by TEM except for 650nm CdSe/CdS/ZnS which is calculated.

† Available at nanoparticle concentration of 50µmol per liter.

96-0810 **Cadmium selenide/cadmium CANdot® sulfide quantum dot (core/shell) kit, 50umol/L in hexane, 550-625nm peak emissions**
NEW→
HAZ **Components available for individual sale. Contains the following:**

48-1040	Cadmium selenide/cadmium sulfide CANdot® quantum dot (core/shell), 50umol/L in hexane, 550nm peak emission	See page 47
48-1046	Cadmium selenide/cadmium sulfide CANdot® quantum dot (core/shell), 50umol/L in hexane, 575nm peak emission	See page 47
48-1052	Cadmium selenide/cadmium sulfide CANdot® quantum dot (core/shell), 50umol/L in hexane, 600nm peak emission	See page 47
48-1057	Cadmium selenide/cadmium sulfide CANdot® quantum dot (core/shell), 50umol/L in hexane, 625nm peak emission	See page 47

air sensitive, (store cold in dark under inert atmosphere)

CADMIUM SELENIDE/CADMIUM SULFIDE/ZINC SULFIDE CANdot® QUANTUM DOT (core/shell/shell) KIT, 50umol/L in hexane, 550-650nm peak emissions

Peak Emission	Particle Size (diameter)	Strem Catalog No. (in hexane)†	Quantum Yield
CdSe/CdS/ZnS core/shell/shell			
550nm	4.6nm	48-1063	>40%
575nm	5.1nm	48-1070	>40%
600nm	6.0nm	48-1075	>40%
625nm	6.6nm	48-1080	>40%
650nm	8.5nm	48-1086	>40%
Kit: 550-650nm		96-0820	>40%

Kit contains 1ml of each of the above 5 products. Ligand capping agent hexadecylamine.

Stable in dispersions >12 months.

*Particle size reported excludes ligand capping agent.

All sizes determined by TEM except for 650nm CdSe/CdS/ZnS which is calculated.

† Available at nanoparticle concentration of 50µmol per liter.

96-0820 **Cadmium selenide/cadmium sulfide/zinc sulfide CANdot® quantum dot (core/shell/shell) kit, 50umol/L in hexane, 550-650nm peak emissions**
NEW→
HAZ **Components available for individual sale. Contains the following:**

48-1063	Cadmium selenide/cadmium sulfide/zinc sulfide CANdot® quantum dot (core/shell/shell), 50umol/L in hexane, 550nm peak emission	See page 47
48-1070	Cadmium selenide/cadmium sulfide/zinc sulfide CANdot® quantum dot (core/shell/shell), 50umol/L in hexane, 575nm peak emission	See page 48
48-1075	Cadmium selenide/cadmium sulfide/zinc sulfide CANdot® quantum dot (core/shell/shell), 50umol/L in hexane, 600nm peak emission	See page 48
48-1080	Cadmium selenide/cadmium sulfide/zinc sulfide CANdot® quantum dot (core/shell/shell), 50umol/L in hexane, 625nm peak emission	See page 48
48-1086	Cadmium selenide/cadmium sulfide/zinc sulfide CANdot® quantum dot (core/shell/shell), 50umol/L in hexane, 650nm peak emission	See page 48

air sensitive, (store cold in dark under inert atmosphere)

Sold in collaboration with CAN for research purposes.

New Products Introduced Since The Strem Chemiker Vol. XXV No. 1

BARIUM (Compounds)

56-7510	Barium nitride (99.7%-Ba) [12047-79-9]	1g
NEW→	Ba ₃ N ₂ ; FW: 439.99; -20 mesh black pwdr.	5g

CALCIUM (Compounds)

20-2025	Calcium nitride (99%-Ca) [12013-82-0]	5g
NEW→	Ca ₃ N ₂ ; FW: 148.25; -200 mesh black pwdr.	25g

CARBON (Elemental forms)

06-0512	Fullerene carbon soot	5g
NEW→	(contains 5-8wt% C ₆₀ /C ₇₀ and higher fullerenes) [131159-39-2] black pwdr.	25g

06-0210	Graphene nanoplatelets (6-8 nm thick x 5 microns wide)	25g
NEW→	black platelet	100g

06-0215	Graphene nanoplatelets (6-8 nm thick x 15 microns wide)	25g
NEW→	black platelet	100g

06-0220	Graphene nanoplatelets (6-8 nm thick x 25 microns wide)	25g
NEW→	black platelet	100g

06-0225	Graphene nanoplatelets aggregates	25g
NEW→	(sub-micron particles, surface area 300m ² /g) black platelet	100g

06-0230	Graphene nanoplatelets aggregates	25g
NEW→	(sub-micron particles, surface area 500m ² /g) black platelet	100g

06-0235	Graphene nanoplatelets aggregates	25g
NEW→	(sub-micron particles, surface area 750m ² /g) black platelet	100g

CARBON (Compounds)

96-7052	Paracyclophane Kit
NEW→	See (page 69).

CERIUM (Compounds)

58-5845	Cerium nitride (99.9%-Ce) [25764-08-3]	250mg
NEW→	CeN; FW: 154.12; -60 mesh pwdr.	1g

EUROPIUM (Compounds)

63-1200	Europium nitride (99.9%-Eu) [12020-58-5]	100mg
NEW→	EuN; FW: 165.97; 60 mesh black pwdr.	500mg

HAFNIUM (Compounds)

72-7750	Tetrakis(diethylamino)hafnium, 99% (99.99+%-Hf, <0.2% Zr)	1g
NEW→	PURATREM [19824-55-6]	5g
amp	Hf[N(CH ₂ CH ₃) ₂] ₄ ; FW: 467.01; light yellow liq.	25g
HAZ	moisture sensitive	

IRIDIUM (Compounds)

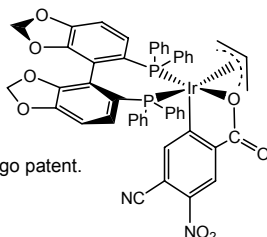
77-5075

NEW→

[(S)-(-)-5,5'-Bis(diphenylphosphino)-4,4'-bi-1,3-benzodioxole][4-cyano-3-nitrobenzenecarboxylato][1,2,3η²-propenyl]iridium(III), min. 98% [1221768-92-8]

C₄₉H₃₅IrN₂O₈P₂; FW: 1033.98; yellow powdr.

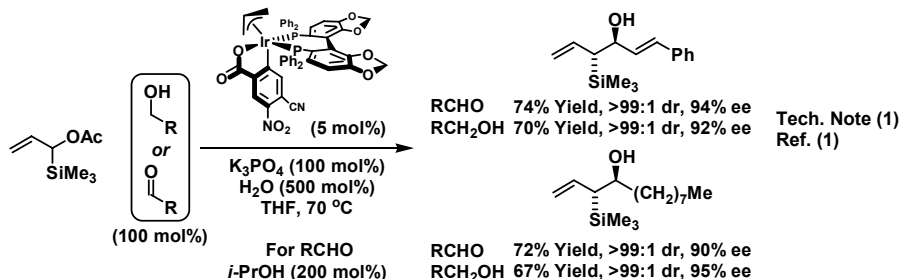
Note: Manufactured under license of Takasago patent.



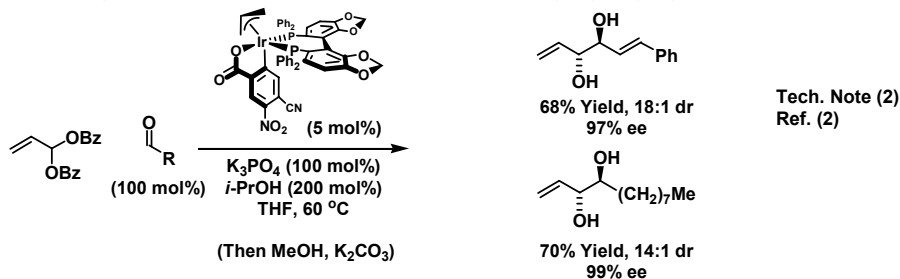
100mg
500mg

Technical Notes:

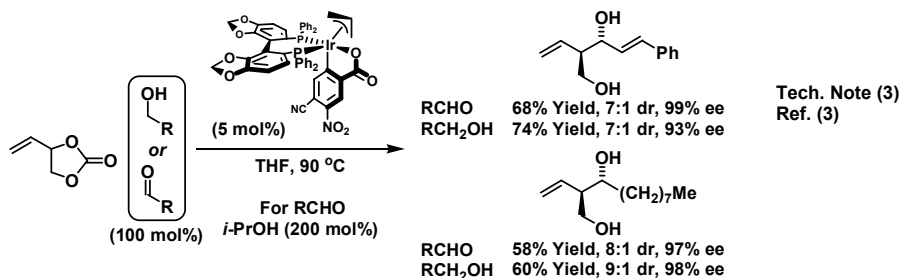
1. Catalyst used for the diastereo- and enantioselective carbonyl (trimethylsilyl)allylation from the alcohol, or aldehyde, oxidation level.



2. Catalyst used for the diastereo- and enantioselective carbonyl (hydroxy)allylation to form anti-1,2-diols.



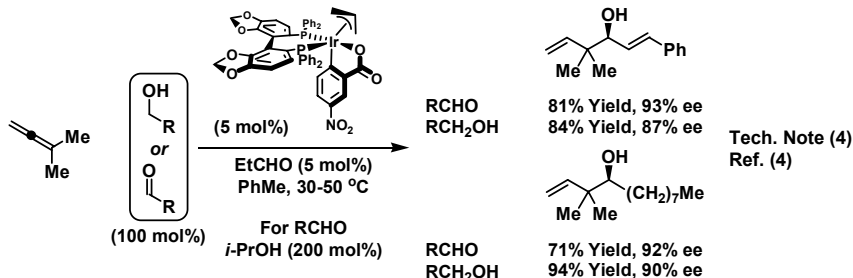
3. Catalyst used for the diastereo- and enantioselective carbonyl (hydroxymethyl)allylation from the alcohol, or aldehyde, oxidation level.



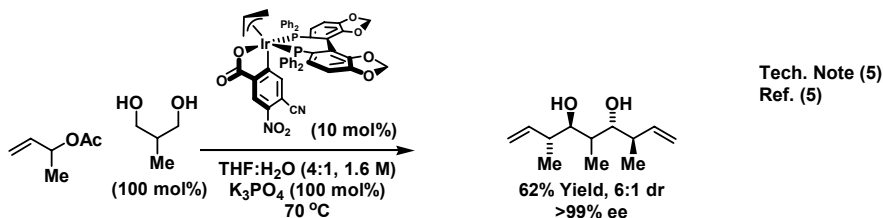
IRIDIUM (Compounds)

77-5075 [(S)-(-)-5,5'-Bis(diphenylphosphino)-4,4'-bi-1,3-benzodioxole][4-cyano-3-nitrobenzenecarboxylato][1,2,3η2-propenyl]iridium(III), min. 98% [1221768-92-8]
NEW→
 (cont.)

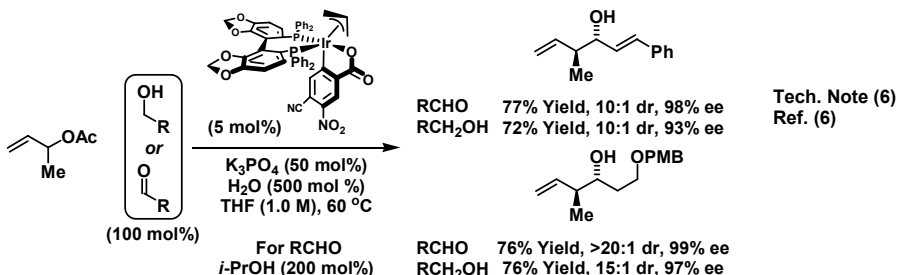
4. Catalyst used for the diastereo- and enantioselective carbonyl tert-prenylation from the alcohol, or aldehyde, oxidation level.



5. Catalyst used for the diastereo- and enantioselective carbonyl double crotylation of 1,3-diols.



6. Catalyst used for the diastereo- and enantioselective carbonyl crotylation from the alcohol or aldehyde oxidation level.



References:

1. *J. Am. Chem. Soc.*, **2010**, 132, 9153.
2. *J. Am. Chem. Soc.*, **2010**, 132, 1760.
3. *J. Am. Chem. Soc.*, **2010**, 132, 4562.
4. *J. Am. Chem. Soc.*, **2009**, 131, 6916.
5. *J. Am. Chem. Soc.*, **2011**, 133, in press.
6. *J. Org. Chem.*, **2011**, 76, 2350.

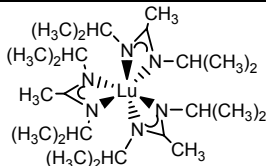
New Products Introduced Since The Strem Chemiker Vol. XXV No. 1

LANTHANUM (Compounds)

57-5737	Lanthanum(III) chloride, lithium chloride complex 0.6M	0.05mole
NEW→	(15wt% ±2wt%) in tetrahydrofuran [10099-58-8]	0.25mole
HAZ	LaCl ₃ ·LiCl; FW: 287.66; colorless to pale yellow liq. <i>moisture sensitive</i> Note: A product of Chemetall. Sold for R&D purposes only.	

LUTETIUM (Compounds)

71-1050	Tris(N,N'-di-i-propylacetamidinato) lutetium(III), 99%	250mg
NEW→	Lu(C₈H₁₇N₂)₃; FW: 598.67;	1g
	white to off-white powdr. Note: Product sold under, use subject to, terms and conditions of label license at www.strem.com/harvard2 .	



MAGNESIUM (Compounds)

12-0815	Methylmagnesium bromide, 3.2M (35wt% ±1wt%)	0.25mole
NEW→	In 2-methyltetrahydrofuran [75-16-1]	1mole
HAZ	CH ₃ MgBr; FW: 119.26; liq. <i>air sensitive, moisture sensitive</i> Note: A product of Chemetall. Sold for R&D purposes only.	

12-0803	sec-Butylmagnesium chloride, lithium chloride complex 1.2M	0.25mole
NEW→	(15wt% ±1wt%) in tetrahydrofuran [15366-08-2]	1mole
HAZ	CH ₃ CH ₂ CH(CH ₃)MgCl·LiCl; FW: 159.26; dark brown liq. <i>air sensitive, moisture sensitive</i> Note: A product of Chemetall. Sold for R&D purposes only.	

12-0810	Ethylmagnesium bromide, 3.4M (40wt% ±1wt%)	0.25mole
NEW→	In 2-methyltetrahydrofuran [925-90-6]	1mole
HAZ	C ₂ H ₅ BrMg; FW: 133.28; dark brown liq. <i>air sensitive, moisture sensitive</i> Note: A product of Chemetall. Sold for R&D purposes only.	

12-0820	Phenylmagnesium bromide, 2.9M (45wt% ±1wt%)	0.25mole
NEW→	in 2-methyltetrahydrofuran [100-58-3]	1mole
HAZ	C ₆ H ₅ BrMg; FW: 136.88; liq. <i>air sensitive, moisture sensitive</i> Note: A product of Chemetall. Sold for R&D purposes only.	

12-0825	i-Propylmagnesium bromide, 2.9M (35wt% ±1wt%)	0.25mole
NEW→	in 2-methyltetrahydrofuran [920-39-8]	1mole
HAZ	(CH ₃) ₂ CHMgBr; FW: 147.30; liq. <i>air sensitive, moisture sensitive</i> Note: A product of Chemetall. Sold for R&D purposes only.	

12-0827	i-Propylmagnesium chloride, lithium chloride complex 1.3M	0.25mole
NEW→	(14wt% ±1wt%) in tetrahydrofuran [1068-55-9]	1mole
HAZ	(CH ₃) ₂ CHMgCl·LiCl; FW: 145.24; yellow-brown liq. <i>air sensitive, moisture sensitive</i> Note: A product of Chemetall. Sold for R&D purposes only.	

12-0832	2,2,6,6-Tetramethylpiperidinylmagnesium chloride, lithium chloride complex 1.0M (18wt% ±2wt%) in toluene/tetrahydrofuran	0.05mole
NEW→	[215863-85-7]	0.25mole
HAZ	C ₉ H ₁₈ NMgCl; FW: 200.00; brown liq. <i>air sensitive, moisture sensitive</i> Note: A product of Chemetall. Sold for R&D purposes only.	

MERCURY (Elemental forms)

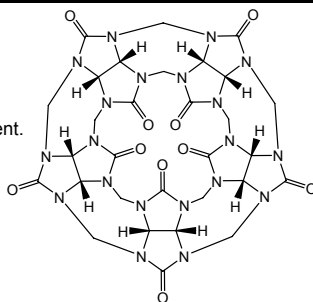
80-1105	Sodium-Mercury Amalgam, 4-5% Na (99.9+%) [11110-52-4]	5g
NEW→	spherical pellets	25g
amp	<i>air sensitive, moisture sensitive</i>	
HAZ		

NANOMATERIALS (Compounds)

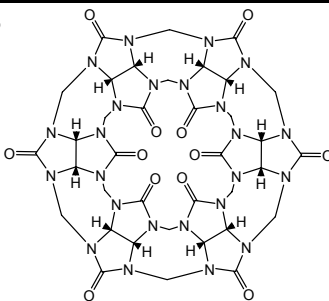
26-0032	Iron(II,III) oxide (Magnetite) aqueous magnetic fluid	2ml
NEW→	[3.5 vol%, Ms = 15-16 kA/m] [1317-61-9]	10ml
	Fe ₃ O ₄ ; black solid (water suspension)	
26-0036	Iron(II,III) oxide (Magnetite) aqueous magnetic fluid	2ml
NEW→	[7.0 vol%, Ms = 30-31 kA/m] [1317-61-9]	10ml
	Fe ₃ O ₄ ; black solid (water suspension)	

NITROGEN (Compounds)

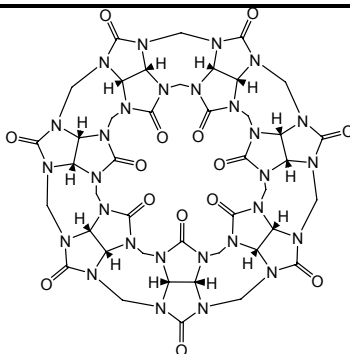
96-7054	Cucurbituril Kit	
NEW→	See (page 67).	
07-1310	Cucurbit[5]uril (CB[5]) ammonium sulfate hydrate, 99+% [259886-49-2]	100mg
NEW→	C ₃₀ H ₃₀ N ₂₀ O ₁₀ ·NH ₄) ₂ SO ₄ ·XH ₂ O; FW: 962.83; white solid Note: Sold for R&D purposes only. US 6365734. Cucurbituril Kit component. See (page 67).	



07-1320	Cucurbit[6]uril (CB[6]) hydrate, 99+%	500mg
NEW→	[80262-44-8] C ₃₆ H ₃₆ N ₂₄ O ₁₂ ·XH ₂ O; FW: 996.82; white solid Note: Cucurbituril Kit component. See (page 67).	



07-1325	Cucurbit[7]uril (CB[7]) hydrate, 99+%	50mg
NEW→	[259886-50-5] C ₄₂ H ₄₂ N ₂₈ O ₁₄ ·XH ₂ O; FW: 1162.96; white solid Note: Sold for R&D purposes only. US 6365734. Cucurbituril Kit component. See (page 67).	



NITROGEN (Compounds)

07-1330

NEW→

Cucurbit[8]uril (CB[8]) hydrate, 99+%

[259886-51-6]

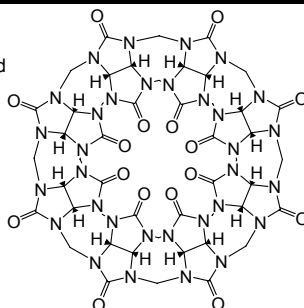
 $C_{48}H_{48}N_{32}O_{16} \cdot H_2O$; FW: 1329.10; white solid

Note: Sold for R&D purposes only.

US 6365734. Cucurbitural Kit component.

See (page 67).

25mg



07-0385

NEW→

N,N'-Di-t-butyl-2,3-diaminobutane, 98%

[1167987-07-6]

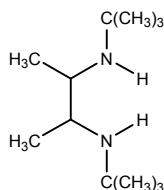
 $(C_4H_9)NHCH(CH_3)CH(CH_3)NH(C_4H_9)$;

FW: 200.36; colorless, viscous liq.

air sensitive

500mg

2g



07-0398

NEW→

Diethylenetriaminepentaacetic acid, 98.5% DTPA (USP) [67-43-6] $(HO_2CCH_2)_2N(CH_2)_2N(CH_2CO_2H)(CH_2)_2N(CH_2CO_2H)_2$; FW: 393.35;

white xtl.

50g

250g

07-0412

NEW→

Diethylenetriaminepentaacetic acid, 99% DTPA [67-43-6] $(HO_2CCH_2)_2N(CH_2)_2N(CH_2CO_2H)(CH_2)_2N(CH_2CO_2H)_2$; FW: 393.35;

white xtl.

25g

100g

07-0610

NEW→

Ethylene glycol-bis(2-aminoethyl)-**N,N,N',N'-tetraacetic acid, 99%**

EGTA [67-42-5]

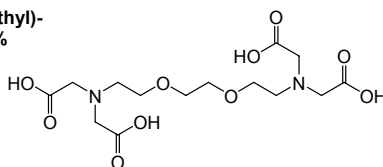
 $(HOOCCH_2)_2N(CH_2CH_2O)_2$ $CH_2CH_2N(CH_2COOH)_2$;

FW: 380.35;

white xtl.

25g

100g



07-4017

NEW→

1-(2,6-Di-i-propylphenyl)-3-(2,4,6-trimethylphenyl)-4,5-dihydro-imidazolium chloride, min. 97%

[866926-59-2]

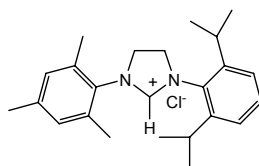
 $C_{24}H_{33}ClN_2$; FW: 384.99;

white to pink solid

air sensitive

500mg

2g



07-1322

NEW→

Perallyloxycucurbit[6]uril (AOCB[6])**potassium sulfate, 94+%** $C_{72}H_{84}N_{24}O_{24} \cdot XK_2SO_4$; FW: 1668.61;

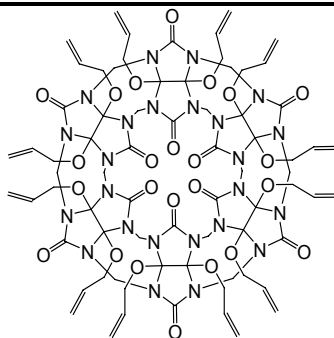
white solid

Note: Sold for R&D purposes only.

US 7388099. Cucurbitural Kit component.

See (page 67).

25mg



OXYGEN (Compounds)

96-7052 Paracyclophane Kit

NEW→ See (page 69).

PALLADIUM (Compounds)

46-0255 Chloromethyl(1,5-cyclooctadiene)palladium(II), 98% [63936-85-6]

250mg

NEW→ $\text{PdCl}(\text{CH}_3)(\text{C}_8\text{H}_{12})$; FW: 265.09; pale yellow powdr.

1g

air sensitive

46-1870 Palladium(II) hexafluoroacetylacetonate, min. 98% [64916-48-9]

250mg

NEW→ $\text{Pd}(\text{CF}_3\text{COCHCOCF}_3)_2$; FW: 520.52; yellow powdr.

1g

5g

PHOSPHORUS (Compounds)

96-4100 Garphos™ Ligand Kit

NEW→ See (page 68).

15-1661 (R)-2,2'-Bis[bis(3,5-dimethylphenyl)phosphino]-4,4',6,6'-tetramethoxybiphenyl, min. 97% (R)-Xyl-Garphos™

100mg

500mg

NEW→ $\text{C}_{48}\text{H}_{52}\text{O}_4\text{P}_2$; FW: 754.87; white xtl.

air sensitive

Note: Sold in collaboration with KCT.

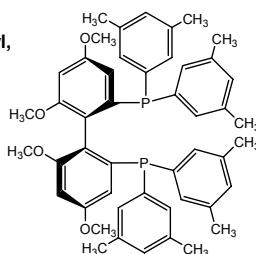
Patent US App No. 61/381,493.

Garphos™ Ligand Kit component.

See (page 68).

Technical Note:

1. See 15-1653 (page 58).



15-1662 (S)-2,2'-Bis[bis(3,5-dimethylphenyl)phosphino]-4,4',6,6'-tetramethoxybiphenyl, min. 97% (S)-Xyl-Garphos™

100mg

500mg

NEW→ $\text{C}_{48}\text{H}_{52}\text{O}_4\text{P}_2$; FW: 754.87; white xtl.

air sensitive

Note: Sold in collaboration with KCT. Patent US App No. 61/381,493.

Garphos™ Ligand Kit component. See (page 68).

Technical Note:

1. See 15-1653 (page 58).

15-1672 (R)-2,2'-Bis[bis(4-methoxy-3,5-di-t-butylphenyl)phosphino]-4,4',6,6'-tetramethoxybiphenyl, min. 97% (R)-DTBM-Garphos™

100mg

500mg

NEW→ $\text{C}_{76}\text{H}_{108}\text{O}_8\text{P}_2$; FW: 1211.61; white xtl.

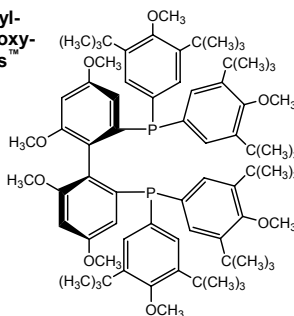
air sensitive, light sensitive

Note: Sold in collaboration with KCT.

Patent US App No. 61/381,493.

Garphos™ Ligand Kit component.

See (page 68).



Technical Note:

1. See 15-1653 (page 58).

15-1673 (S)-2,2'-Bis[bis(4-methoxy-3,5-di-t-butylphenyl)phosphino]-4,4',6,6'-tetramethoxybiphenyl, min. 97% (S)-DTBM-Garphos™

100mg

500mg

NEW→ $\text{C}_{76}\text{H}_{108}\text{O}_8\text{P}_2$; FW: 1211.61; white xtl.

air sensitive, light sensitive

Note: Sold in collaboration with KCT. Patent US App No. 61/381,493.

Garphos™ Ligand Kit component. See (page 68).

Technical Note:

1. See 15-1653 (page 58).

PHOSPHORUS (Compounds)

15-1666

NEW→

(R)-2,2'-Bis[bis(4-methoxy-3,5-dimethylphenyl)phosphino]-4,4',6,6'-tetramethoxybiphenyl, min. 97% (R)-DMM-Garphos™
C₅₂H₆₀O₈P₂; FW: 874.98; white xtl.

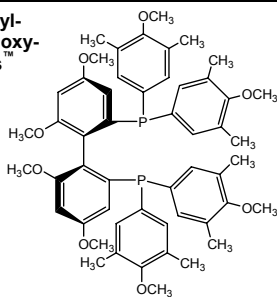
air sensitive

Note: Sold in collaboration with KCT.

Patent US App No. 61/381,493.

Garphos™ Ligand Kit component.

See (page 68).



100mg

500mg

Technical Note:

1. See 15-1653 (page 58).

15-1667

NEW→

(S)-2,2'-Bis[bis(4-methoxy-3,5-dimethylphenyl)phosphino]-4,4',6,6'-tetramethoxybiphenyl, min. 97% (S)-DMM-Garphos™
C₅₂H₆₀O₈P₂; FW: 874.98; white xtl.

air sensitive

Note: Sold in collaboration with KCT. Patent US App No. 61/381,493.

Garphos™ Ligand Kit component. See (page 68).

Technical Note:

1. See 15-1653 (page 58).

100mg

500mg

15-1663

NEW→

(R)-2,2'-Bis[bis(3,5-trifluoromethylphenyl)phosphino]-4,4',6,6'-tetramethoxybiphenyl, min. 97% (R)-BTfM-Garphos™
C₄₈H₂₈F₂₄O₄P₂; FW: 1186.64; white xtl.

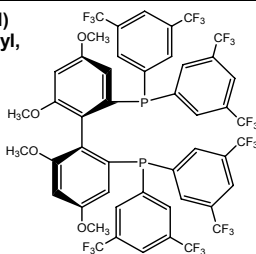
air sensitive

Note: Sold in collaboration with KCT.

Patent US App No. 61/381,493.

Garphos™ Ligand Kit component.

See (page 68).



100mg

500mg

Technical Note:

1. See 15-1653 (page 58).

15-1664

NEW→

(S)-2,2'-Bis[bis(3,5-trifluoromethylphenyl)phosphino]-4,4',6,6'-tetramethoxybiphenyl, min. 97% (S)-BTfM-Garphos™
C₄₈H₂₈F₂₄O₄P₂; FW: 1186.64; white xtl.

air sensitive

Note: Sold in collaboration with KCT. Patent US App No. 61/381,493.

Garphos™ Ligand Kit component. See (page 68).

Technical Note:

1. See 15-1653 (page 58).

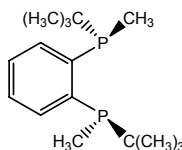
100mg

500mg

15-0166

NEW→

(R,R)-(+)-1,2-Bis(di-t-butylmethylphosphino)benzene (R,R)-BenzP* [919778-41-9]
C₁₆H₁₈P₂; FW: 282.34; white xtl.;
[α]_D +223° (c 0.54, AcOEt)
air sensitive

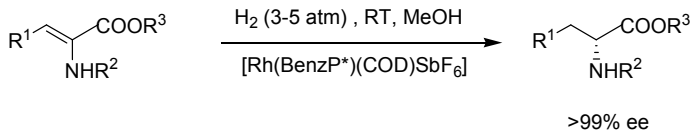


50mg

250mg

Technical Note:

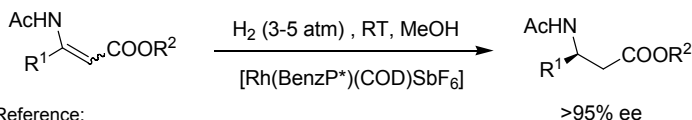
1. The rhodium complex of BenzP* is highly active in the asymmetric hydrogenation of various functionalized alkenes (ee >99%).



PHOSPHORUS (Compounds)

15-0166 (R,R)-(+)-1,2-Bis(di-t-butylmethylphosphino)enzene (R,R)-BenzP*
NEW→ [919778-41-9]
 (cont.)

Technical Note (cont.)



Reference:

1. *Org. Lett.*, **2010**, 12, 4400.

15-0167 (S,S)-(-)-1,2-Bis(di-t-butylmethylphosphino)benzene (S,S)-BenzP*
NEW→ C₁₆H₁₈P₂; FW: 282.34; white xtl.; [α]_D -223° (c 0.54, AcOEt);
 m.p. 125-126°
air sensitive

50mg
 250mg

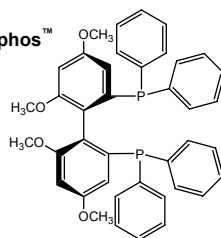
Technical Note:

1. See 15-0166 (page 57).

15-1653 (R)-2,2'-Bis(diphenylphosphino)-4,4',6,6'-
NEW→ tetramethoxybiphenyl, min. 97% (R)-Ph-Garphos™
 C₄₀H₃₆O₄P₂; FW: 642.66; white xtl.
air sensitive

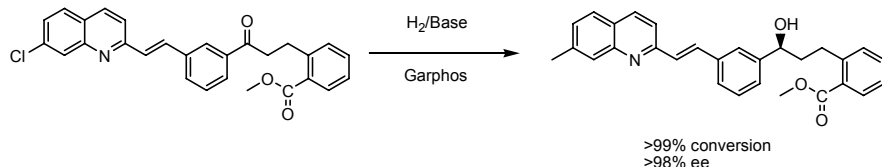
100mg
 500mg

Note: Sold in collaboration with KCT.
 Patent US App No. 61/381,493. Garphos™
 Ligand Kit component. See (page 68).

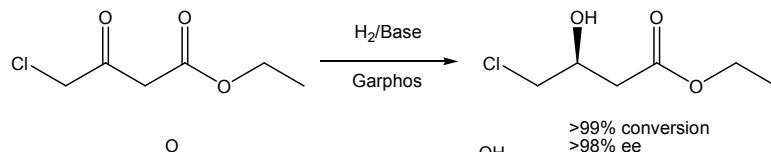


Technical Note:

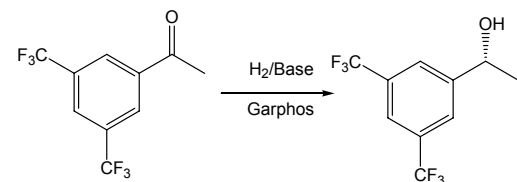
1. Chiral ligand used in the preparation of hydrogenation catalysts with exceptionally high activity and selectivity.



Tech. Note. (1)
Ref. (1)



Tech. Note. (2)
Ref. (1)



Tech. Note. (3)
Ref. (1)

S:C = 100,000:1
 >99% conversion
 >99% ee

Reference:

1. US Patent Application No. 61/381,493.

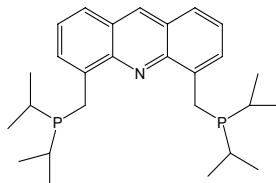
PHOSPHORUS (Compounds)

15-1654 (S)-2,2'-Bis(diphenylphosphino)-4,4',6,6'-tetramethoxybiphenyl, min. 97% (S)-Ph-Garphos[™] 100mg
NEW→ 500mg
 $C_{40}H_{36}O_4P_2$; FW: 642.66; white xtl.
 air sensitive
 Note: Sold in collaboration with KCT. Patent US App No. 61/381,493.
 Garphos[™] Ligand Kit component. See (page 68).

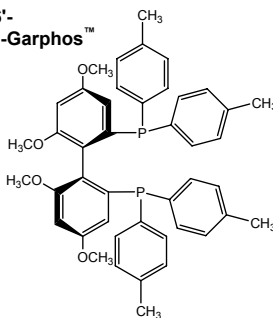
Technical Note:

1. See 15-1653 (page 58).

15-0415 4,5-Bis-(di-i-propylphosphino-methyl)acridine, 98+% [1101230-28-7] 50mg
NEW→ 250mg
 $C_{27}H_{38}NP_2$; FW: 439.55; yellow xtl.
 air sensitive
 Note: Patents: US provisional 61/087,708, PCT/IL2009/000778.



15-1657 (R)-2,2'-Bis(di-p-tolylphosphino)-4,4',6,6'-tetramethoxybiphenyl, min. 97% (R)-Tol-Garphos[™] 100mg
NEW→ 500mg
 $C_{44}H_{44}O_4P_2$; FW: 698.77; white xtl.
 air sensitive
 Note: Sold in collaboration with KCT. Patent US App No. 61/381,493.
 Garphos[™] Ligand Kit component. See (page 68).



Technical Note:

1. See 15-1653 (page 58).

15-1658 (S)-2,2'-Bis(di-p-tolylphosphino)-4,4',6,6'-tetramethoxybiphenyl, min. 97% (S)-Tol-Garphos[™] 100mg
NEW→ 500mg
 $C_{44}H_{44}O_4P_2$; FW: 698.77; white xtl.
 air sensitive
 Note: Sold in collaboration with KCT. Patent US App No. 61/381,493.
 Garphos[™] Ligand Kit component. See (page 68).

Technical Note:

1. See 15-1653 (page 58).

15-0405 1,2-Bis(phenylphosphino)ethane [18899-64-4] 500mg
NEW→ 2g
 $(C_6H_5)_2PCH_2CH_2P(C_6H_5)_2$; FW: 246.22; colorless to yellow liq.
 pyrophoric

amp
 HAZ
 NO UPS



PHOSPHORUS (Compounds)

15-0570

NEW→

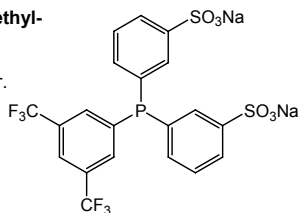
Bis(3-sulfonatophenyl)(3,5-di-trifluoromethyl-phenyl)phosphine, disodium salt, min. 97% DANPHOS [1289463-82-6]

$C_{20}H_{13}F_6Na_2O_6PS_2$; FW: 604.39; white powdr.

Note: Sold under license from UAB

for research purposes only.

PCT/EP2010/065531.



100mg

500mg

Technical Note:

1. Water soluble phosphine.

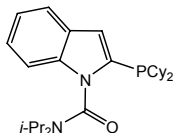
15-1086

NEW→

2-(Dicyclohexylphosphino)-N,N-bis(1-methylethyl)-1H-indole-1-carboxamide, min. 98% Amidole-Phos [1067175-36-3]

$C_{27}H_{41}N_2OP$; FW: 440.60;

white to off-white powdr.; m.p. 192.1-193.8°

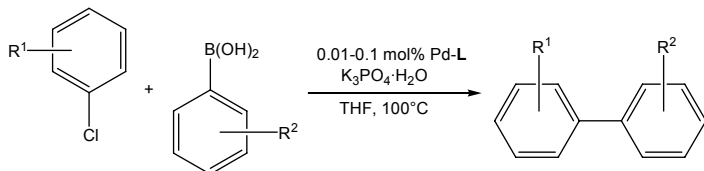


100mg

500mg

Technical Note:

1. Suzuki-Miyaura Coupling of Aryl Chlorides (low catalyst loading).



$R^1 = \text{Me, MeO, NH}_2, \text{CO}_2\text{Me, COMe, pyr}$; $R^2 = \text{Me, Np, Bu}$

up to 99% yield

Tech. Note (1)
Ref. (1)

Reference:

1. *J. Org. Chem.* **2008**, 73, 7803.

15-1087

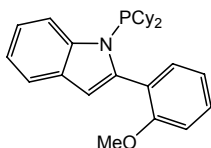
NEW→

1-(Dicyclohexylphosphino)-2-(2-methoxyphenyl)-1H-indole, min. 98% NPCy o-Andole-Phos [947402-60-0]

$C_{27}H_{34}NOP$; FW: 419.54;

white to off-white powdr.;

m.p. 131.1-132.5°

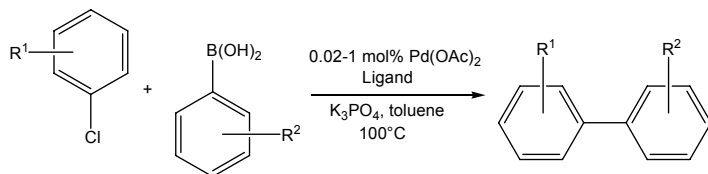


100mg

500mg

Technical Note:

1. Suzuki-Miyaura Coupling of Aryl and Hetero-aryl Chlorides.



$R^1 = \text{Me, MeO, NH}_2, \text{CO}_2\text{Me, COMe, pyr}$; $R^2 = \text{Me, Np, Bu}$

up to 99% yield

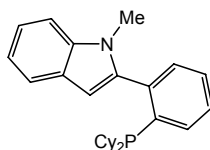
Tech. Note (1)
Ref. (1)

Reference:

1. *Org. Lett.* **2007**, 9, 2795.

PHOSPHORUS (Compounds)

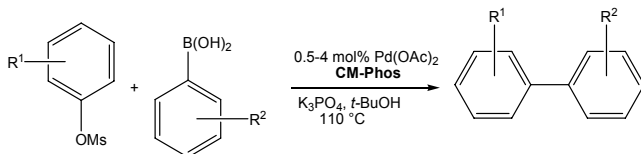
15-1088
NEW→
2-[2-(Dicyclohexylphosphino)phenyl]-1-methyl-1H-indole, min. 98% CM-Phos
 [1067883-58-2]
 $C_{27}H_{34}NP$; FW: 403.54;
 white to off-white powdr.;
 m.p. 171.9-174.9°



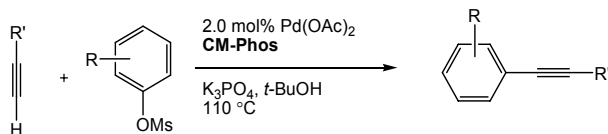
100mg
 500mg

Technical Notes:

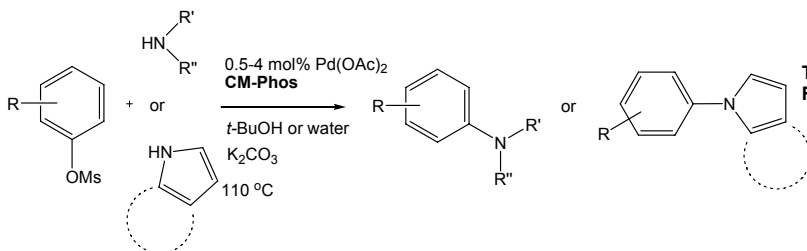
1. Suzuki-Miyaura Coupling of Aryl Mesylates bearing alkyl, methoxy, aldehyde, keto, nitrile, ester, and heteroaryl substitution.
2. Sonogashira Coupling of Aryl Mesylates, $R' = \text{alkyl, aryl}$; $R = C(O)R, COOMe, CHO, CN$.
3. Buchwald-Hartwig Amination of Aryl Mesylates, $R = \text{cyano, chloro, methoxy, keto, ester and etc.}$
4. Additional catalyzed reactions include Cyanation of functional Aryl Mesylates and Chlorides (Ref. 4,5); Hiyama Coupling of Aryl Mesylates (Ref. 6); Direct Arylation of Heterocycles with Aryl Mesylates (Ref. 7); Borylation of Aryl Mesylates (Ref. 8).



Tech. Note (1)
Ref. (1)



Tech. Note (2)
Ref. (2)

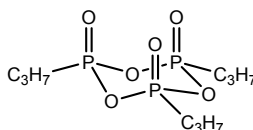


Tech. Note (3)
Ref. (3)

References:

1. *Angew. Chem. Int. Ed.*, **2008**, 47, 8059.
2. *Chem. Eur. J.*, **2010**, 16, 9982.
3. *Angew. Chem. Int. Ed.*, **2008**, 47, 6402.
4. *Angew. Chem. Int. Ed.*, **2010**, 49, 8918.
5. *Org. Lett.*, **2011**, 13, 648.
6. *Org. Lett.*, **2009**, 11, 317.
7. *Chem. Eur. J.*, **2011**, 17, 761.
8. *Chem. Eur. J.*, **2011**, 17, 6913.

15-9159
NEW→
HAZ
2,4,6-Tripropyl-2,4,6-trioxo-1,3,5,2,4,6-trioxatri-phosphorinane (Propylphosphonic acid anhydride 50% solution in N,N-dimethylformamide) [68957-94-8]
 $(C_3H_7O_2P)_3$; FW: 318.20;
 slightly yellow to brown liq.



10g
 50g

15-9160
NEW→
HAZ
2,4,6-Tripropyl-2,4,6-trioxo-1,3,5,2,4,6-trioxatriphosphorinane (Propylphosphonic acid anhydride 50% solution in ethyl acetate) [68957-94-8]
 $(C_3H_7O_2P)_3$; FW: 318.20; slightly yellow to brown liq.

10g
 50g

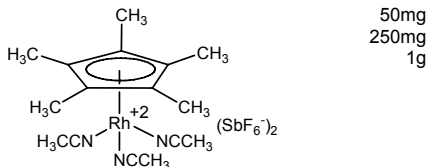
PHOSPHORUS (Compounds)

15-9155 **Vinylphosphonic acid, min. 90% [1746-03-8]** 50g
 $\text{CH}_2=\text{CHP}(\text{O})(\text{OH})_2$; FW: 108.00; colorless to pale-yellow liq. 250g
NEW→
 HAZ

15-9158 **Vinylphosphonic acid dimethyl ester, min. 90% [4645-32-3]** 50g
 $\text{CH}_2=\text{CHP}(\text{O})(\text{OCH}_3)_2$; FW: 136.10; colorless liq. 250g
NEW→
 HAZ (store cold)

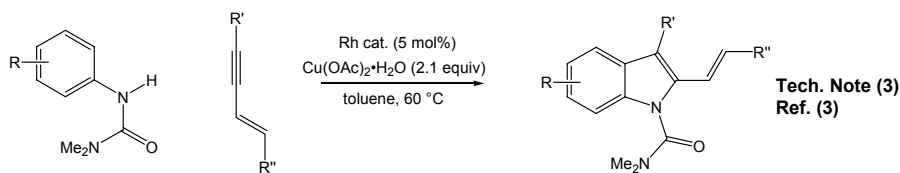
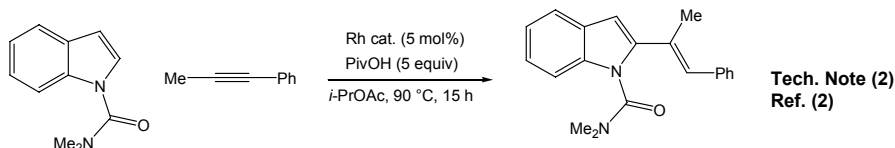
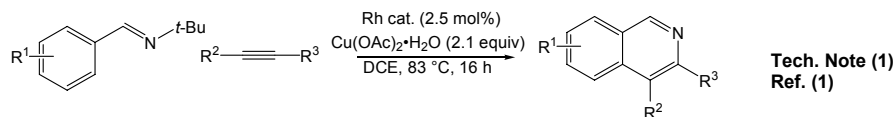
RHODIUM (Compounds)

45-2160 **Tris(acetonitrile)pentamethylcyclopentadienylrhodium(III) hexafluoroantimonate, min. 98% [59738-27-1]**
 $[\text{Rh}(\text{C}_{10}\text{H}_{15})(\text{CH}_3\text{CN})_3]^+(\text{SbF}_6^-)_2$;
 FW: 832.79; light yellow powdr.



Technical Notes:

1. Catalyst used for the oxidative, cross-coupling/cyclization of aryl aldimines and alkynes.
2. Catalyst used for the intermolecular hydroarylation of alkynes.
3. Catalyst useful for the **Fagnou Indole/Pyrrole Synthesis**.



References:

1. *J. Am. Chem. Soc.*, **2009**, 131, 12050.
2. *J. Am. Chem. Soc.*, **2010**, 132, 6910.
3. *Angew. Chem. Int. Ed.*, **2011**, 50, 1338.

RUTHENIUM (Compounds)

44-0217

NEW→

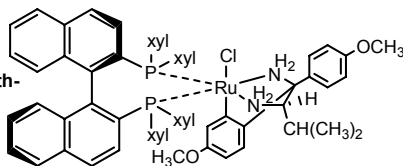
Chloro((R)-(+)-2,2'-bis
[di(3,5-xylyl)phosphino]-1,
1'-binaphthyl)][(2R)-(-)-1-
(4-methoxyphenyl)-1'-(4-meth-
oxyphenyl-kC)-3-methyl-
1,2-butanediamine]
ruthenium(II)

(R)-RUCY™-XylBINAP

C₇₁H₇₃ClN₂O₂P₂Ru₂; FW: 1184.82; yellow to dark brown/green solid
air sensitive

Note: Manufactured under license of Takasago patent application no.
JP2010-104552. Takasago BINAP Ru Diamine Catalyst Kit
component. Takasago ATH Catalyst Kit component.

Visit www.strem.com.



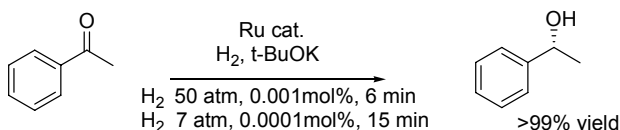
250mg

1g

5g

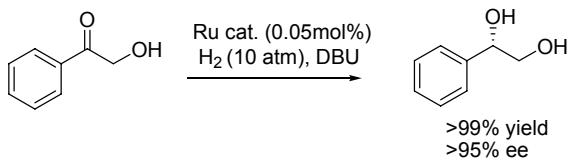
Technical Note:

1. Catalyst used for the rapid, and highly selective hydrogenation of ketones.

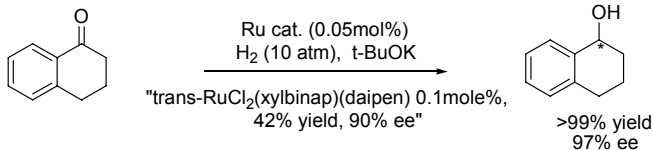


Tech Note (1)
Ref. (1,2)

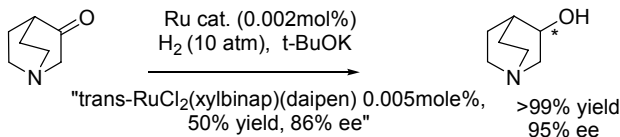
"trans-RuCl₂(xylbinap)(daipen) 0.002%, 120 min"



Tech. Note (2)
Ref. (1,2)



Tech. Note (3)
Ref. (1,2)



Tech. Note (4)
Ref. (1,2)

References:

1. Patent Application No. JP2010-104552.
2. J. Am. Chem. Soc., **2011**, 133, 10696.

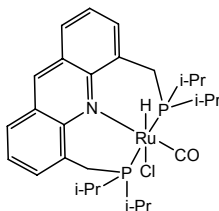
While supplies last, with any purchase of a Takasago product, receive 100mg of 44-0217 at no additional charge. Supplies are limited. This Bonus Offer is limited to one bonus per customer order. Please add 100mg of 44-0217 at the time your order is placed.

RUTHENIUM (Compounds)

44-0525

NEW→

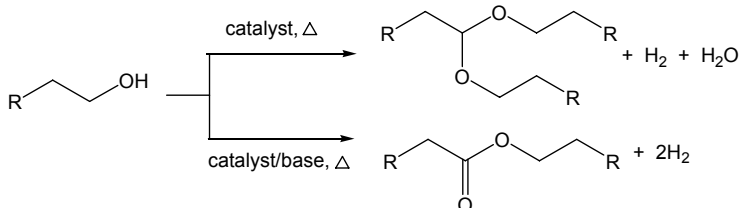
**Chlorocarbonylhydrido[4,5-bis-(di-*i*-propylphosphinomethyl)acridine] ruthenium(II), min.98%
Milstein Acridine Catalyst [1101230-25-4]
C₂₈H₄₀ClNOP₂Ru; FW: 605.09; orange solid
air sensitive
Note: Patents: US provisional 61/087,708, PCT/IL2009/000778.**



25mg
100mg

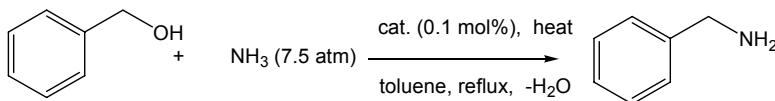
Technical Notes:

- Useful ruthenium catalyst for the direct conversion of alcohols to acetals and esters.



**Tech. Note (1)
Ref. (1)**

- Useful ruthenium catalyst for the selective synthesis of amines directly from alcohols and ammonia.



**Tech. Note (2)
Ref. (2)**

References:

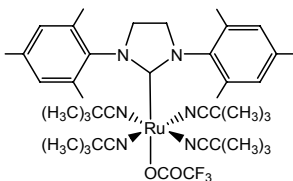
- J. Am. Chem. Soc.*, **2009**, 131, 3146.
- Angew. Chem. Int. Ed.*, **2008**, 47, 8661.

44-7712

NEW→

**Trifluoroacetato[4,5-dihydro-1,3-bis(2,4,6-trimethylphenyl)imidazol-2-ylidene]tetra(2,2-dimethylpropanenitrile) ruthenium(II) trifluoroacetate [1034198-65-6]
C₄₅H₆₂F₆N₆O₄Ru; FW: 966.08; yellow xtl.**

Note: Sold under license from ITCF for research purposes only. DE 102008008299, US 12/866.806.



100mg
500mg

Technical Note:

- Cationic ruthenium(II) complex useful for UV-induced, ring-opening metathesis polymerization.

Reference:

- Angew. Chem. Int. Ed.*, **2008**, 47, 3267.

SODIUM (Elemental forms)

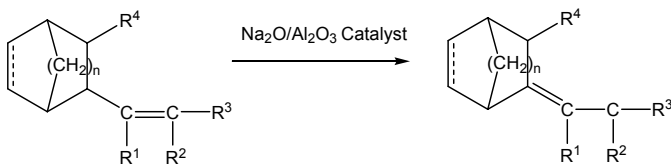
80-1105

NEW→

**Sodium-Mercury Amalgam, 4-5% Na (99.9+%)
SEE MERCURY SECTION (page 54)**

SODIUM (Compounds)

11-1007	Sodium oxide/sodium on alumina, Olefin Isomerization Catalyst	10g
NEW→	(Na₂O 11.5-13.5%, Na 1.8-3.0%)	50g
HAZ	Na ₂ O/Na; white solid <i>moisture sensitive</i>	



Catalyst benefits:

- Very active and highly selective olefin isomerization catalyst
- Highly resistant to catalyst poisons (tetrahydroindene, cyclopentadiene, etc.)

Uses:

- Diene monomer in the production of EPDM rubber.
- Scent carrier for flavors and fragrances.

STRONTIUM (Compounds)

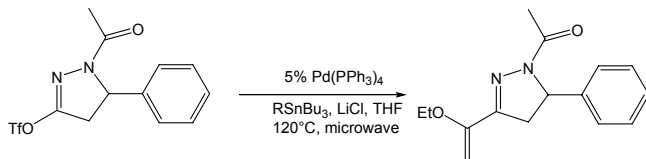
38-3840	Strontium hydride (99.5%-Sr) [13598-33-9]	1g
NEW→	SrH ₂ ; FW: 89.64; -60 mesh gray powdr.	5g
38-3860	Strontium nitride (99.5%-Sr) [12033-82-8]	1g
NEW→	Sr ₃ N ₂ ; FW: 290.87; -60 mesh tan powdr.	5g

TIN (Compounds)

50-1150	N,N'-Di-t-butyl-2,3-diamidobutanetin(II), 98%	250mg
NEW→	[1268357-44-3]	1g
amp	C ₁₂ H ₂₆ N ₂ Sn; FW: 317.06; white to off-white powdr. (store cold) Note: US Patent Application 61/320,069 filed April 1, 2010. Product sold under, use subject to, terms and conditions of label license at www.strem.com/harvard3 .	
50-1815	Tetrakis(dimethylamino)tin(IV), 99% TDMASn [1066-77-9]	1g
NEW→	Sn[N(CH ₃) ₂] ₄ ; FW: 295.01; colorless liq.; b.p. 51° (15mm)	5g
amp	<i>moisture sensitive</i>	
98-4050	Tetrakis(dimethylamino)tin(IV), 99% TDMASn, 50-1815, contained in 50 ml Swagelok® cylinder for CVD/ALD [1066-77-9]	10g
NEW→	Sn[N(CH ₃) ₂] ₄ ; FW: 295.01; colorless liq.; b.p. 51° (15mm)	
HAZ	<i>moisture sensitive</i>	
50-3015	Tributyl(1-ethoxyvinyl)tin, 97% [97674-02-7]	1g
NEW→	(C ₄ H ₉) ₃ Sn(C ₄ H ₇ O); FW: 361.16; colorless liq.	5g
		25g

Technical Note:

1. Versatile tin reagent used for the introduction of a 1-ethoxyvinyl group via a Stille cross-coupling reaction, (palladium-catalyzed coupling of an organohalide (or pseudohalide) with an organotin compound).



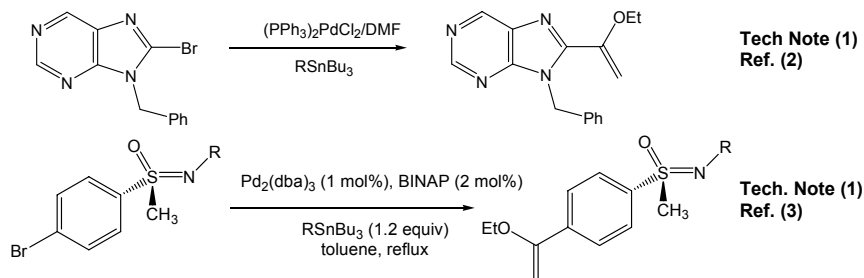
Tech. Note (1)
Ref. (1)

TIN (Compounds)

50-3015 Tributyl(1-ethoxyvinyl)tin, 97% [97674-02-7]

NEW→
(cont.)

Technical Note (cont):



References:

1. *J. Org. Chem.*, **2009**, 74, 6390.
2. *J. Org. Chem.*, **2007**, 72, 8577.
3. *J. Org. Chem.*, **2005**, 70, 2346.

YTTERBIUM (Compounds)

70-1000 Tris(N,N'-di-i-propylacetamidato)

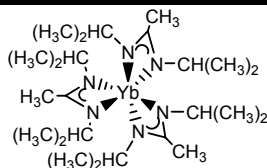
NEW→

ytterbium(III), 99%

Yb(C₈H₁₇N₂)₃; FW: 596.74;

white to off-white powdr.

Note: Product sold under, use subject to, terms and conditions of label license at www.strem.com/harvard2.



250mg

1g

ZINC (Compounds)

30-3020 2,2,6,6-Bis(tetramethylpiperidine)zinc, lithium chloride complex

NEW→

HAZ

0.35M (12wt% ±2wt%) in toluene/tetrahydrofuran [207788-38-3]

C₁₈H₃₆Zn; FW: 317.87; amber to brown liq.

air sensitive, moisture sensitive

Note: A product of Chemetall. Sold for R&D purposes only.

.025mole

30-3050 Zinc arsenide (99.5%-Zn) [12006-40-5]

NEW→

Zn₃As₂; FW: 346.01; 1/8" gray pieces

5g

25g

30-3012 Zinc chloride 2.2M (25wt% ±1wt%) in 2-methyltetrahydrofuran

NEW→

HAZ

[7646-85-7]

ZnCl₂; FW: 136.28; liq.

air sensitive, moisture sensitive

Note: A product of Chemetall. Sold for R&D purposes only.

0.25mole

1mole

CUCURBITURIL KIT

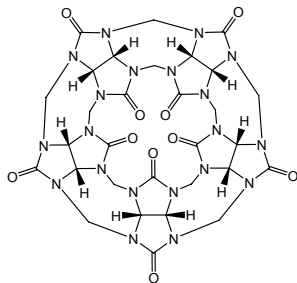
96-7054

Cucurbituril Kit

Components available for individual sale.

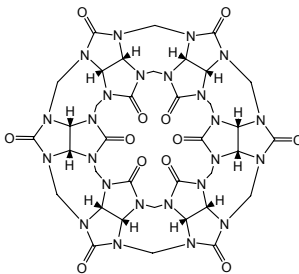
NEW→

Contains the following:



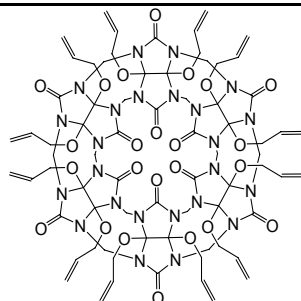
07-1310

100mg



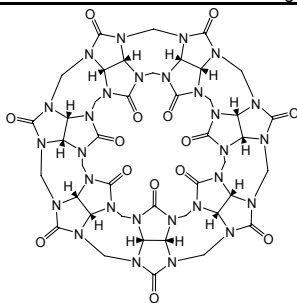
07-1320

500mg



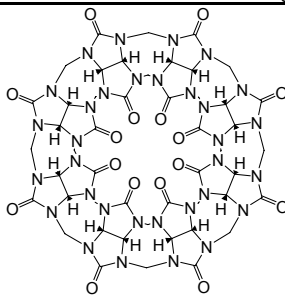
07-1322

25mg



07-1325

50mg



07-1330

25mg

- | | | |
|---------|--|-------------|
| 07-1310 | Cucurbit[5]uril (CB[5]) ammonium sulfate hydrate, 99+% | See page 54 |
| | [259886-49-2] | |
| 07-1320 | Cucurbit[6]uril (CB[6]) hydrate, 99+% | See page 54 |
| | [80262-44-8] | |
| 07-1325 | Cucurbit[7]uril (CB[7]) hydrate, 99+% | See page 54 |
| | [259886-50-5] | |
| 07-1330 | Cucurbit[8]uril (CB[8]) hydrate, 99+% | See page 55 |
| | [259886-51-6] | |
| 07-1322 | Peralloyoxycucurbit[6]uril (AOCB[6]) potassium sulfate, 94+% | See page 55 |

Garphos™ Ligand Kit

96-4100

Garphos™ Ligand Kit

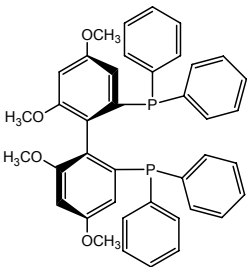
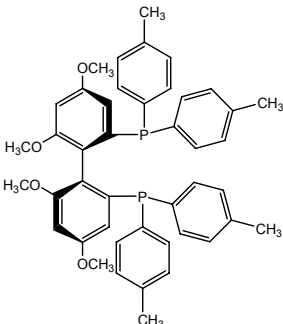
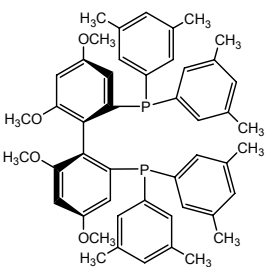
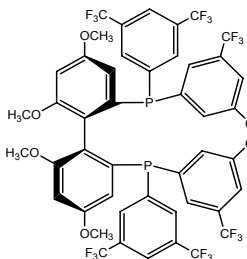
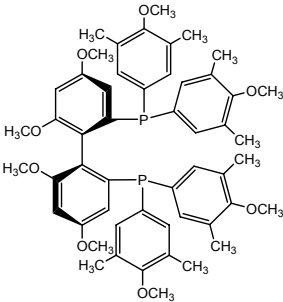
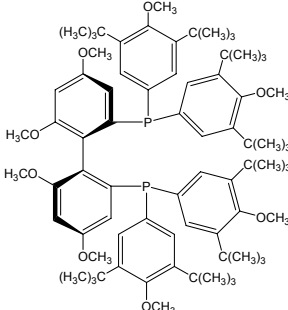
NEW→

Sold in collaboration with KCT.

Patent US App No. 61/381,493.

Components available for individual sale.

Contains the following:

		100mg
15-1653	(R)-Ph-Garphos™	
15-1654	(S)-Ph-Garphos™	
		100mg
15-1657	(R)-Tol-Garphos™	
15-1658	(S)-Tol-Garphos™	
		100mg
15-1661	(R)-Xyl-Garphos™	
15-1662	(S)-Xyl-Garphos™	
		100mg
15-1663	(R)-BTM-Garphos™	
15-1664	(S)-BTM-Garphos™	
		100mg
15-1666	(R)-DMM-Garphos™	
15-1667	(S)-DMM-Garphos™	
		
15-1672	(R)-DTBM-Garphos™	
15-1673	(S)-DTBM-Garphos™	
15-1653	(R)-2,2'-Bis(diphenylphosphino)-4,4',6,6'-tetramethoxybiphenyl, min. 97% (R)-Ph-Garphos™	See page 58
15-1654	(S)-2,2'-Bis(diphenylphosphino)-4,4',6,6'-tetramethoxybiphenyl, min. 97% (S)-Ph-Garphos™	See page 59
15-1657	(R)-2,2'-Bis(di-p-tolylphosphino)-4,4',6,6'-tetramethoxybiphenyl, min. 97% (R)-Tol-Garphos™	See page 59
15-1658	(S)-2,2'-Bis(di-p-tolylphosphino)-4,4',6,6'-tetramethoxybiphenyl, min. 97% (S)-Tol-Garphos™	See page 59
15-1661	(R)-2,2'-Bis[bis(3,5-dimethylphenyl)phosphino]-4,4',6,6'-tetramethoxybiphenyl, min. 97% (R)-Xyl-Garphos™	See page 56
15-1662	(S)-2,2'-Bis[bis(3,5-dimethylphenyl)phosphino]-4,4',6,6'-tetramethoxybiphenyl, min. 97% (S)-Xyl-Garphos™	See page 56
15-1663	(R)-2,2'-Bis[bis(3,5-trifluoromethylphenyl)phosphino]-4,4',6,6'-tetramethoxybiphenyl, min. 97% (R)-BTM-Garphos™	See page 57
15-1664	(S)-2,2'-Bis[bis(3,5-trifluoromethylphenyl)phosphino]-4,4',6,6'-tetramethoxybiphenyl, min. 97% (S)-BTM-Garphos™	See page 57
15-1666	(R)-2,2'-Bis[bis(4-methoxy-3,5-dimethylphenyl)phosphino]-4,4',6,6'-tetramethoxybiphenyl, min. 97% (R)-DMM-Garphos™	See page 57
15-1667	(S)-2,2'-Bis[bis(4-methoxy-3,5-dimethylphenyl)phosphino]-4,4',6,6'-tetramethoxybiphenyl, min. 97% (S)-DMM-Garphos™	See page 57
15-1672	(R)-2,2'-Bis[bis(4-methoxy-3,5-di-t-butylphenyl)phosphino]-4,4',6,6'-tetramethoxybiphenyl, min. 97% (R)-DTBM-Garphos™	See page 56
15-1673	(S)-2,2'-Bis[bis(4-methoxy-3,5-di-t-butylphenyl)phosphino]-4,4',6,6'-tetramethoxybiphenyl, min. 97% (S)-DTBM-Garphos™	See page 56

PARACYCLOPHANE KIT

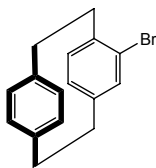
96-7052

NEW→

Paracyclophane Kit

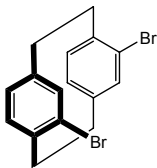
Components available for individual sale.

Contains the following:



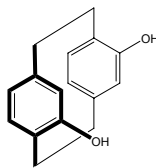
06-0104

500mg



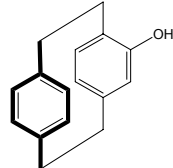
06-0460

250mg



08-0700

100mg



08-2027

250mg

06-0104 racemic-4-Bromo[2.2]paracyclophane, min. 95% [1908-61-8]

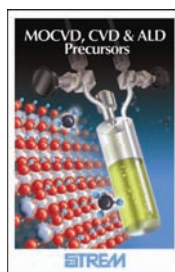
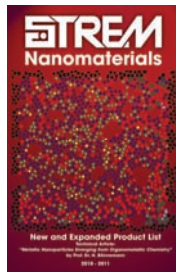
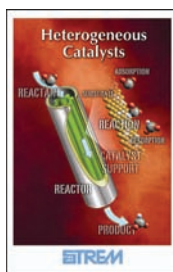
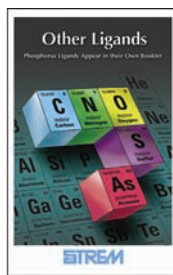
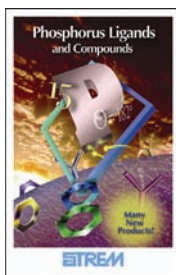
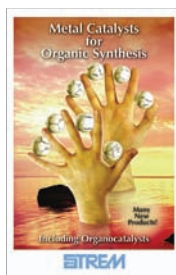
Visit www.strem.com

06-0460 racemic-4,12-Dibromo[2.2]paracyclophane, min. 95%
[23927-40-4]

08-0700 racemic-4,12-Dihydroxy[2.2]paracyclophane, min. 97%
[612492-27-0]

08-2027 racemic-4-Hydroxy[2.2]paracyclophane, min. 97% [157018-15-0]

AVAILABLE BOOKLETS



THE STREM CHEMIKER

STREM CHEMICALS, INC.

7 Mulliken Way

Newburyport, MA 01950-4098 U.S.A.

Tel.: (978) 499-1600 Fax: (978) 465-3104

(Toll-free numbers below US & Canada only)

Tel.: (800) 647-8736 Fax: (800) 517-8736

OUR LINE OF RESEARCH CHEMICALS

Electronic Grade Chemicals

Fullerenes

High Purity Inorganics & Alkali Metals

Ionic Liquids

Ligands & Chiral Ligands

Metal Acetates & Carbonates

Metal Alkoxides & beta-Diketonates

Metal Alkyls & Alkylamides

Metal Carbonyls & Derivatives

Metal Catalysts & Chiral Catalysts

Metal Foils, Wires, Powders & Elements

Metal Halides, Hydrides & Deuterides

Metal Oxides, Nitrates, Chalcogenides

Metalloenes

Nanomaterials

Organofluorines

Organometallics

Organophosphines & Arsines

Porphines & Phthalocyanines

Precious Metal & Rare Earth Chemicals

Volatile Precursors for MOCVD, CVD & ALD

Bulk Manufacturing, Custom Synthesis

cGMP facilities

Visit our website at www.strem.com.
Stock status now on-line.

